

Aurora Marie Fosli Flataker

# Voltage-dependency of loads and its role in voltage control strategies

Master's thesis in Energy and Environmental Engineering  
Supervisor: Kjell Sand  
June 2019

**NTNU**  
Norwegian University of Science and Technology  
Faculty of Information Technology and Electrical  
Engineering  
Department of Electric Power Engineering



Aurora Marie Fosli Flataker

# Voltage-dependency of loads and its role in voltage control strategies

Master's thesis in Energy and Environmental Engineering  
Supervisor: Kjell Sand  
June 2019

Norwegian University of Science and Technology  
Faculty of Information Technology and Electrical Engineering  
Department of Electric Power Engineering





## Abstract

A voltage control strategy can be defined as a deliberate choice made by the distribution system operator to keep voltages in the network in the lower or higher part of the allowed voltage band defined in voltage quality standards. The goal of implementation of a strategy can be reduction of network losses, peak power or the energy demanded by the loads in the network. The response of a given network to a voltage control strategy depends on the network topology and network components as well as the voltage-dependency of the connected loads. Knowledge about loads' dependency on voltage is therefore crucial for assessment of voltage control strategies.

Different load types respond differently to voltage changes. This thesis investigates the voltage-dependency of selected household appliances by laboratory experiments. The measurements obtained from the laboratory are used to express the voltage-dependency of the tested loads by two commonly used load models, namely the ZIP model and the exponential model. Both models capture the voltage-dependency of the modelled load. The load model coefficients are estimated from the laboratory test data by utilising curve fitting techniques.

The tested devices are:

- induction cooktop
- electrical space heater (resistance heater)
- heat pump
- washing machine
- tumble dryer

The laboratory tests examine the voltage dependency of the tested devices and investigate how the load behaviour changes through the operation cycles of the loads and varies with user-defined settings. It is found that the load behaviour changes between different user-defined settings. The washing machine exhibits fundamentally different load-to-voltage behaviour in different part of the operation cycle, while the induction cooktop shows fundamentally different voltage-dependency depending on the user-defined setting selected for the cooking application. Moreover, the heat pump and tumble dryer tested feature technology which is not common in conventional heat pump and tumble dryers. Their load behaviour differs significantly from load behaviour of the conventional-technology heat pumps and tumble dryers found in literature.

For the DSO, generally the *aggregate effect* of several individual customers and appliances is of interest. Also for assessing the response of a potential voltage control strategy, the aggregate response of all appliances connected and used at a given period in time is the main concern. Therefore, this thesis also addresses how the knowledge about behaviour of individual loads can be used to make aggregate load models. This is especially interesting and challenging when voltage control strategies shall be implemented in a network with considerable shares of closed-loop loads connected to it.

Closed-loop loads are loads containing one or more control loops, typically thermostat controls for controlling the duty-cycle of heating and cooling loads. For such loads, it is not enough to examine the loads' instantaneous response to voltage change. By the fact that the applied voltage influences the duty-cycle of the load, one need to take into account how the voltage scheme influences the aggregate effect of the change in the duty-cycles of the appliances. In the thesis one example of a simulation of the aggregate effect of thermostatically controlled water heaters for different applied voltages is included. The result of the simulation indicates that peak power demand can be reduced by applying

higher voltages. This is interesting since voltage control strategies implemented by DSOs in other countries exploits the positive load-to-voltage dependency of the load by reducing voltage to achieve reduction in power and/or energy demand.

Voltage-dependency of loads plays a key role in determining the outcome of a given voltage control strategy. This thesis can provide insight in voltage-dependency and load behaviour of selected household appliances and in how this knowledge can be used for load model aggregation and assessment of voltage control strategies. Further, it provides an overview of the concept of voltage control strategies and reviews strategies implemented by DSOs.

## Sammendrag

En spenningsreguleringsstrategi kan sees på som et bevisst valg tatt av nettselskapet om å holde spenningene i nettet i den nedre eller øvre delen av det tillatte spenningsbåndet gitt i Forskrift om leveringskvalitet (FoL). Målet med en slik strategi kan være reduksjon av nettap, makseffekt eller energiforbruket til lastene som er knyttet til nettet. Hvordan nettet responderer på en gitt spenningsreguleringsstrategi avhenger av nettopologien og komponenter i nettet i tillegg til spenningsavhengigheten til tilknyttede laster. Kunnskap om lastens spenningsavhengighet er derfor avgjørende for å vurdere spenningsreguleringsstrategier.

Denne masteroppgaven undersøker spenningsavhengigheten til utvalgte elektriske husholdningsapparater. Målingene fra laborieforsøkene brukes til å uttrykke apparatens spenningsavhengighet ved hjelp av to mye brukte lastmodeller, nemlig ZIP-modellen og eksponentialmodellen. Begge modellene uttrykker aktivt og reaktivt effektforbruk som funksjon av påtrykt spenning. I oppgaven estimeres koeffisientene i lastmodellene med utgangspunkt i måledata fra labforsøkene ved hjelp av kurvetilpasning (minste kvadraters metode).

Apparatene som testes er:

- Induksjonsovn
- Panelovn
- Varmepumpe
- Vaskemaskin
- Tørketrommel

Labforsøkene undersøker spenningsfølsomheten til apparatene og hvordan lastens karakteristikk endrer seg gjennom apparatens driftssyklus og varierer mellom ulike innstillinger valgt av brukeren. Resultatene viser at lastkarakteristikken til apparatene avhenger av hvilken innstilling brukeren velger. Vaskemaskinen har svært ulik spenningsfølsomhet i ulike deler av vaskeprogrammet, mens induksjonsovnen har svært ulik spenningsfølsomhet for de ulike innstillinger brukeren av ovnen kan velge mellom. Teknologien brukt i varmpumpen og tørketrommelen som er testet i forbindelse med oppgaven er annerledes enn teknologien som er mest vanlig i slike apparater. Lastkarakteristikken deres viser seg å skille seg vesentlig fra lastkarakteristikken til varmpumper og tørketromler som er basert på konvensjonell teknologi.

Nettselskap forsyner ulike typer kunder med ulike typer elektriske apparater. For nettselskapet er det vanligvis den aggregerte lasten som er av interesse. Dette gjelder også for vurdering av spenningsreguleringsstrategier. Derfor er problemstillinger knyttet til aggregering av last tatt med i denne oppgaven. Aggregering av last er særlig interessant og utfordrende når spenningsreguleringsstrategier skal implementeres i nett med betydelig andel termostatstyrt last eller andre laster med innebygde reguleringsløsninger.

For termostatstyrte laster er det ikke tilstrekkelig å undersøke hvordan effektforbruket til lasten påvirkes av en spenningsendring umiddelbart etter at spenningsendringen finner sted. Siden spenningen også påvirker driftssyklusen til termostaten - altså hvor lenge lasten står på om gangen før termostaten slår den av - må man ta hensyn til hvordan virkningen av spenningsendring er over tid. Denne masteroppgaven presenterer et eksempel på hvordan man kan simulere virkningen av spenningsregulering på en aggregert last bestående av termostatstyrte varmtvannsberedere. Resultatene fra simuleringene indikerer at den aggregerte lastens maksimaleffekt reduseres ved høyere spenningsnivå. Dette er interessant siden spenningsreguleringsstrategier implementert av nettselskap i

andre land antar en positiv spenningsavhengighet (altså at effektforbruket reduseres ved lavere spenningsnivå).

Lasters spenningsavhengighet er avgjørende for utfallet av en spenningsreguleringsstrategi. Denne oppgaven kan gi innsikt i spenningsavhengigheten til et utvalg husholdingsapparater og hvordan denne kunnskapen kan brukes for å lage aggregerte lastmodeller og til å vurdere spenningsreguleringsstrategier. Videre gir oppgaven oversikt over konseptet spenningsreguleringsstrategi og gjennomgår strategier som er implementert i distribusjonsnett.

## Acknowledgement

This master thesis is written spring 2019 and is the work marking the end of the five-year Master of Science study program Energy and Environmental Engineering at NTNU.

I would like to express my gratitude to those who have helped me with this thesis.

Firstly, I would like to thank my supervisor Kjell Sand for help and support during the whole process from finding the topic of the thesis until finalizing the work. His feedback and perspectives have been very valuable for me, both related to the specific topic and about scientific work in general. In addition, Arnt-Magnar Forseth from TrønderEnergi Nett (TEN) and researcher Nicolai Feilberg, who has been working together with TEN during the last years on topics related to this thesis, have provided insight and perspectives which has been useful and inspiring in the work with the thesis.

A special thanks to Nicolai Feilberg for sharing his results and methodology from simulations on water heaters as well as the regression analysis performed on the measurement data from Huseby in Trondheim.

In the work with the thesis I also got the opportunity to learn how voltage control is implemented in the distribution networks of the DSOs NTE and TEN. Thanks to Rue Paulsen (NTE) Arnt-Magnar Forseth (TEN) and Svein Skjevik (TEN) for the time and effort.

I also want to thank the staff at the Service lab at NTNU for helping me with the equipment and test setup. Especially I want to express my gratitude to Bård Almås, who has helped me a lot in this regard and has been very patient and solution oriented when problems have occurred during the lab tests and when I needed some extra guidance with the equipment or software.

## Table of contents

Abstract .....	i
Sammendrag .....	iii
Acknowledgement .....	v
Table of contents .....	vi
List of figures .....	viii
List of tables .....	x
Definitions .....	xi
Abbreviations .....	xiii
1 Introduction .....	1
<b>Part I - Voltage control and voltage control strategies .....</b>	<b>4</b>
2 Voltage control and voltage quality .....	5
2.1 Voltage control in distribution grids .....	5
3 Voltage control strategies .....	9
3.1 Introduction .....	9
3.2 VC strategies implemented by DSOs worldwide .....	10
3.3 Assessment of VC strategies .....	11
4 Discussion .....	12
<b>Part II - Voltage-dependency of individual loads and network losses .....</b>	<b>14</b>
5 Introduction .....	14
6 Load modelling .....	17
6.1 ZIP model .....	18
6.2 Exponential model .....	19
7 Network components - losses in lines, cables and transformers .....	20
7.1 No-load losses .....	20
7.2 Variable losses .....	20
8 Lab test: Voltage dependency of individual loads .....	22
8.1 Objective .....	22
8.2 Approach .....	22
8.3 Equipment and test setup .....	23
8.4 Curve fitting - Finding load model parameters from measurement data .....	25
8.5 Results and discussion .....	26
9 Discussion .....	47

<b>Part III - Aggregated loads and -load modelling .....</b>	<b>50</b>
10 Measurement-based and component-based load modelling .....	51
10.1 Component-based load modelling.....	51
11 Modelling and aggregation of thermal closed-loop loads.....	55
11.1 Example: simulation of aggregated effect of water heaters .....	56
12 Discussion .....	60
<b>Part IV - Conclusion and further work.....</b>	<b>61</b>
13 Conclusion.....	61
14 Further work .....	62
References .....	64
Appendices.....	68

## List of figures

Figure 2-1: One-line diagram showing a simplified network with one MV feeder and two LV feeders. It shows the distribution of VC resources that often are available for DSOs. ....	7
Figure 3-1: Illustration of a radial feeder below a distribution transformer and voltage drops towards the end of the feeder for different VC strategies. The VQ-requirements for supply voltage variations are shown as red dotted lines. ....	9
Figure 5-1: Illustration of a radial LV-feeder and some of the electrical appliances that might be found behind a supply point for a residential customer. ....	14
Figure 6-1: Diagram with different lad models categorised as static and dynamic models. From [4].	17
Figure 8-1: Illustration of the test setup showing the main components of the setup and the connection between them. The Power Supply is fed the local distribution network. It outputs an adjustable voltage which feeds the device under test (DUT). The Power Analyser measures voltages and currents. ....	23
Figure 8-2: Power Analyser configuration 1ph with neutral (TN).....	24
Figure 8-3: Power Analyser configuration 1ph without neural (IT).....	24
Figure 8-4: Curve fit example. The data points are plotted together with the fitted ZIP model and exponential model curves. The residual between one datapoint and the ZIP model curve is shown. ..	25
Figure 8-5: Schematic representation of an induction cooktop. From [40] .....	27
Figure 8-6: Induction cooktop load curves. Active power for different user-defined settings. All tests are performed with 230V test voltage. ....	28
Figure 8-7: Induction cooktop, 800W setting. ....	29
Figure 8-8: Induction cooktop, 1600W setting .....	29
Figure 8-9: Induction cooktop, 300W setting .....	29
Figure 8-10: Induction cooktop, MaxPower setting. Three different tests at 207V are shown (_xxx are the measurements-numbers of the respective tests) .....	29
Figure 8-11: Electric space heater. Measured voltage together with measured active power from the voltage dependency test of the full-power setting.....	31
Figure 8-12: Electric space heater. Measured voltage together with measured active power from the voltage dependency test of the half-power setting. ....	31
Figure 8-13: Electric space heater. Measured voltage together with measured reactive power from the voltage dependency test of the full-power setting.....	32
Figure 8-14: Electric space heater. Measured voltage together with measured reactive power from the voltage dependency test of the half-power setting .....	32
Figure 8-15: Illustration showing the basic operation and components of a heat pump. From [46] ....	33
Figure 8-16: Measured active and reactive power load curves for heat pump during a test. The heat pump was supplied with 230V voltage for the whole period except for the two events marked as "voltage tests". Under the voltage tests the voltage was changed between 210 and 250V. The heat pump was first run with 24°C as target temperature. After ca 2800 seconds (ca 45 min) the target temperature was changed to 21°C.....	34



Figure 8-17: Heat pump, active power and voltage for voltage-dependency test. ....	35
Figure 8-18: Heat pump, reactive power and voltage for voltage-dependency test. ....	35
Figure 8-19: Heat pump, active power and voltage for voltage-dependency test. ....	36
Figure 8-20: Heat pump, reactive power and voltage for voltage-dependency test. ....	36
Figure 8-21: Air conditioner load curve from measurements in [49]. Figure a show the measurement time series in hourly resolution. Fig. b shows one of the hours in minute resolution. ....	37
Figure 8-22: Heat pump power demand from measurements of 11 hours of operation. ....	37
Figure 8-23: Washing machine load curves for different washing programs .....	39
Figure 8-24: Washing machine load curve from measurements of a washing cycle from [49] .....	40
Figure 8-25: Washing machine load curves from measurements of four different washing cycles from [51] .....	40
Figure 8-26: Washing machine load curve from measurements of a washing cycle from [49] .....	40
Figure 8-27: Active and reactive power demand for washing machine throughout washing cycle for different voltages. Each time step equals 0.25 seconds. The washing cycle stages washing, heating, rinse and spin are marked in the figure. ....	41
Figure 8-28: Drying programs active power demand.....	44
Figure 8-29: Load curves from four differed dryers measured in [51].....	46
Figure 8-30: Load curves of drying programs for two different clothes dryer models measured in [49] .....	46
Figure 10-1: One-line diagram showing one radial MV-feeder. The upstream transformer (HV/MV) as well as some downstream transformers (MV/LV) are shown. Parts of the LV network downstream of the MV/LV transformers are shown. The figure illustrates different points of load aggregation. Different load aggregation points are relevant depending on which part of the network that is subject to analysis. ....	53
Figure 11-1: Heat demand and power demand from a 24-hour simulation of the aggregate effect of 1000 thermostatically controlled water heaters. The heat demand for each eater heater come from Monte Carlo simulation. The corresponding electric power demand for a water heater is a result of the heat demand and thermostat-controlled heating element’s duty-cycle to keep the water in the water heater between threshold values. Each water heater has a nominal power of 2kW, but is here supplied with 0.9pu (207V) and therefore only supplying 1620Watts.....	58
Figure 11-2: The heat demand is the same as for Figure 11-1 (refer to explanation above). Here however, the supply voltage for each water heater is 1 pu (230V) and thus each heating element delivers 2kW as long as they are active. ....	58
Figure 11-3: Expected values and 95% confidence interval resulting from 100 independent simulations of the aggregated effect of 1000 thermostatically controlled water heaters. Voltage of 1pu corresponds to 230V. ....	59

## List of tables

Table 8-1: Induction cooktop. Average active and reactive power for different user-defined settings (time step 50-800, i.e. excluding the start-up behaviour) .....	28
Table 8-2: Induction cooktop load model coefficients for ZIP and exponential load models. Model parameters are listed for different user-defined settings. For the 300W and 800W settings, two sets of load model coefficients are included, namely for "on-state" and "off-state", i.e. when the active power demand is peaking and close-to-zero respectively. ....	30
Table 8-3: Durations of the on- and off-states for the 300W and 800W- settings for the induction cooktop .....	30
Table 8-4: Load model parameters for ZIP and exponential load models for the resistance heater at half- and full-power settings .....	32
Table 8-5: Washing machine cycle broken down to three stages: cleaning/washing, rinse and spin. .	38
Table 8-6: Average values of active and reactive power, true power factor and current and voltage THD for the tested washing machine programs. Tests are performed with 230V test voltage.....	40
Table 8-7: Load model parameters for ZIP and exponential load models for the washing machine 40°C cotton program. Model parameters for each stage in the washing cycle are listed. ....	42
Table 8-8: Average active and reactive power values for different drying programs .....	45
Table 8-9: Load model parameters for ZIP and exponential load models for the heat pump dryer for the Time Dry-setting .....	46
Table 9-1: Summarising table for the curve fitting results. The results are simplified to categorise each tested appliance as either constant impedance, constant current or constant power. When relevant, individual settings or parts of operation cycle are categorised independently. ....	48

## Definitions

**SUPPLY POINT** – In this thesis “supply point” is used referring to the same concept as “Point of supply” and “supply terminals” defined in [2]:

“point in a distribution network designated as such and contractually fixed, at which electric energy is exchanged between contractual partners

Note – The point of supply may be different from the boundary between the electricity supply system and the user’s own installation or from the metering point.”

For describing load concepts, the definitions given by the IEEE Task Force on Load Representation for Dynamic Performance, presented in [3] (1993) are used:

**LOAD** - The term “load” can have several meanings in power system engineering. including:

- a) A device. connected to a power system, that consumes power,
- b) The total power (active and/or reactive) consumed by all devices connected to the power system,
- c) A portion of the system that is not explicitly represented in a system model. but rather is treated as if it are a single power-consuming device connected to a bus in the system model.
- d) The power output of a generator or generating plant.

Note: for the purpose of this thesis, the definitions a) and b) are the most relevant.

**LOAD COMPONENT** - A load component is the aggregate equivalent of all devices of a specific or similar type, e.g., water heater, mom air conditioner, fluorescent lighting.

**LOAD CLASS** - A load class is a category of load, such as, residential, commercial, or industrial. For load modelling purposes, it is useful to group loads into several classes, where each class has similar load composition and load characteristics.

**LOAD COMPOSITION** - The fractional composition of the load by load components. This term may be applied to the bus load or to a specific load class.

**LOAD CLASS MIX** - The fractional composition of the bus load by load classes.

**LOAD CHARACTERISTIC** - A set of parameters, such as power factor, variation of P with v, etc., that characterize the behaviour of a specified load. This term may be applied to a specific load device, a load component, a load class, or the total bus load.

**LOAD MODEL** - A load model is a mathematical representation of the relationship between a bus voltage (magnitude and frequency) and the power (active and reactive) or current flowing into the bus load. The term “load model” may refer to the equations themselves or the equations plus specific values for the parameters (e.g., coefficients, exponents) of the equations. Depending on the computational implementation of these equations in a specific program, the load power or current may not be calculated explicitly, but it is useful to think of the model in these terms.

Some additional definitions for load modelling are taken from [4]:

**LOAD MODEL CATEGORY** – A group of different electrical devices used in various end-use applications, which, for the purpose of load modelling, have the same or similar characteristics with respect to their active and reactive power demands and also demonstrate similar responses to variations in voltage and frequency, therefore allowing them to be represented by the same load model.

Note: One load model category may be further divided into several sub-categories (e.g. category of motor loads may be divided into single-phase and three-phase motor sub-categories, while the category of non-linear power electronic loads may be divided in three general sub-categories: without power factor correction circuit (PFC), with passive PFC, and with active PFC).

**END-USE LOAD TYPE** - A group of individual loads with the same specific purpose, which may have the same or different electrical characteristics. Note: E.g. incandescent lamps, compact fluorescent lamps, high-intensity discharge lamps and LED light sources all belong to the same “lighting load” type although they have different electrical characteristics and should be represented by different load model categories.

**LOAD CURVE OR LOAD PROFILE** - A graphical depiction or analytical representation of the observed (i.e. measured), or estimated (i.e. forecasted) variations in active and/or reactive power demand of a load during a specified time period, where variations in demand are correlated with the actual time at which they occur.

## Abbreviations

ASHP	- Air Sourced Heat Pump
CVR	- Conservation Voltage Reduction
DETC	- De-Energized Tap Changer
DG	- Distributed Generation
DSO	- Distribution System Operator
DUT	- Device Under Test
EV	- Electric Vehicle
FoL	- Forskift om leveringskvalitet
GSHP	- Ground Sourced Heat Pump
HV	- High Voltage
HVAC	- Heating, Ventilation and Air Conditioning
LDC	- Line Droop Compensation
LM	- Load Management
LV	- Low Voltage
MV	- Medium Voltage
NEK	- Norsk Elektroteknisk Komite
OLTC	- On-Load Tap Changer
pu	- Per Unit
QoS	- Quality of Supply
RMS	- Root Mean Square
SCADA	- Supervisory Control and Data Acquisition
TSO	- Transmission System Operator
VC	- Voltage Control
VQ	- Voltage Quality

# 1 Introduction

## Background

Voltage is a parameter in the power system which must be controlled to minimize network losses, control reactive power flow and maintain system stability as well as to make sure that all network components and connected devices are operated within their design limits. For the distribution system operators (DSOs), one main goal of voltage control is to keep the supply voltage at the supply terminals within the limits as defined in voltage quality standards. Furthermore, the power and energy demanded by loads connected to the network is to varying extent dependent on the supplied voltage. Consequently, voltage control is not only a necessary measure for securing optimal operation of the system given a load situation, it can also be used actively to change the load situation in the grid.

Due to the climate crisis and the associated increased focus on renewable energy, energy-efficiency and electrification of sectors like transportation, new challenges are introduced to the system operators. In Norway, increased penetration of power-demanding appliances like Electric Vehicles (EVs) and replacement of energy-demanding appliances with more energy-efficient but power-demanding appliances, has led to that power demand is increasing more rapidly than energy demand[5]. At the same time system operators face vast investments to reinforce networks due to aging of components[6].

Optimization of the utilization of the existing network and choosing cost-efficient alternatives to meet the introduced challenges is necessary to minimize investment and operation costs. Reduction of energy losses and energy consumption are other aspects relevant in an era where climate change mitigation and sustainability should be incorporated in all sectors and on all levels. One possibility that can be exploited is the potential granted by voltage control to choose a *voltage control strategy*, through which energy and/or power demand in the system can be reduced.

The relevance of voltage control is likely to increase as new voltage control technologies with higher switching speeds and more advanced control logics are deployed in networks. Moreover, the observability of the network increases with the deployment of smart meters and other metering infrastructure. These developments enhance the DSOs possibilities to operate the grids closer to operational limits.

A question that could be asked is then how a voltage control strategy should look to achieve the desired goals. One voltage control strategy implemented by DSOs in other countries is the so-called Conservation Voltage Reduction. This strategy implements voltage reductions with the objective to reduce the total energy demand in the system, i.e. reduce the sum of the network losses and the energy demanded from loads connected to the system. A different possible objective of a voltage control strategy could be peak power reduction.

The response of a network to a voltage control strategy is determined by the voltage-dependency of the loads connected to the system as well as the voltage-dependency of the network losses. Since all networks have different characteristics and because the connected loads are not the same in all networks, the voltage-dependency can vary between networks.

Therefore, to be able to estimate how a VC strategy will impact the power system in question, knowledge about the voltage-dependency of loads and network components is necessary. One way to assess VC strategies before their implementation is by performing load flow simulations on a model of the network to calculate network losses and power demand when different voltages are applied. To obtain realistic results from this type of simulation, the models of the network components, generation units and connected loads used in the simulation must capture the relevant behaviour of the real system.

The load models must hence capture the voltage dependency of the active and reactive power drawn by the loads. Two widely used load models which incorporates the load-to-voltage behaviour are the ZIP model and the exponential load model. The coefficients in these models must be selected so that the models reflect the load behaviour of the load that is to be modelled. An approach to determining the relevant load model coefficients is to use a bottom-up procedure where knowledge of load behaviour of individual loads forms the basis for finding the load behaviour of the aggregate load.

Load model parameter values for commonly used electrical appliances are presented in various references, like [1], [7], [8], [9, p. 310]. Load model parameters for individual appliances and for aggregate models from various publications are listed in [4]. However, since load characteristics are constantly changing with technology development and entering of new products to the market, it is necessary to do test on modern electrical appliances to keep load models up to date. The importance of updating and improving load models is emphasized in reference [3], [7], [10].

## Scope and thesis contributions

In this thesis, load model coefficients of household appliances are estimated by testing the voltage-dependency of loads in the laboratory and fitting the behaviour to load models by utilization of curve fitting techniques.

Moreover, based on the results from the lab work, literature review and a simulation example performed by Nicolai Feilberg and presented in this thesis, it is discussed how the knowledge about individual appliances can be used on an aggregated level.

Voltage control strategies are addressed by looking at the voltage control technologies typically available in distribution grids and reviewing strategies implemented by DSOs.

The contributions from this thesis include:

- Overview of voltage control technologies in distribution networks. Since these per today are the available resources that can be used for implementing potential VC strategies, the limitations and opportunities introduced by them must be borne in mind when considering VC strategies.
- Review of voltage control strategies implemented in distribution networks. Even if it is desired to choose strategies with other objectives and other means of implementation, experience from research and real-world implementation of other strategies can provide useful insight.
- Methodology and results from laboratory tests of the household appliances listed below. The tests are devoted to examining the voltage dependency of the tested devices as well as investigating how the load behaviour changes through the operation cycles of the loads and varies with user-defined settings. The test results are used to find load model parameters for the tested devices for two commonly used load models, namely the ZIP model and the exponential load model.
  - Induction Cooktop
  - Resistance space heater
  - Heat pump
  - Washing Machine
  - Tumble dryer with heat pump technology
- Overview of methods for load model aggregation, i.e. how knowledge about the load behaviour of individual loads can be used and aggregated to understand the behaviour of a group of individual loads.

- Measurement data from the laboratory tests are included as appendix and can be used in later research. The data contains measurements of harmonic currents and voltages which are not analysed in this thesis but can be interesting in further work.
- The measurements are performed in the Smart House connected to the Smart grid laboratory at NTNU. The results from the tests can be valuable in later work in the laboratory. For example, the knowledge about the load profiles and voltage-dependency of the individual appliances can serve as reference if voltage-dependency tests of aggregated loads are to be conducted. In addition, for work with demand side flexibility and smart-home solutions, knowledge about the load profiles of the individual loads can be useful.

## Thesis structure

The thesis is divided into three main parts:

- Part I – Voltage control and voltage control strategies
- Part II – Voltage-dependency of individual loads and network losses
- Part III – Aggregated loads and -load modelling

Each part address important aspects of the topic of voltage control strategies, load modelling and load's dependency on voltage. Each part is divided into chapters and subchapters. In the end of each part, there is a chapter which discuss and summarise the content of the part.

Part I introduce the concept of voltage control and voltage quality. Further, an overview of the voltage control technologies widely used in distribution systems is given. The concept of voltage control strategies is introduced, and voltage strategies implemented by DSOs are reviewed.

Part II focus on the voltage-dependency of individual loads. The voltage dependency of loads can be expressed in terms of different load models. Load modelling is an important field of study within electrical engineering, as many applications in planning and operation of power system relies on simulations of the power system in different situations (e.g. load flow studies and stability analysis). In the simulations it is necessary to model the loads connected to the network as well as the network itself and the generation units. Therefore, in this part of the thesis load modelling is addressed in general terms followed by more detailed information about the two load models used in the load modelling in the thesis. These models are the ZIP load model and exponential load model. Moreover, the results from the laboratory work is presented and discussed in this part.

Part III is devoted to aggregation of loads. In this part, the two main approaches to load model aggregation is presented, namely the measurement-based and component-based approaches. The emphasis is on the latter since the laboratory results from Part II is more relevant for this approach. Further, the complexity added to the load modelling when the individual loads feature thermostatic controls or other control loops is addressed. Such loads are referred to as closed-loop loads and are highly relevant in a Norwegian contexts by the fact that water and space heating constitute major parts of the residential load. Due to its high relevance, an example of simulation of closed-loop loads is included. The example is a simulation of the aggregate effect of voltage-dependency of water heaters. The simulation is performed by Nicolai Feilberg. The simulation work has not been published previously, and is therefore presented in the thesis with his permission due to the relevance of the methodology and results.



## **Part I - Voltage control and voltage control strategies**

This part contains the following chapters:

Chapter 2 – addresses voltage control and presents the relevant voltage quality requirements for voltage control strategies. Further, the voltage control technologies typically available in distribution grids are presented.

Chapter 3 – addresses the concept of voltage control strategies and reviews some voltage control technologies implemented in real-world networks as well as some relevant simulation and measurement results relevant for the topic.

Chapter 4 – summarises and discusses some aspects of chapter 2 and 3.

## 2 Voltage control and voltage quality

Network components like lines and transformers, generation units and all electrical loads connected to the grid are design to operate under voltages within a certain range and of a given quality. Too high voltages can amongst other cause dielectric breakdown of insulation, whereas too low voltages can cause malfunction of motors and risk of overheating of power electronic devices. Per IEC definition (ref [2]), voltage control is “*the adjustment of the network voltages to values within a given range*”. System operators implements voltage control to keep network components within operation limits, reduce network losses, maintain system stability and to secure satisfactory voltage quality for the connected customers.

Voltage quality (VQ) is one of more aspects related to the electrical supply which is regulated to make sure all connected customers receives a satisfactory “Quality of electricity supply” (QoS)<sup>1</sup>. Voltage quality is regulated through standards where limits and indicative values for different phenomena related to voltage quality are given. The European standard is EN50160[11]. In Norway, VQ requirements are incorporated in *Forskrift om leveringskvalitet* (FoL)[12]. Voltage phenomena subject to requirements include harmonics, unbalance, flicker, dips and swells. [11], [12]

In this thesis, load modelling is viewed in the context of voltage control strategies. The most relevant voltage quality phenomena in this context is the “supply voltage variations” (Norwegian: langsomme variasjoner i spenngens effektivverdi). Supply voltage variations are the slowest voltage variations subject to requirements in VQ standards. In FoL ([12]) it is stated that ***the RMS-voltage averaged over a one-minute interval should be kept within a range of +/- 10% of the nominal voltage***. This involves that the DSOs must make sure that the voltage at all supply points (the point where a customer is connected to the grid) are within these limits. Hence, the upper and lower limits are 253 and 207V for a nominal voltage of 230V. This has to be accounted for by the DSOs both in planning (when selecting line cross sections, transformer ratings, etc) and in operation of the grid (operation of voltage controls, etc).

The voltage applied to the individual appliances within a customers’ electrical installations may to a varying extent differ from the voltage delivered at the supply point due to losses within the customers’ installation itself. According to [13], the NEK<sup>2</sup> recommendation for maximum voltage drop within an electrical low voltage installation is 4%. Thus, if a 230V voltage is delivered at the supply point, the appliance with the worst location in the installation would experience a voltage of 220,8 V.

### 2.1 Voltage control in distribution grids

The author has been in contact with two Norwegian DSOs, NTE and TrønderEnergi Nett, to learn how voltage control is implement in their grids[14], [15]. Based on VC implementation in their grids and literature (amongst others [6], [16]–[20]), an overview over voltage control as traditionally implemented

---

<sup>1</sup> Voltage quality, continuity of supply and commercial quality are aspects incorporated in “Quality of the electricity supply”. QoS definition from [2]: “Collective effect of all aspects of performance in the supply of electricity

Note – The quality of the electricity supply includes security of electricity supply as a prerequisite, reliability of the electric power system, power quality and customer relationships ”

<sup>2</sup> NEK = Norsk Elektroteknisk Komite, committee for managing electrotechnical standards/norms. The standard referred to in [13] is NEK 400 2006:525 for electrical low voltage installations.

in distribution grids will be given in this subchapter. The exact implementation may of course be different between DSOs and in different grid areas.

The VC resources that normally are available in distribution grids are tap-changers in transformers and capacitor banks. Tap-changers regulates the secondary voltage of the transformer by adjusting the winding ratio of the transformer. [18] Capacitor banks are normally connected in parallel (shunt) to the grid. By injecting reactive power to the grid they contribute to loss reduction and can provide voltage control. [16]

The voltage controllers are in general distributed as follows. See Figure 2-1 for illustration.

- On-load tap changers (OLTCs) in power transformers (transforming from HV- to MV-level)
  - Can operate under load.
  - In the conventional types, the position of the taps is changed by a mechanical mechanism.[18]
  - Are normally controlled by an Automatic Voltage Controller (AVC) which based on measurements and build-in logic determines when tap-changing shall be executed. [19]
- De-energized tap changers (DETC) in distribution transformers (transforming from MV- to LV-level)
  - Cannot operate under load. Tap position is changed manually.
  - Due to the manual operation and need for de-energizing before tap-changing, the tap position is rarely changed. The tap is either left in the same position for the whole lifetime of the transformer, or the tap position is changed periodically or in irregular intervals to meet long-term variations due to load-growth, system expansion or seasonal changes.
- Capacitor banks in the MV network.
  - Some are fixed (not switchable) and installed to provide VAR-compensation at all times.
  - Others are switchable and can be connected or disconnected according to the load situation and VC needs. They can feature multiple capacitors in parallel which can be connected/disconnected to provide step-wise (discrete) voltage control.[16], [20, p. 453]. In NTE's grid the capacitor banks have only one "step" and is typically connected before the winter and disconnected in the spring to provide compensation in the high-load season. The connection/disconnection is operated from the SCADA system. [14]

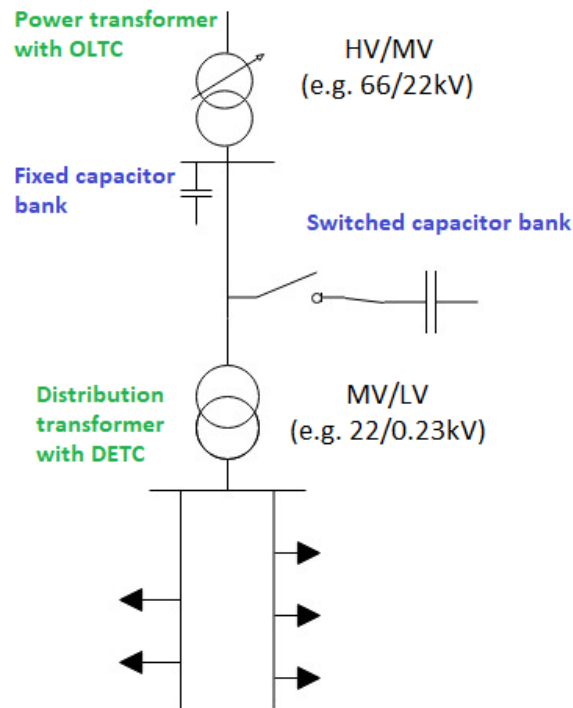


Figure 2-1: One-line diagram showing a simplified network with one MV feeder and two LV feeders. It shows the distribution of VC resources that often are available for DSOs.

The AVC controlling the On load tap-changers can feature more or less sophisticated algorithms for making the control decisions.[19] The most commonly logics implemented are the two listed below, of which the former is most widely used in Norwegian distribution networks. [17]

1. Load Tap Changer (LTC)
  - Voltage measurement is performed at the secondary side of the transformer
  - The AVC controls the secondary voltage of the transformer to lie within a deadband selected by the DSO. Typically, a time-delay of 30-90 seconds is implemented to limit the number of tap-changing operations. I.e. if the measured voltage is outside the deadband, the AVC waits a given time period before demanding change of tap position.
2. Line Droop Compensation (LDC)
  - In addition to voltage measurement, the secondary side current is measured.
  - By taking the loading current into account, the control objective for the LDC is to control the voltages of the remote point to lie within a given dead band. Normally the “remote point” is the far end of the feeder where the voltage is expected to be lowest. The LDC simulates the voltage drop across the feeder based on the current measurement and the line impedance.

In addition to the mentioned technologies, there exist a large variety of other voltage control technologies which are used in some distribution grids. These includes voltage boosters[21], distribution transformers with OLTCs, OLTCs with power-electronic operated tap-changing mechanism[18], FACTS

devices like Static Var Compensator (SVC)[22] and voltage control implemented in distributed generation units. These generally offer enhanced controllability of voltage in the network:

- OLTCs in distribution transformers, DGs with reactive power control as well as voltage boosters and battery storage systems located on LV-feeders enable voltage control closer to the end-users.
- SVCs and other FACTS devices as well as OLTCs with power-electronic tap-changer offer high switching speeds.
- Instead of voltage control in discrete steps, many voltage control technologies can control voltage in continuous steps (e.g. voltage boosters and various power electronic- and reactor-based devices[22])

### 3 Voltage control strategies

#### 3.1 Introduction

Provided that all customers receive a voltage of satisfactory quality – is there a “smart” way to control the voltage?

The figure illustrates a radial LV distribution feeder assuming no distributed generation and thus a voltage drop towards the end of the feeder. The blue curve illustrates the voltage drop along the feeder for a given load situation. All the connected customer receives a voltage within the +/-10% VQ-limits, with relatively large margins both to the upper and lower limits. In this given case, the DSO would have the possibility to make a deliberate choice to aim for a higher voltage or a lower voltage. I.e. the DSO could choose to implement “voltage control strategy A” or “voltage control strategy B” illustrated in the figure. In either case, all supply voltages are in compliance with the VQ requirements for supply voltage variations.

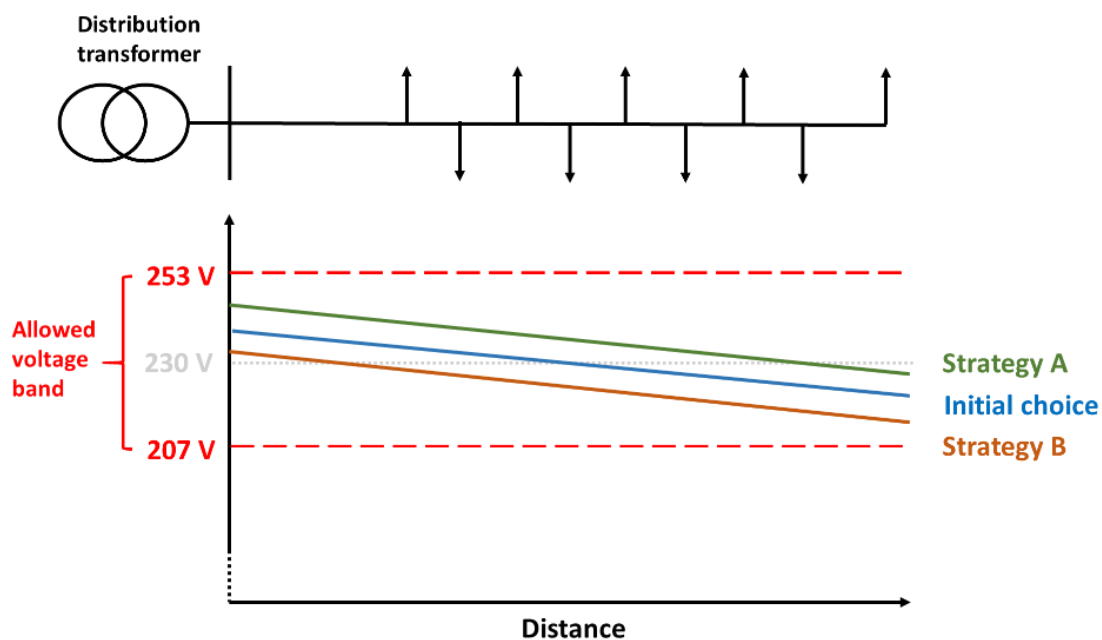


Figure 3-1: Illustration of a radial feeder below a distribution transformer and voltage drops towards the end of the feeder for different VC strategies. The VQ-requirements for supply voltage variations are shown as red dotted lines.

Whether it would be preferable to go with strategy A or B depends on several factors.

- It may depend on which goal one wants to achieve by implementing the selected strategy. Goals potentially achievable by controlling the voltage in a more optimal way include network loss reduction, reduction of end-user energy demand and peak power reduction.
- It depends on the characteristics of the network for which the strategy is to be implemented. It is namely not granted that two different networks respond to a given voltage regime in the same way. Even the same network may respond to a given voltage change in different ways depending on the instance of time in which it takes place. The reason for this is that voltage dependency

of the power and energy consumption as well as losses vary between load types and network components. This will be more closely discussed in part II of this thesis.

The next subchapter presents some VC strategies implemented by DSOs and studied in literature.

## 3.2 VC strategies implemented by DSOs worldwide

A voltage control strategy which has been implemented in networks in the U.S.[23], [24], Canada[25], Ireland and Australia is Conservation Voltage Reduction (CVR)[26]. This strategy works under the assumption that the aggregated load in the system has a positive voltage dependency, i.e. a reduction in the voltage causes a reduction in power demand.

In [26] the voltage reduction techniques utilized by the utilities which have implemented CVR schemes are summarised. Most of the utilities have implemented CVR by using OLTCs in transformers, often in combination with Var-compensation from capacitor banks[27][26]. In most of the cases reviewed in [26], line droop compensation (LDC) is implemented in the OLTC. Some utilities have also adopted CVR as a part of a closed-loop voltage-var control regime utilizing measurements from different locations in the network to determine the best voltage/var control actions during certain time periods.[26] The latter shows greater energy savings and is adaptive to dynamic system changes, at the expense of being more complex and involving higher costs.[26]

According to [26], the range of energy savings achieved in the networks where CVR schemes are implemented ranges from 0.3% to 1% for a voltage reduction of 1%. An evaluation of CVR (including simulations) from 2010 estimated that a full deployment of CVR in the U.S. can give 3% annual energy savings[27].

One can distinguish between short-term CVR and long-term CVR. The objective of the former is to reduce peak demand. This is implemented by lowering the voltage in the time window where the power-reduction is desired. For long-term CVR on the other hand, the voltage is reduced permanently with the objective to save energy. [26] In the literature on CVR reviewed in this thesis, it seems like energy savings is the main concern. Peak power reduction seems to rather be a positive side effect of the implemented energy-saving regime than the primary objective of the implemented schemes.

A different voltage control strategy is demonstrated in field trials in a UK network and is referred to as Voltage-Led Voltage Management.[28], [29] The basic assumption upon which it works is the same as for CVR; namely that the voltage-power relationship is positive. However, the objective and the control philosophy are very different from CVR. As described in [28] “voltage-led LM is a power-focused scheme that provides DNOs with a new source of flexibility to help – for instance– the transmission system operator balancing generation and demand.” As oppose to CVR, which typically reduces the voltage as much as possible to exploit the energy savings potential in the grid, in the voltage-led LM scheme, the voltage is only reduced when it is needed and to the extent it is needed to provide the required service.[28] The implemented duration of the voltage reduction is maximum 60 minutes. Other possible applications of the scheme than providing the TSO with balancing flexibility, include peak load reduction to defer investments in the distribution network. [29]

In the work with this thesis it has not been found examples of CVR or voltage-led LM schemes implemented in Norwegian distribution networks. There has however, been projects in Norway with the goal of assessing how voltage increase can influence networks losses. As part of the project VoltageReg, simulations are run to investigate how voltage influenced the network losses for a grid with high share of thermostatically controlled loads (water heaters and space heaters).[17] From the theoretical and simulation-based study it is found that there could be potential for a 15% loss reductions through a 10%

voltage increase. However, the coincident factor of the studied loads (i.e. the fraction of the total installed power for water heaters and space heater respectively being “active”/”on” at the same time instant) showed to play a prominent role in determining the network losses. It is concluded by the authors that there are significant uncertainties related to the achievable network loss reductions due to lack of knowledge about the actual load and coincident factors in Norwegian distribution networks.

Additionally, measurements performed and analysed by the DSO TrønderEnergi Nett and researcher Nicolai Feilberg, shows results which are interesting in voltage control context. Measurement data from several years of measurements from a power transformer and the downstream distribution transformers in an area called Huseby (close to Trondheim, Norway) has been collected.

Regression analysis on the measurement data indicates that the voltage dependency of the load measured at the primary substation varies through the day, being negative in some hours and positive in others. The negative load-to-voltage relationship coincide with the period of peak power demand in the morning hours. The hypothesis extracted from this result is that controlling the voltage to higher levels in the periods with negative voltage-power relationship and lower levels in the periods with positive voltage-power relationship, could be implemented as a means of load shifting.

### 3.3 Assessment of VC strategies

Different methods can be used to assess how a given VC strategy impacts the network where it has been or shall be implemented. Quantifying the effects of an VC strategy is challenging since there are several other factors than the voltage which influences the power and energy-consumption of loads (e.g. temperature/weather, changes in electricity use over time due to new appliances and demographic changes, changed user behaviour, stochastic user-behaviour, etc.). For CVR, the commonly used methods for estimating the effects are discussed in [26]. Some methods are used to assess the effects of CVR after it has been implemented. The following two methods can be used to assess the VC scheme *before* its implementation:

- a. Synthesis-based method: The overall CVR effects of a circuit is estimated by aggregating the load-to-voltage behaviours of load components or load classes. [26]
- b. Simulation-based method: measured load in a circuit with CVR is compared with load flow simulation results from load flow simulations on a model of the same circuit without CVR. If CVR is not yet implemented in a real network, simulations can be used to compare scenarios with and without CVR. [26]

The two methods can be used to estimate how a VC strategy is likely to impact the considered network. For both methods, knowledge about the load and the network in question is necessary.



## 4 Discussion

In this part of the thesis, the concept of voltage control strategies is introduced, including a brief review of VC strategies implemented by DSOs and how the effect of VC strategies can be assessed. A prerequisite for implementation of a VC strategy is to have VC technologies available in the network. Therefore, an overview over VC technologies penetrating distribution grids is given. Moreover, the VC strategy can only be implemented if the voltage quality at all supply points can still be guaranteed.

The headroom in choice of strategy and in its implementation depends on:

- Available VC resources.
  - A limitation of the tap-changer technologies widely used in distribution networks is that they only offer voltage control in discrete steps. Also, the number of steps is limited, which limits how high or low the secondary voltage of the transformer can potentially be controlled to be.
  - If the set-points in the AVC for the OLTCs can only be manually operated (which is often the case), it is unrealistic to choose a voltage strategy which requires a dynamically changing set-point. It is however possible to choose a lower or higher set-point for the AVC on a general basis. This will involve that the voltage is either always lower or always higher than the “initial choice” of set-point would imply. For strategies where it is desirable to change the set-point according to the load behaviour, more advanced AVCs are necessary.
    - Line Droop Compensation is one way to take into account the loading of the network. The set-point is not changing, but since the voltage being controlled is the end-of-feeder voltage, the controlled end-of-feeder voltage is the same in both high-load and low-load situations.
    - If the load-to-voltage relationship is changing with time and its desired to regulate the voltage to be higher in some periods and lower in others, it must be possible to change set-point dynamically.
- Available margins to the VQ-limits
  - When several feeders are fed from the same transformer, the “worst feeders” determines the headroom for voltage control.
    - Feeders with light load, low losses and/or distributed generation will have the supply points with the highest voltages
    - Feeders with high load, larger losses (weak network) and no distributed generation will have the supply points with the lowest voltages.
  - Feeders with flat voltage profiles are the ones with the greatest potential of keeping the voltage at more optimal levels for most supply points. I.e. feeders with low network impedance or local voltage controllers located along the feeder.
- Level of detailed knowledge about the voltage and load situation in the grid
  - Keeping voltages closer to the VQ-limits requires monitoring of voltage at strategic places in the network to make sure the VQ-requirements are not sacrificed for the purpose of some VC strategy goal.
  - The roll-out of smart meters increase the observability of the network and can contribute to giving the DSOs valuable information about the actual conditions in the network.
  - Additional real-time monitoring with higher time resolutions than available from the smart meters is required if it is desired to operate the grid with small voltage margins.

The traditional approach to solving voltage quality problems is grid reinforcements. Estimations from [6] shows that voltage control can be more cost-efficient than grid reinforcements in certain cases. If DSOs to a larger extent implement different types of voltage controls in the grid, the relevance of investigating the effects of VC strategies increase. Moreover, the trend towards deploying more real-time monitoring, using state estimation and more detailed load and generation predictions and modelling will increase the DSO's knowledge overview of available margins and real-time situation in the grid and thereby give increased opportunities for VC strategy implementation.

The VC strategies reviewed in the thesis which are implemented by DSOs in other countries exploit the positive load-to-voltage dependency of the loads in their networks. What seems to be the main concern where CVR is implemented is energy savings (the net effect of less demand from connected loads + reduction/increase of losses). However, since electricity prices in Norway are generally lower than in other countries and by the fact that the electricity production in Norway is almost 100% renewable, the motivation to save energy to reduce costs and CO<sub>2</sub>-emissions may be lower here than in the reviewed cases of CVR.

Peak demand on the other hand, is a hot topic in the Norwegian energy business. EVs, electric ferries and other power demanding appliances are penetrating the grids<sup>3</sup>. According to [5] (from 2016), the Norwegian power demand has increased more rapidly than the energy demand during the last years. Reinvestments of grid components are often driven by peak demand (thermal limits of components and voltage drops along feeders). VC strategies with the objective of reducing peak demand may therefore be more relevant than energy-conservation regimes in a Norwegian context.

The effect of a given VC scheme depends on the network and the voltage-dependency of the loads connected to the network. Knowledge about the load composition in the network and the loads dependency of voltage is therefore crucial for assessing different voltage control strategies before their implementation.

---

<sup>3</sup> Statistics showing the increase of registered EVs and plug-in hybrid vehicles (PEHVs) in Norway since 2010: <https://elbil.no/elbilstatistikk/>

## Part II - Voltage-dependency of individual loads and network losses

### 5 Introduction

As an electrical power engineer, one may be used to seeing a load as an arrow in a one-line diagram. Behind the arrow there is often tens, hundreds, thousands or even millions of individual appliances. An electrical load can be a water kettle or a washing machine, a cold storage at a fish landing facility or grocery store, an electric vehicle (EV) charging at  $7\text{kW}^4$  or an electric ferry charging at  $7\text{MW}^5$ . The figure below illustrates the diversity of appliances hidden behind the supply point of a household.

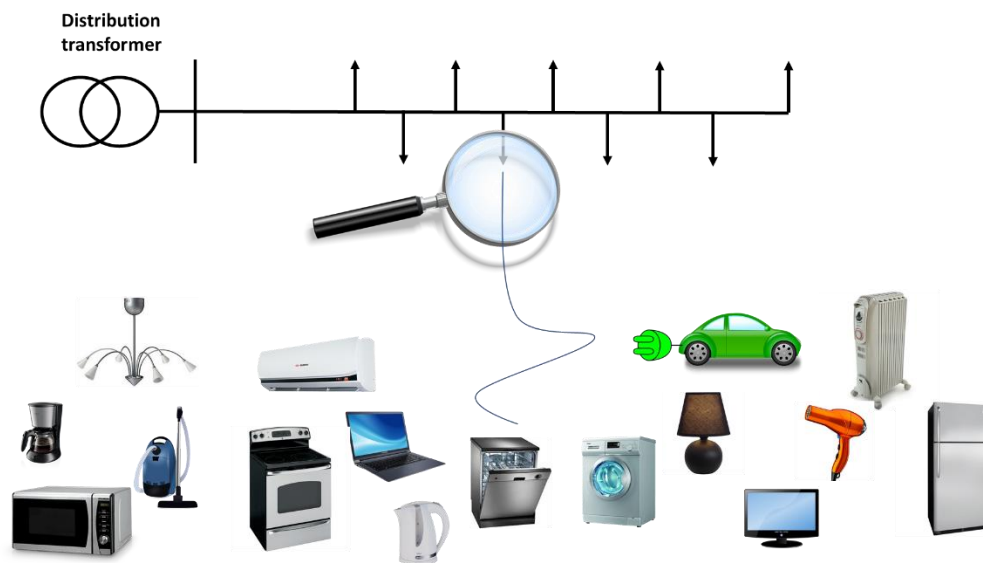


Figure 5-1: Illustration of a radial LV-feeder and some of the electrical appliances that might be found behind a supply point for a residential customer.

Each individual load has electrical characteristics including the load's active and reactive power demand. The power demand may depend on:

- The voltage applied to the load
- The frequency of the voltage applied to the load
- Controllers internally in the load, e.g.:
  - a thermostatic control measuring the temperature of the water in the water kettle and turning the power off when the water is boiling
  - power electronic controllers in the EV charger responsible of controlling the charging cycle, for instance with the objective to increase the EV battery lifetime.

Each of the individual loads' electrical characteristics are determined from of which components they are build, how these components are connected as well as from the internal controllers.

---

<sup>4</sup> Home-charging for EVs in 230V-networks (<https://elbil.no/lade-med-hjemmeladeboks/>)

<sup>5</sup> Ferry coming in 2021, Molde-Horten (Norway): <https://industriinorge.no/samferdsel/rekordrask-lading-pa-norges-viktigste-fergestrekning/>

Since power system operation and planning relies heavily on modelling and simulations, it is necessary to model the electrical loads and their electrical characteristics. In [10] the goal of load modelling is described as “developing simple mathematical models to approximate load behaviours.”. A load model should be able to give a realistic picture of the real loads while at the same time being simple enough to be practical in the applications for which it shall be used. This is not a trivial task due to the diversity of loads and the stochastic behaviour of the utilization of the loads:

- For each type of electrical appliance there exist many suppliers and different models, which all may have different electrical characteristics
  - Miele and Bosch probably do not build their washing machines the exact same way. Moreover, washing machines sold in 2003 do not have the same features as those sold in 2019.
  - Many appliances also have numerous options for the user to choose from (e.g. to wash the clothes at 40 or 60 °C, with extra rinse or without centrifuging).
- Since one electrical appliance’s working cycle may involve different tasks demanding utilization of different components, the electrical characteristics for the same appliance can vary throughout the working cycle. E.g. a drying cycle of a clothes dryer often alternates between two modes of operation: heating of the air and rotation of the drum to move the laundry.
- User behaviour, weather conditions, seasonal changes and changes in the “load stock” over time causes the load composition (i.e. how much of which type of load being used at a certain time instant) to change with time.

Traditionally, load modelling has not been the top priority in power system industry and academia. Modelling of generators and the transmission and distribution equipment has been given more attention[3]. In the 1980s major blackouts caused by voltage collapse[30, p. 64], followed by failing attempts to simulate the events in the current power system models, resulted in increased attention on load modelling. In the 1990s the IEEE Task Force on Load Representation for Dynamic Performance reviewed the load modelling practice and gave recommendations on load model development and use[3], [4], [10] Due to renewed interest in load modelling amongst others due to the increasing penetration of DGs and power-electronic interfaced loads, Cigré established a working group “C4.605: Modelling and Aggregation of loads in flexible power networks in 2010. Their findings and recommendations on load modelling are summarised in the report [4].

For the purpose of assessing voltage control strategies, it is crucial to investigate how the active and reactive power consumed by loads in the power system depend on the applied voltage. One way to assess this, is to develop load models for the network area for which a voltage control strategy should be implemented and use the model in load flow analysis for different scenarios to investigate how different strategies impact the system losses, peak power demand and energy demand of the loads.

This chapter will introduce different load models used in the power system industry and academia today. Two commonly used load models are the ZIP model and the exponential models. These models are used in the thesis for modelling the voltage dependency of the electrical household appliances that are tested in the lab. Therefore, these two models will be described in detail.

Load models can be used both for describing the characteristics of individual loads (e.g. a specific washing machine) or a group of loads (e.g. the sum of all the individual loads connected to a busbar). One approach to find aggregate load models is referred to as the component-based approach, which is a bottom-up approach. The bottom layer is knowledge of individual load component’s load characteristics. For instance, how a washing machine’s power consumption depends on the applied voltage. The

next step for finding the aggregate load model, is knowledge about the composition of different load components, i.e. how large fraction the washing machine or the heat pump constitute of the total load.

The aggregation of loads will be discussed in closed detail in part III of this thesis. In part II, we will concentrate on the load characteristics of the individual loads. The outline of part II of the thesis is as follows:

In chapter 6, load modelling will first be addressed in general terms before looking more deeply into the two load models in focus in this thesis: the ZIP model and the exponential model.

Since network losses depend on voltage and the network loading, for assessment of VC strategies it is also important to take into account how a VC scheme affects the losses in the system. It might even be a goal of the VC strategy to reduce losses. Therefore, network losses is addressed in a designated chapter (ch.7) to give an overview over how voltage and loading may impact the losses.

In chapter 8, the lab work conducted in this thesis is presented. Five household appliances are tested to investigate their voltage dependency. Through data analysis of the measurement data model parameters for the ZIP- and exponential models are found to model the devices' voltage dependencies. The methodology used in the lab work is explained and the results obtained from the tests is presented.

Chapter 0 concludes this part of the thesis and discuss some findings from the laboratory tests.

## 6 Load modelling

«The goal of load modelling is to develop simple mathematical models to approximate load behaviours.» [10]. Real loads have several characteristics that can potentially be captured in a model. One such characteristic is how the load responds to a rapid change in voltage or frequency. Another is the loads' "steady-state"-dependency on voltage and frequency. Different models may capture these characteristics in different ways (or not at all). The preferred choice of model both depend on which types of loads that is to be modelled and for which application the model is to be used.

There exist many different load models which are used in academia, industry and adopted in open-source and commercial software. One often distinguishes between static and dynamic models. In both groups there exist several models. The figure below is taken from the Cigré WG C4.605 report on load modelling and shows a classification of different load models divided into static and dynamic models.

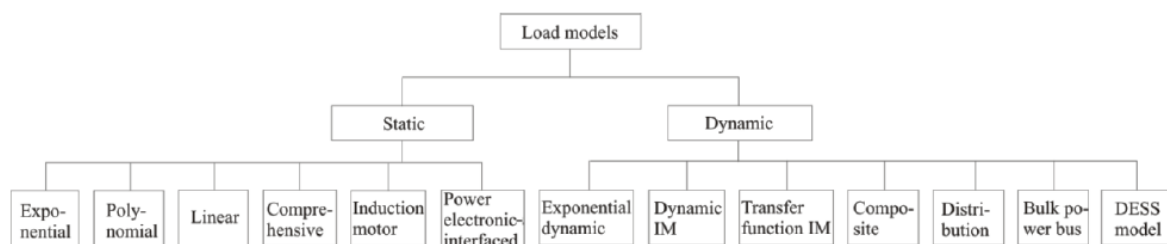


Figure 6-1: Diagram with different load models categorised as static and dynamic models. From [4]

Static models are mostly used for power flow analysis and voltage stability studies. They are normally used for representing aggregate loads that lack participation of large induction motors and electrical drives in the overall load mix[4]. For load mixed with significant contributions of large induction motors and electrical drives, the dynamic load models are the most widely used. [4]

A survey carried out by the same work group[31] revealed that for steady-state analysis, more than 80% of the surveyed utilities used constant power-model and none of the models included in the representation in the above figure. Amongst the European utilities surveyed, the share sticking to the constant-power model is 89%. "The constant power model" models the load as constant power load. I.e. it assumes that the active and reactive power drawn by the connected load is independent of voltage and frequency. The remaining 11% of the respondents uses the polynomial model (ZIP model). The survey also revealed that static models are the most widely used, both for steady-state and dynamic power system studies.

For the purpose of assessing voltage control strategies, the loads' steady-state dependency on voltage is the main concern. Maintaining the frequency is the responsibility of the TSO. From the DSO perspective, the frequency is a parameter which cannot be controlled. Therefore, the frequency-dependency of loads are not further discussed in this thesis. The load models chosen in the thesis are independent of frequency.

The load models addressed in this thesis are the ZIP and exponential models. The ZIP model is a variant of the load model referred to as "Polynomial model" in the above figure. The selected models will be presented in subsequent subchapters. The lab work conducted in the thesis are aimed at finding the voltage dependency of the tested loads. Based on the lab tests, the measured data is used to fit the behaviour of the tested devices into these two load models.

Both the ZIP and exponential models represent loads as a function of the voltage. According to the survey on industry practice for load modelling[31], they are used for both steady-state and dynamic analysis. An advantage of the two models is that they model the voltage dependency of loads in an intuitive way with a physical meaning. The models are simple and can be applied both to individual load components and to aggregated loads. Although they do not model dynamic loads accurately (e.g. induction motors), the models can be combined with dynamic models to form so-called *composite load models*. [10] By combining the ZIP or exponential model with for instance induction motor model, more accuracy can be added to models used for dynamic studies.

## 6.1 ZIP model

The ZIP model represents the active and reactive power load as functions of the applied voltage as a second-degree polynomial and is also referred to as a “Polynomial model”. The expressions for the active and reactive power loads ( $P_l$  and  $Q_l$ ) are shown in the equations below. The name “ZIP” comes from the fact that this model represents the load as a combination of a constant impedance (Z), a constant current (I) and a constant power load (P).

$$P_l = P_n \left( Z_p \left( \frac{V_l}{V_n} \right)^2 + I_p \frac{V_l}{V_n} + P_p \right)$$

where

$$Z_p + I_p + P_p = 1$$

$$Q_l = Q_n \left( Z_q \left( \frac{V_l}{V_n} \right)^2 + I_q \frac{V_l}{V_n} + P_q \right)$$

where

$$Z_q + I_q + P_q = 1$$

$V_l$ = voltage applied to the load

$P_l$  and  $Q_l$ : active and reactive power drawn by the load when the voltage  $V_l$  is applied to it

$V_n$  = nominal voltage

$P_n$  and  $Q_n$ : active and reactive power drawn by the load at nominal voltage  $V_n$

$Z_p, I_p, P_p$  = ZIP-coefficients for active power

$Z_q, I_q, P_q$ =ZIP-coefficients for reactive power

The coefficients are constrained to sum up to one. The coefficients represent the fractions of the total load which comprises constant power, constant current and constant power respectively. Two variants of the ZIP model are being used:

- The constrained ZIP model
  - An additional constraint is applied to the model, namely that each coefficient must have a value in the interval 0-1. When this constraint is applied it is easy to compare ZIP model parameters of different loads, since the coefficients represent the “percentage” of the load being constant power, constant current and constant impedance. E.g. If the coefficients are  $Z=0.4$ ,  $I=0.4$  and  $P=0.2$ , 40% of the load exhibits constant impedance and constant current characteristics respectively, and 20% exhibit constant power characteristics.
- The accurate ZIP model

- The additional constraint is not applied. Thus, the coefficients are allowed to be greater than one or negative. Since this model introduces less constraints in the modelling procedure, the model tends to represent the real load behaviour more accurately. However, model coefficients for different loads cannot be compared as intuitively as for the constrained model. Due to the higher accuracy, this model is chosen for the lab tests in this thesis.

If  $Z=1$  and the other parameters are 0, the load is a pure constant power load. Similarly, if  $I=1$  and the other coefficients are 0, the load is a pure constant current load.  $P=1, I=Z=0$  represents a constant power load.

The ZIP model is used by the Nordic TSOs in power system network planning for representation of the voltage dependency of loads. An additional factor is added to the ZIP model to account for the load's frequency-dependency (this methodology is frequently used and addressed in [4], [9, p. 273], [10]). In this thesis, frequency dependency of loads is not regarded.

## 6.2 Exponential model

The exponential load model formulation is shown in the below equations, for active and reactive power respectively. Pure constant impedance loads are modelled with exponent  $n=2$ , constant current loads with  $n=1$  and constant power loads with  $n=0$ .

Loads that are not pure constant impedance, constant current or constant power are modelled with exponents that lie somewhere in between 0 and 2, or even outside this interval.[3] In this thesis, the exponents are not constrained to be within the interval 0-2 and are therefore in some cases negative or greater than 2.

$$P_l = P_n \left( \frac{V_l}{V_n} \right)^{n_p}$$

$$Q_l = Q_n \left( \frac{V_l}{V_n} \right)^{n_q}$$

$V_l$  = voltage applied to the load

$P_l$  and  $Q_l$ : active and reactive power drawn by the load when the voltage  $V_l$  is applied to it

$V_n$  = nominal voltage

$P_n$  and  $Q_n$ : active and reactive power drawn by the load at nominal voltage  $V_n$

$n_p, n_q$  = exponents for active and reactive power



## 7 Network components - losses in lines, cables and transformers

Network losses can be divided into two groups: variable and no-load losses. The no-load losses (also referred to as fixed losses) do not vary with the loading of the network (i.e. the current flowing through the network components). They are present as long as the components are electrically energized. The variable losses vary with the loading (i.e. the current). [34], [35]

Both lines, cables and transformers cause variable and no-load losses. In the following subchapters a brief introduction to the fixed and variable losses is given.

In 2016, the energy demand in Norway is 133TWh, of which ca 80 TWh is delivered through the local distribution system (MV and LV networks). The same year, the distribution losses accounted for 4.1 TWh. [36]

From the voltage control strategy point of view, it is important to look at how the losses are influenced by the voltage scheme.

### 7.1 No-load losses

No-load losses or fixed losses is energy dissipated by network component as a result of being connected to the network and being energized[35]. Hence, these losses are present at all times when a voltage is applied to the network components, independently of the loading. In general, about one quarter to one third of the network losses are no-load losses.[34] The majority of the no-load losses are caused by transformers[35].

99% of the no-load losses in transformers takes place in the core is a combination of hysteresis and eddy-current losses[37]. These are often referred to as core-losses or iron-losses. Other no-load losses present in power systems include different types of dielectric losses. In high voltage networks, corona partial discharges cause losses. In underground cables, dielectric losses in the insulation is a source of no-load losses. [35]

The no-load losses are dependent on voltage, but is regarded as being “fixed” since the voltage variations in the network in general are relatively small[35]. However, according to [26], CVR schemes (i.e. voltage reduction) can reduce the transformer core losses.

### 7.2 Variable losses

The variable losses depend on the loading of the system. For both lines and transformers, the main cause of variable losses is the joule heating caused by the current flowing in conductors (i.e. in transformer windings and line/cable conductors). The joule heating is referred to as  $I^2R$ -losses or ohmic losses and has the following form for a three-phase system:

$$P_{loss} = 3I^2R$$

$I$ = single-phase current

$R$ = Resistance of each phase conductor

The conductor resistance is a function of the wire diameter, the conductor material's resistivity, the length of the conductor as well as conductor temperature. The resistance increases with increasing conductor temperature. Thus, the losses are higher in high-load situations than low-load situations both due to the larger current and higher resistance.

From a voltage control perspective, variable losses can be reduced by reducing current flowing through the network components. Depending on the type of load present in the network, this could involve either increasing or reducing the voltage. Constant-power loads draw more current when the applied voltage is reduced, constant impedance loads draw less current when voltage is reduced, while constant current loads draw the same current independently of the voltage. Since both active and reactive power flows contribute to the current flowing in the network, the voltage response of both active and reactive power load influences the variable losses.

## 8 Lab test: Voltage dependency of individual loads

This chapter presents results from measurements performed in the Smart Grid Laboratory at NTNU. The voltage dependency of the following household appliances is tested:

- Induction cooktop
- Electric space heater
- Heat pump
- Washing machine
- Clothes dryer (tumble dryer featuring heat pump technology)

For all the tested devices, load model coefficients for the ZIP- and exponential load models were estimated using curve fitting techniques.

The first subchapters present the objective of the tests and the methodology followed. The equipment and test-setup are described in a designated subchapter. Subsequently, the principle and methodology of the curve fitting is explained.

In chapter 8.5 each of the tested devices are discussed in separate subchapters. For each device, some background information about the type of device is given, followed by an explanation of how the tests for the respective device is performed. The results from the tests are presented and discussed.

### 8.1 Objective

The goal of the tests is to find the voltage dependency of household appliances. Knowledge about the loads' voltage dependencies and load profiles is useful when assessing the impact of different voltage control strategies in the network. In addition, load modelling is highly relevant for other power system engineering applications. Hence, the results from these tests can both benefit the further work with assessing voltage strategies as well as being a contribution to the work with improving load models for other applications.

### 8.2 Approach

The lab tests and data analysis contain two basic steps:

1. Apply different voltages to the device under test (DUT) and measure active and reactive power
2. Estimate the load model coefficients for the DUT based on the measurement data by utilisation of curve fitting techniques

Some of the tested devices have changing electrical characteristics throughout the cycle. They also offer several settings for the user to choose from (e.g. washing at 40°C or 60°C). For these devices two types of tests are performed:

1. Tests of different settings to capture the diversity in load behaviour depending on the user-defined setting. For these tests, nominal voltage (230V) is applied.
2. Tests of the same setting when different voltages are applied to capture the voltage dependency of the load. For these tests, voltages in the +/-10% voltage band from the VQ standard (FoL[12]) is applied. I.e. voltages in the range 207-253V. For most devices, voltages of 210, 220, 230, 240 and 250V is used.

The measured parameters in the tests are current and voltage. Based on the measurements, the measurement device calculates other power system parameters. The measurement device logs the parameters for a user-defined and logs those for each time step.

The time interval chosen for logging is 0.25 seconds, which is the most fine-grained time interval available for the measurement device. For each time interval, both the minimum, maximum and average value for the time interval for each parameter is logged. From inspecting the data sets it is found that there is small (normally no) difference between the min, max and average values. In the curve fitting, average values of several time intervals are used. Therefore, the average values are used in plotting and curve fitting in the thesis

### 8.3 Equipment and test setup

This chapter describes the equipment used during the tests together with explanation on how the equipment is connected and used. Details about the test equipment is included in appendix A.

The tests are performed in the National Smart Grid Laboratory[38] at NTNU. As part of the laboratory, there is an apartment, referred to as the “Smart House”, equipped with state-of-the-art electrical household appliances. All tests are performed inside the Smart House.

One household electrical appliance is tested at the time. The three main components in each test setup are:

- A programmable Power Supply (ITECH 7626). This serves as the adjustable voltage supplying unit of the test setup. Hereafter referred to as the Power Supply.
- A power analyser (Fluke 438-II), used to measure current and voltage and log relevant parameters. Hereafter referred to as the Power Analyser.
- The household appliance to be tested. Hereafter referred to as the Device Under Test (DUT).

The below figure illustrates the test setup.

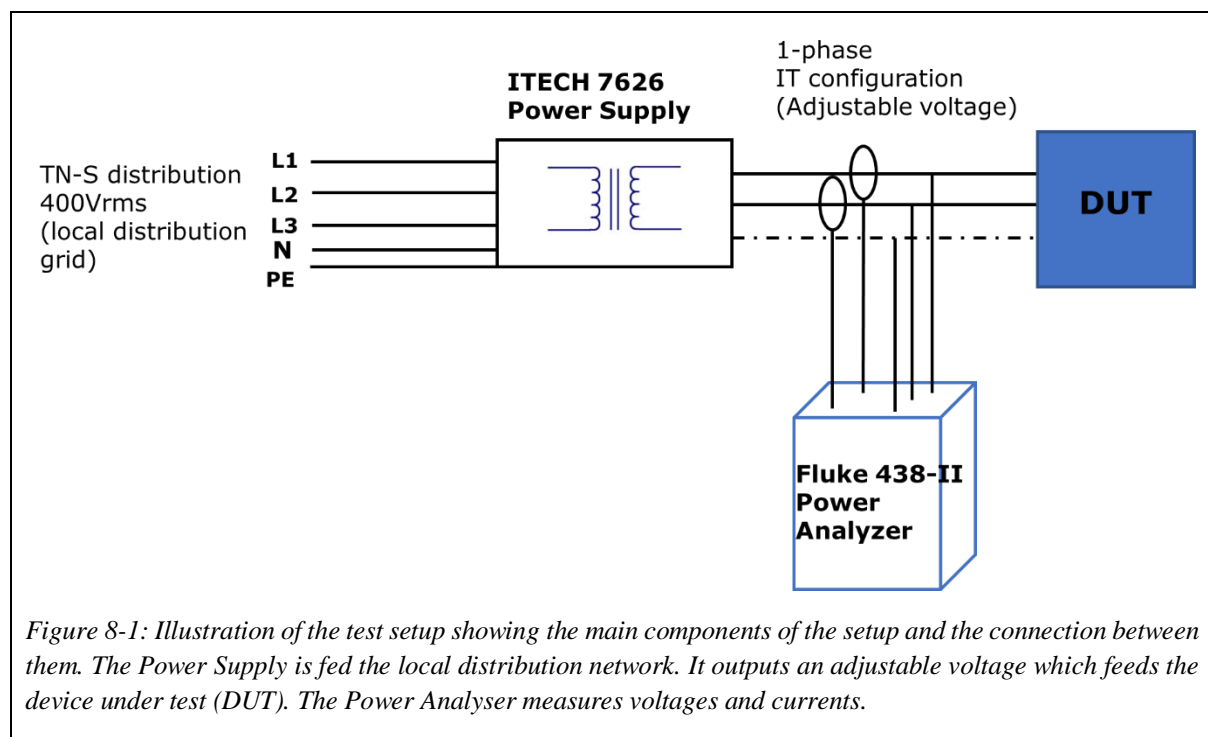


Figure 8-1: Illustration of the test setup showing the main components of the setup and the connection between them. The Power Supply is fed the local distribution network. It outputs an adjustable voltage which feeds the device under test (DUT). The Power Analyser measures voltages and currents.

The Power Supply takes a 3ph 400V voltage as input and can output 1ph power with voltages ranging from 0 to 300Vrms. Both waveform, frequency and RMS-voltage are adjustable. The voltage output from the Power Supply is manually controlled during the tests to give the desired output voltage. 50 Hz sinewave is selected in all tests, while the RMS-voltage is adjusted to the desired level for each test.

The DUT is connected to the Power Supply via an extension cable which is plugged into one of the CEE 7/3 sockets on the Power Supply front panel. The overcurrent limit of these sockets is 10A. Consequently, this setup is limited to testing of electrical appliances drawing currents of maximum 10A.

The Power Analyser measures current and voltage and calculates other relevant parameters (active and reactive power, THD, etc) based on these measurements. It can log a user-defined set of parameters over a time period and store the data internally in an SD card. Later, the time series can be downloaded from the Power Analyser's SD card to a computer.

The Power Analyser can be used for 1ph and 3ph test setups with different configurations. The preferred Power Analyser configuration for the test setup in this thesis would be the 1ph IT configuration showed in Figure 8-3. The reason for this is that the secondary side of the Power Supply is not grounded, and its power output therefore corresponds to an IT network configuration. However, during the testing of the test setup it was discovered that the Fluke Power Analyser firmware V05.07 has a bug in the IT configuration. Therefore, the TN configuration showed in Figure 8-2 is used instead.

Consequently, the Power Analyser configuration does not comply with the real configuration of the setup. This leads to some unmeaningful data in the acquired measurement time series. For the data analysis performed in the thesis, this does not cause problems. It is however important that if the data is used for future research within other projects, the users of the data are aware of which data is and is not meaningful. Some further explanation regarding this is provided in appendix A.1.1.

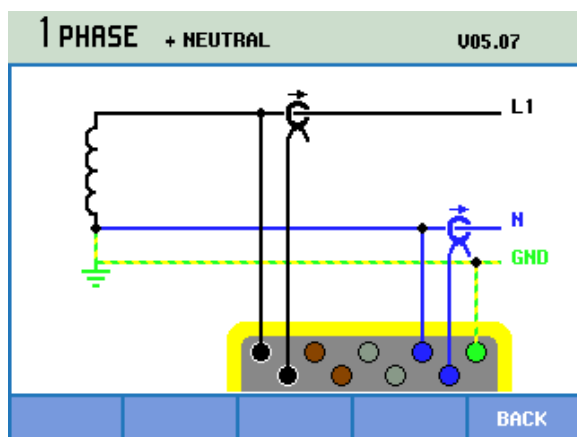


Figure 8-2: Power Analyser configuration 1ph with neutral (TN)

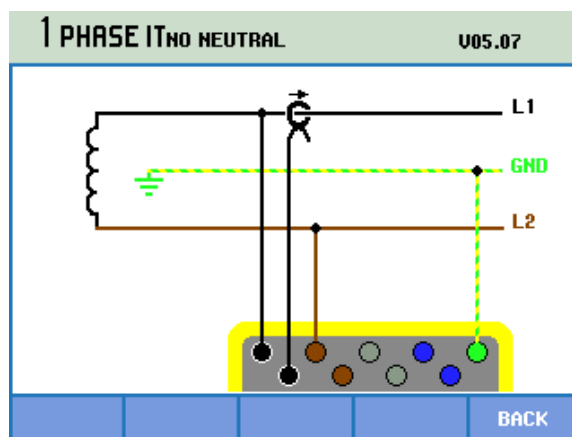


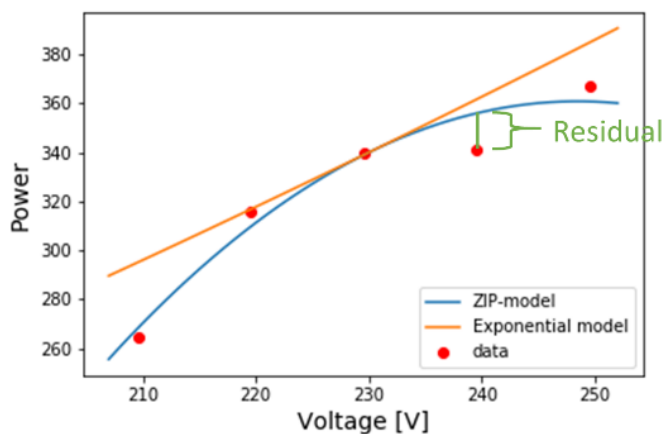
Figure 8-3: Power Analyser configuration 1ph without neutral (IT)

## 8.4 Curve fitting - Finding load model parameters from measurement data

After having performed the tests in the lab, the acquired measurement data must be analysed to find the model coefficients for the relevant models. The models chosen in this thesis is the ZIP model and exponential model presented in chapter 6.1 and 6.2. For each tested appliance the load model parameters are found using least squares minimization as implemented in Python LMFIT package[39].

The basic idea of least squares minimization is to find the curve for which the residuals between the curve and the data points to be fitted are minimized. The below figure shows an example of a curve fit performed in this thesis. The red dots are the data points for which load model parameters should be found in this case. The blue and orange curves show the fitted ZIP model curve and the exponential model curve respectively. In the figure, the “residual” between one of the datapoints and the fitted ZIP model curve is shown. In the curve fit, the sum of the square of all residuals is minimized.

The minimization problem is solved by an iterative method (Levenberg-Marquardt method). The method requires a set of initial guesses for the parameters to be optimized. It runs several iterations with small changes in the parameter values until the set of parameters is found for which the objective function is minimized. The objective function in the least squares problem is the one shown in equation 1.



$$\text{Minimize} \left[ \sum_i^N [\text{Residual}_i]^2 \right] \quad (1)$$

N= number of datapoints  
i = the i-th datapoint  
Residual = the distance between the data point i and the curve to be fitted

Figure 8-4: Curve fit example. The data points are plotted together with the fitted ZIP model and exponential model curves. The residual between one datapoint and the ZIP model curve is shown.

Recall the ZIP and exponential models from chapter 0. For the ZIP model, the coefficients to be optimized in the least squares minimisation are  $Z_p$ ,  $I_p$  and  $P_p$  for the active power model. The other parameters in the model are  $V_n$  (the nominal voltage) and  $P_n$  (the nominal active power). The nominal voltage and power should be fixed parameters given as input in the minimization problem and not be changed in the minimization.

Further details regarding the curve fitting procedure is included in appendix B.

A challenge in finding the load model parameters is to choose meaningful datasets to use in the curve fitting algorithm. The scope of the thesis is to find load model parameters reflecting the steady-state behaviour of the tested loads. Therefore, the load behaviour for instance in the beginning of the load cycle that seems to be atypical compared to the rest of the cycle is excluded from the datasets.

For the washing machine and the induction cooktop, the load behaviour is found to be changing throughout the cycle. In these cases, one has to make a decision on which part of the cycle the load model should reflect. It could be possible to find load model parameters which reflects the “average behaviour” of the load throughout the cycle. Alternatively, one can split the load cycle into different parts with similar behaviour and find the load model parameters for each of the parts individually. The preferred approach may depend on the application of the model. Therefore, in some cases, both approaches are used to provide future users of the results with the choice to use the results fitting his application.

## 8.5 Results and discussion

This chapter is divided into subchapters for each tested device. For each device, the following points are presented:

1. Working principle and background information about the type of device
2. Results from the laboratory tests and curve fitting
3. Observations from the results and comparison with results from literature.

### 8.5.1 Induction cooktop

#### 8.5.1.1 Working principle and deployment

Induction cooktops have experienced an increasing popularity and deployment during the last decades. According to a Norwegian consumer magazine article from 2010<sup>6</sup>, around 50% of households were using this type of cooking device at that time.

For an induction cooktop, heat is produced directly in the cooking pot by joule heating caused by eddy currents circulating in the cooking pot. One of the main components of the cooktop is a planar coil located underneath the cooktop surface. This coil is fed with an alternating current of high frequency (20kHz-100kHz[40], [41]). The alternating current induces an alternating magnetic field which passes through the metallic cooking pot. The magnetic field give rise to eddy currents flowing in the metal. Due to the resistivity of the vessel, the eddy currents heat the vessel through joule heating ( $I^2R$ ). [40], [41]

A schematic representation of an induction cooktop is shown in the figure below. It shows the three main components: A converter converting the 50Hz AC to a DC current, an inverter responsible of turning the DC into an AC of the desired frequency, and finally the coil where the magnetic field is induced from the alternating current.

---

<sup>6</sup> <https://www.dinside.no/bolig/snart-har-halvparten-av-oss-induksjon/61739067>

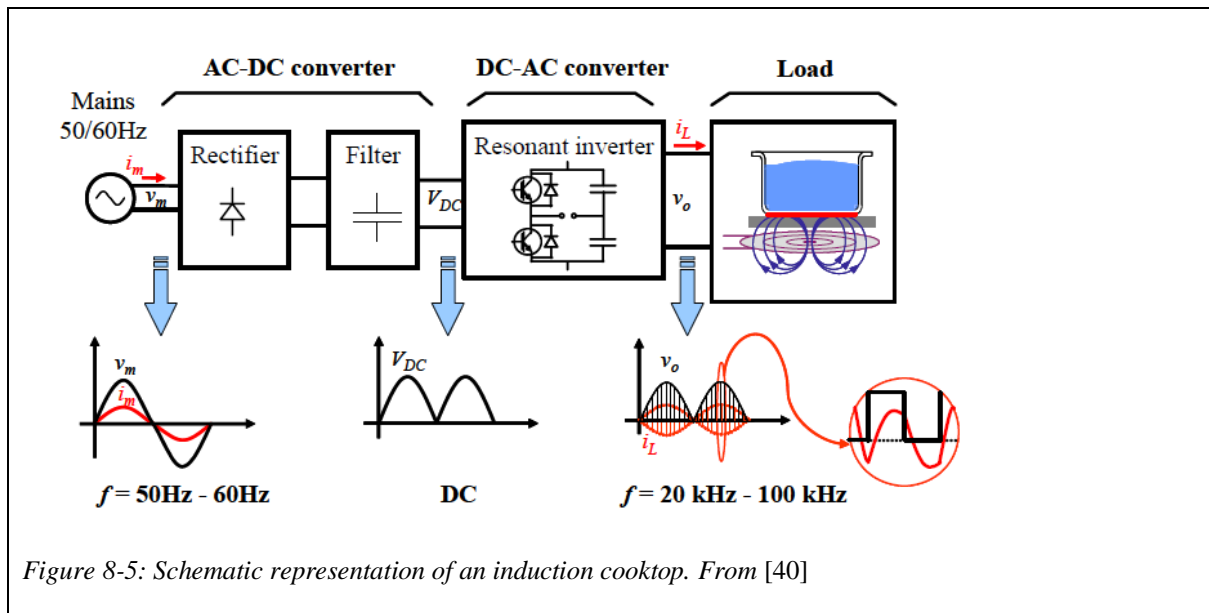


Figure 8-5: Schematic representation of an induction cooktop. From [40]

According to [40], induction cooktops available for domestic use delivers powers up to 5.5 kW. Different inverter technologies and control methods are presented which are being researched and used in commercially available cooktops. One interesting feature being discussed in the reference is different approaches to allow for different power outputs. One way of achieving this is to implement controls that switches the inverter on and off with given time intervals to achieve an average power output corresponding to the desired power output. Other technologies implement power output control by controlling the frequency of the AC output from the inverter.

### 8.5.1.2 Test details

The induction cooktop tested in this thesis is a standalone induction cooker. According to information from a vendor [42], the cooktop offers 17 different settings including the possibility to choose power output or target temperature. In the lab tests the following settings are tested:

- Settings tested with different applied voltages:
  - 1600W
  - 800W
  - 300W
  - Max Power
- Additional settings tested to obtain more information on how the load profile is for different user-defined settings. These are only tested at 230V.
  - 500W
  - 1100W

All tests are performed with the same pan filled with 1 litre of water. The initial temperature of the water is measured before starting each test. To ensure similar starting conditions for each test, the cooktop is cooled down to room temperature between each test. For most of the test, the cooktop is left on until the water temperature reaches approximately 100°C. Further details are provided in appendix C.1.



### 8.5.1.3 Results

Figure 8-6 shows the active power for each of the tested settings. In Table 8-1 the average values for active and reactive power, true power factor as well as THD for current and voltage is listed for the different settings.

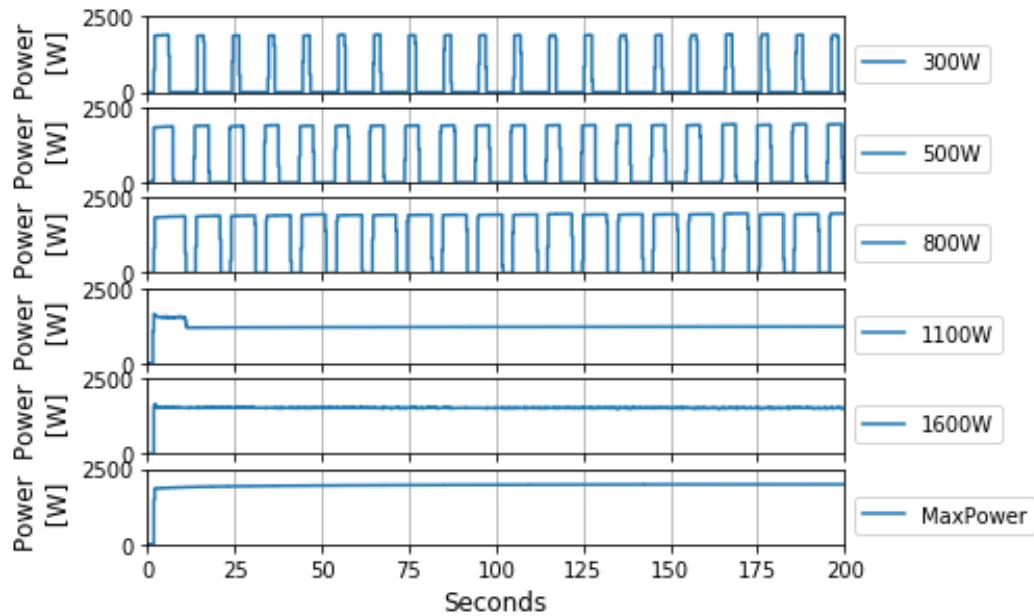


Figure 8-6: Induction cooktop load curves. Active power for different user-defined settings. All tests are performed with 230V test voltage.

	<b>P [W]</b>	<b>Q [VAR]</b>
<b>300W</b>	372	-125
<b>500W</b>	764	-168
<b>800W</b>	1339	-229
<b>1100W</b>	1205	-268
<b>1600W</b>	1522	-278
<b>MaxPower</b>	1965	-292

Table 8-1: Induction cooktop. Average active and reactive power for different user-defined settings (time step 50-800, i.e. excluding the start-up behaviour)

Three types of load curve characteristics depending on the user-defined setting can be observed:

- For low power settings, the load has a “on -and off”-behaviour, alternating between intervals of peak active power and intervals with close-to-zero active power. The time-intervals for the on-state is controlled such that the average power corresponds to the chosen power setting (Table 8-1 shows that the average power values does not correspond as well to the chosen setting in all cases. See 800W setting). The power drawn in the on-state is close to independent of the chosen setting (i.e. is the same for 300, 500 and 800 W settings).
- For higher power settings, the active power drawn is more constant (although varying in a range approximately 50W around what seems to be the “target power”).
- There seems to also exist a “Max-power” mode of the cooktop. In this mode, the active power is increasing for the one-two first minutes. The rate-of-change of the active power decelerates with time.

The four figures below show the active and reactive power for the settings for which voltage tests are conducted. The 300W and 800W in “on-state” as well as the MaxPower setting exhibit close to constant-impedance characteristics for the active power, while the 1600W has a close to constant-power characteristic. Table 8-2 contain the load model parameters. For the 300W and 800W settings, two sets of load model coefficients are included, namely for "on-state" and “off-state”. The durations of the on- and off-states are shown in Table 8-3.

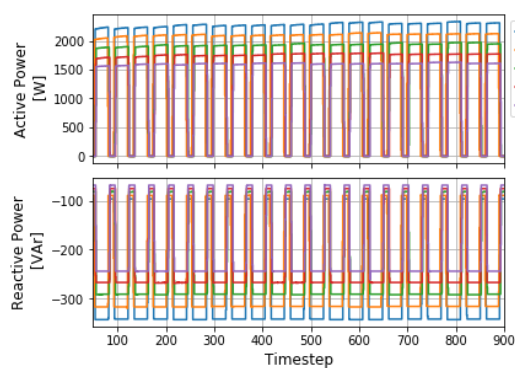


Figure 8-7: Induction cooktop, 800W setting.

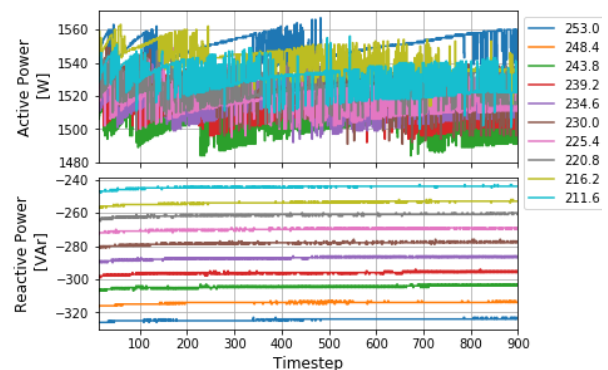


Figure 8-8: Induction cooktop, 1600W setting

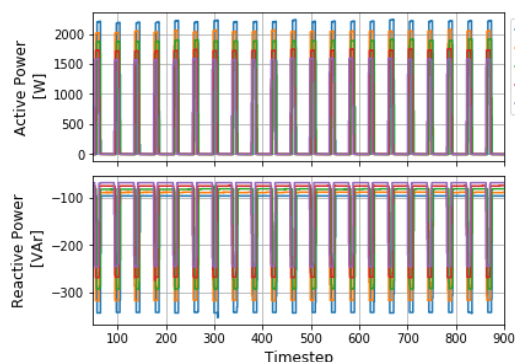


Figure 8-9: Induction cooktop, 300W setting

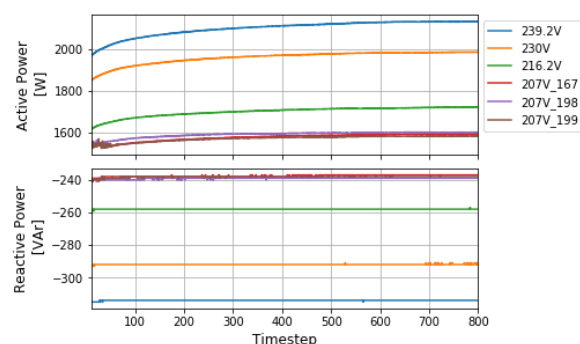


Figure 8-10: Induction cooktop, MaxPower setting. Three different tests at 207V are shown (\_xxx are the measurements-numbers of the respective tests)

	$P_n$ [W]	$Q_n$ [VAR]	$Z_P$	$I_P$	$P_P$	$Z_Q$	$I_Q$	$P_Q$	np	nq
<b>1600W</b>	1519	-280	1.52	-3.07	2.55	1.03	-0.51	0.48	-0.01	1.56
<b>300W (on)</b>	1902	-296	0.74	0.44	-0.18	0.68	0.57	-0.25	1.92	1.92
<b>300W (off)</b>	-6	-82	-6.17	14.9	-7.75	0.20	1.54	-0.75	2.51	1.95
<b>800W (on)</b>	1952	-295	0.91	0.21	-0.12	0.66	0.61	-0.27	2.04	1.94
<b>800W (off)</b>	-5	-82	5.68	-8.15	3.47	0.32	1.33	-0.65	3.23	1.96
<b>MaxPower</b>	1971	-295	1.03	-0.03	0.00	0.84	0.25	-0.08	2.04	1.93

Table 8-2: Induction cooktop load model coefficients for ZIP and exponential load models. Model parameters are listed for different user-defined settings. For the 300W and 800W settings, two sets of load model coefficients are included, namely for "on-state" and "off-state", i.e. when the active power demand is peaking and close-to-zero respectively.

Setting	On-state [seconds]	Off-state [seconds]
<b>300W</b>	2	8
<b>800W</b>	7	3

Table 8-3: Durations of the on- and off-states for the 300W and 800W- settings for the induction cooktop

Further details about the curve fits performed for the respective voltage tests can be found in appendix D.1.

## 8.5.2 Electric space heater (resistance heater)

### 8.5.2.1 Working principle and deployment

Space heating is the end use in the residential load sector responsible for the highest share of the electricity consumption[43]. According to [44], 96% of households have electric space heating as only heating source or in combination with other sources. Resistance heaters (used by 82% of households) and floor heating (72% of households) are the most widely used electric heating sources. Air-to-air heat pump is an increasingly used heating technology (24% of households had one/more heat pumps in 2012).

Resistance heaters exploit the principle of joule heating to transfer electrical power to heat. Some types are also equipped with fans to increase the circulation of air surrounding the heater. Thermostatic controls are often implemented to be able to control the temperature in the room to a user-specified target

temperature. To keep the temperature close to the target temperature, the heating elements are turned on and off to adjust the heating output to the measured temperature of the air.

### 8.5.2.2 Test details

The tested space heater has three modes of operation- full power, half power, and off-state. It is thermostatically controlled with user defined target-temperature ranging from 8-29 °C or “Max”.

The tests are performed choosing the ‘Max’ temperature setting. Hence, the duty cycle of the thermostat control is not taken into account in the test. The goal of the test is solely to investigate the voltage dependency of the space heater given that the thermostat target temperature is higher than the measured temperature in the room.

The space heater is tested at both full power and half power. For each test, the applied voltage is changed in steps of 10V and 5 V between 210 and 250V (and a short period of 260V for the full power mode).

### 8.5.2.3 Results

The below figure shows the voltage plotted together with the active and reactive power respectively. The figures on the left hand side are for the max power mode, the ones to the right is for half power.

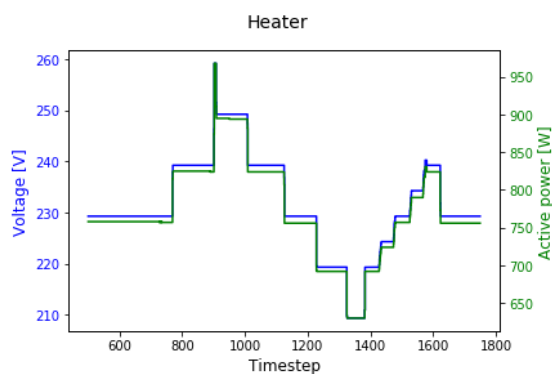


Figure 8-11: Electric space heater. Measured voltage together with measured active power from the voltage dependency test of the full-power setting

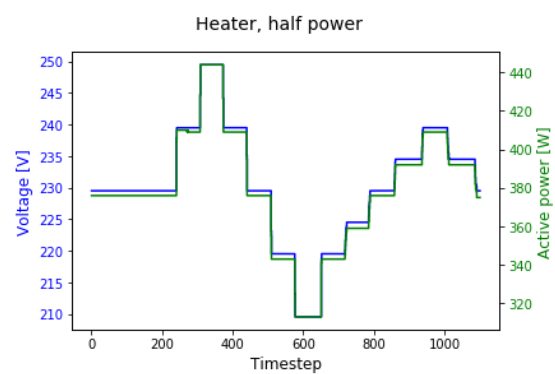


Figure 8-12: Electric space heater. Measured voltage together with measured active power from the voltage dependency test of the half-power setting.

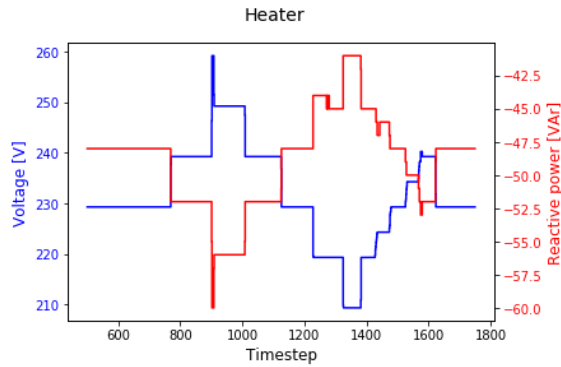


Figure 8-13: Electric space heater. Measured voltage together with measured reactive power from the voltage dependency test of the full-power setting

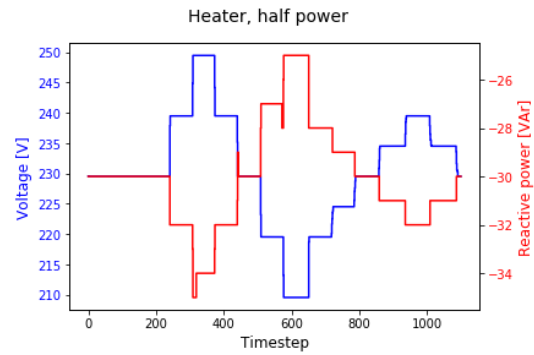


Figure 8-14: Electric space heater. Measured voltage together with measured reactive power from the voltage dependency test of the half-power setting

The table below summarise the load model coefficients and nominal active and reactive power for the two settings full and half power.

	$P_n$ [W]	$Q_n$ [VAR]	$Z_P$	$I_P$	$P_P$	$Z_Q$	$I_Q$	$P_Q$	np	nq
<b>Full power</b>	762	-48	0.86	0.30	-0.15	2.45	-3.09	1.64	2.01	1.81
<b>Half power</b>	377	-30	1.08	-0.15	0.07	-1.40	4.53	-2.13	2.01	1.73

Table 8-4: Load model parameters for ZIP and exponential load models for the resistance heater at half- and full-power settings

#### 8.5.2.4 Observations

From the plots and the load model coefficients it can be observed that the tested resistance heater exhibits a load characteristic close to constant impedance. This is expected since the operation of the heater is based on joule heating.

Another observation from the tests is that the power responds instantaneously to the voltage changes.

In the tests performed in this thesis, the duty cycle of the thermostatic control is not investigated. In part III of the thesis, it will be discussed how thermostatic loads like the tested space heater can be modelled.

## 8.5.3 Heat pump

### 8.5.3.1 Working principle and deployment

Although in Norway resistance heating is still the heating source penetrating the majority of households, heat pumps are increasingly used[44]. In 2017 the estimated number of heat pumps in Norway was one million, demanding 6TWh of electrical energy[45].

Heat pumps and air conditioners exploit the thermodynamic laws to “move” heat from one place to another by use of a refrigerant. The below figure shows the basic operating principle of a heat pump and its four main components. The exact thermodynamics of the operation is outside the scope of this thesis, but a simplified explanation of heat pump operation will be given in the following.

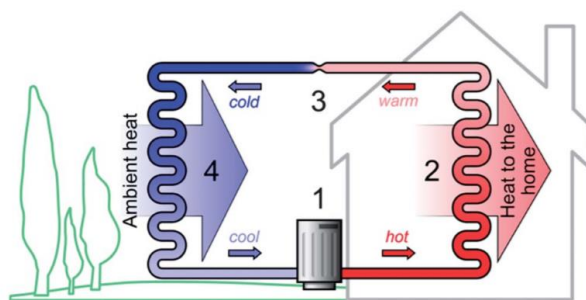


Figure 8-15: Illustration showing the basic operation and components of a heat pump. From [46]

Component 2 and 4 in the illustration are heat exchangers. A refrigerant flows through the system and the heat exchangers. The basic principle of operation is that heat is transferred from a medium with high temperature to a medium with lower temperature. The “ambient heat” in the figure can be either heat in the outside air in the case of an air sourced heat pump (ASHP), or heat in the ground in the case of a ground sourced heat pump (GSHP). The indoor heat exchanger can either exchange heat directly to the inside air, or to a water based central heating system. [46] The heat pump type tested in this thesis is an ASHP which exchanges heat directly to the air. Such systems are referred to as air-to-air systems. Air-to-air is the most widely used heat pump technology in Norwegian households[45].

To be able to extract heat from the outside air, the temperature of the refrigerant must be lower than that of the ambient air when flowing through the outdoor heat exchanger. Once the refrigerant reaches the indoor heat exchanger, the temperature of the refrigerant must be higher than the air of the indoor room to release heat to the indoor air. To achieve this, there is a compressor (component 1) increasing the pressure of the refrigerant on its way to the indoor unit. On the way back outside, the refrigerant’s pressure is reduced through an expansion valve (component 3).

The working concept of an air conditioner is the same. Then the refrigerant flow is reversed and thus extracting heat from the inside air moving it to the outside air. By using a reversible valve, the direction of the refrigerant flow can be changed to work either as a heat pump or an air conditioner depending on the heat or cool demand in the room/house.

In addition to the four main components shown in the above figure, both the indoor and outdoor unit have fans to increase the circulation of the air through the heat exchangers. According to [47], for air

conditioners, the compressor contributes to the major part of the electricity consumption (ca 80%), whereas the two fans together contributes to the remaining 20%.

Basic heat pumps feature a fixed-speed compressor which can only operate at either full-speed or no-speed. Therefore, to maintain the desired indoor temperature, such heat pumps turns regularly on and off [46], [48].

More advanced heat pumps/air conditioners may have two different compressors for different speeds to allow two different intensities for heating/cooling. [46] Better speed-control can be achieved by using inverter technology [46], [48]. The heat pump tested in this thesis features inverter technology. According to [48], this works as follows: “The inverter, or VFD (Variable speed drive), uses a rectifier to convert the incoming alternating current (AC) to direct current (DC), then uses pulse-width modulation in an electrical inverter to produce AC of a desired frequency. The variable- frequency ac drives a brushless motor, or an induction motor, as the speed of an induction motor is proportional to the frequency of the AC. The compressor can then run at different speeds.”

### 8.5.3.2 Test details

To investigate the voltage dependency of the hat pump, two tests are performed:

- Test with target temperature of 24 °C. After the voltage dependency test, the target temperature was lowered to 21 °C to observe how the heat demand influence the power demand.
- Test with target temperature of 30 °C.

For both tests, the heat pump is left on until a stable power consumption is observed. Then, voltage is changed in steps of 5 or 10 V between 210 and 250V.

An additional test at 23 °C target temperature is done to observe the load curve for a longer time period (11 hours). The purpose of this test is to observe the load behaviour at nominal voltage.

### 8.5.3.3 Results and observations

The below figure shows the recorded time series for the heat pump with 24°C and 21°C target temperatures respectively. The two voltage tests performed during the recording are marked in the figure.

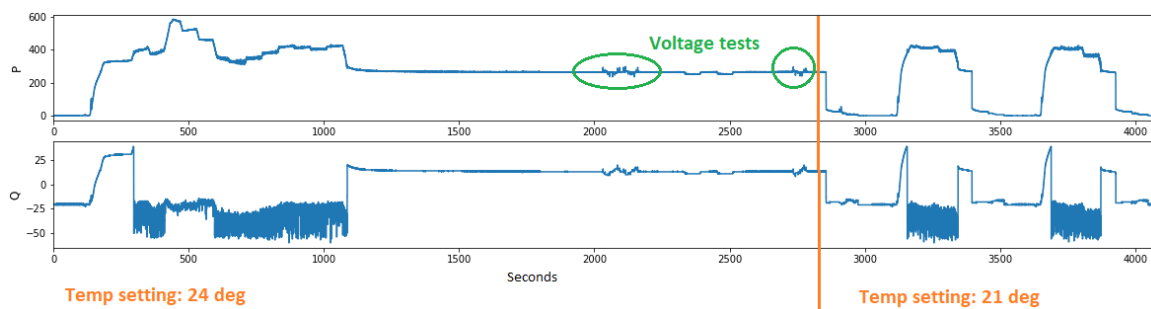
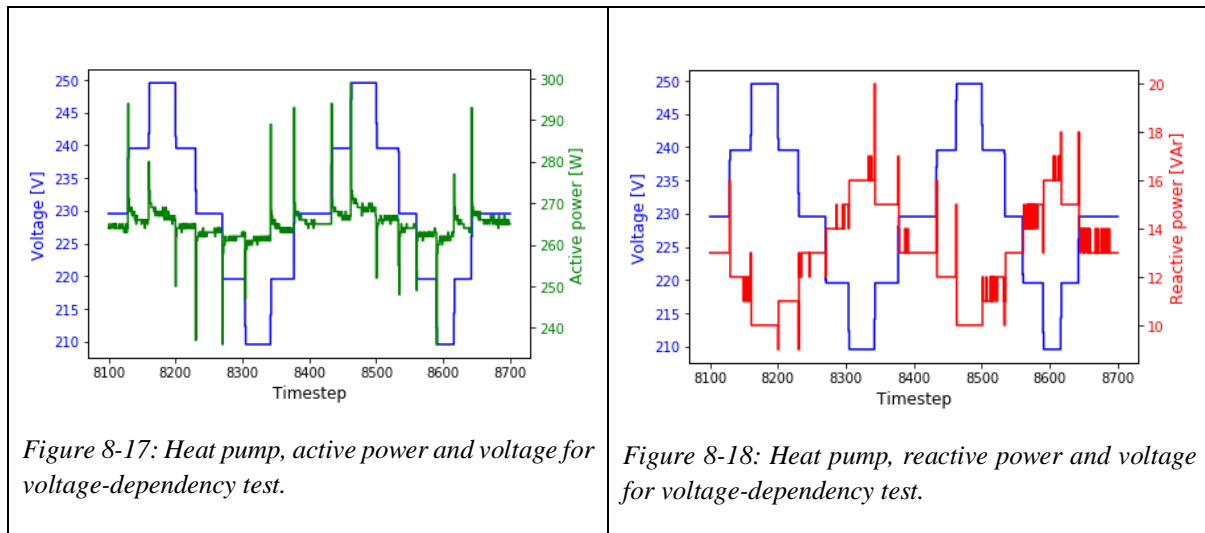


Figure 8-16: Measured active and reactive power load curves for heat pump during a test. The heat pump was supplied with 230V voltage for the whole period except for the two events marked as "voltage tests". Under the voltage tests the voltage was changed between 210 and 250V. The heat pump was first run with 24°C as target temperature. After ca 2800 seconds (ca 45 min) the target temperature was changed to 21°C

The voltage tests are carried out by changing the voltage stepwise in steps of 10V between 210 and 250V. The below figures show the voltage together with the active and reactive power respectively.

From the plots one can observe that following each voltage change, there is a rapid change in the power. After this transient, the power consumption stabilises. A small voltage dependency can be observed in the steady-state power consumption.



A different test is done with temperature setting 30 °C. The measured room temperature when starting the test is 22.5 °C. In this test, the power demand increased the first 5-7 minutes of operation until it reached an active power demand of about 1.1kW. Hence, the measured power demand in this test is significantly higher than the one from the test described above. The reason for this is probably that the heat pump adjusts the power demand (and thus the delivered heating power delivered to the room) according to the temperature gradient between the measured room temperature and the temperature setting.

The below figures show the voltage tests performed for the timeseries where 30deg setting is selected. For the active power, the similar behaviour as for the above-mentioned test can be observed in this test. The reactive power is positive (inductive) in the test presented above and is decreasing with increasing power. In this test, the reactive power is negative (capacitive) with decreasing absolute value for increasing voltage. I.e. the absolute value of the reactive power is decreasing with increasing voltage in both cases.



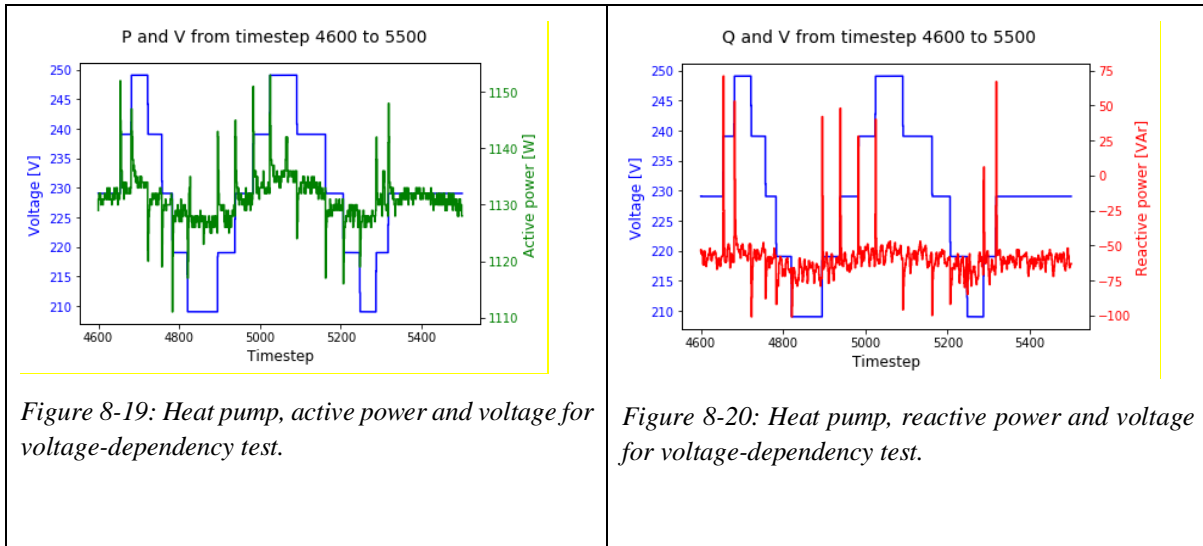


Figure 8-19: Heat pump, active power and voltage for voltage-dependency test.

Figure 8-20: Heat pump, reactive power and voltage for voltage-dependency test.

The active and reactive power demands are varying during heat pump operation, depending indoor and outdoor temperatures and the difference between the selected temperature and the measured indoor temperature. The voltage dependency observed from the performed tests on the other hand, is very small (at least when disregarding the transient behaviour following a voltage change). It can therefore be argued that finding model parameters which captures the very small changes in the voltage is of little use when the other factors impact the power demand in a much larger scale. The curve fit results obtained for both of the tests discussed above gives parameters values close to constant power behaviour. When using the constrained ZIP model in the curve fits (bounding the ZIP coefficients to the interval 0-1), the obtained curve fit result yields  $Z=0$ ,  $I=0$ ,  $P=1$  (i.e. constant power characteristics) for both active and reactive power.

For modelling voltage dependency of the tested heat pump, a constant power characteristic seems like a fair simplification. The more challenging and interesting task for modelling heat pump loads of this type (inverter based) is rather to model how the power consumption varies with time due to a varying heat demand and outdoor temperatures. This can be done using a closed-loop model. This is discussed in part III of the thesis.

The tested heat-pump features inverter technology to adjust the compressor speed. Compared to load curves found in literature, the load curve obtained from measurements shows a smoother load profile.

In [49], measurements on two domestic air conditioners is made. Their load profiles resemble the fixed-speed compressor type. One of them is shown in the below figure.

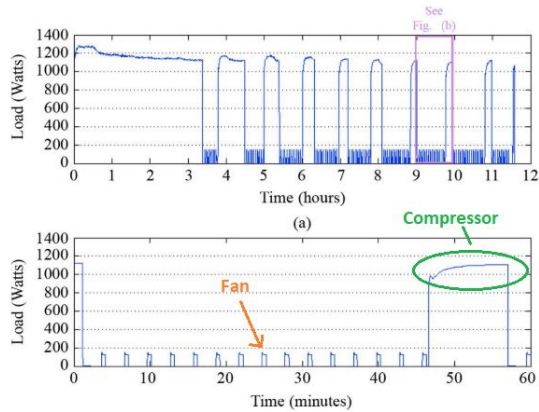


Figure 8-21: Air conditioner load curve from measurements in [49]. Figure a show the measurement time series in hourly resolution. Fig. b shows one of the hours in minute resolution.

The below figure shows the active and reactive power demand from a test performed in this thesis. Measurements are logged pump during 11 hours of operation. Note that the measurement is conducted during daytime (11AM to 10PM) in the spring, when outdoor temperatures are around 13 °C. On cold days, the power demand will be higher, and the load curve may look different. as lower outdoor temperatures increase the heat demand (due to heat loss through walls/windows) and decrease the heat pump efficiency.

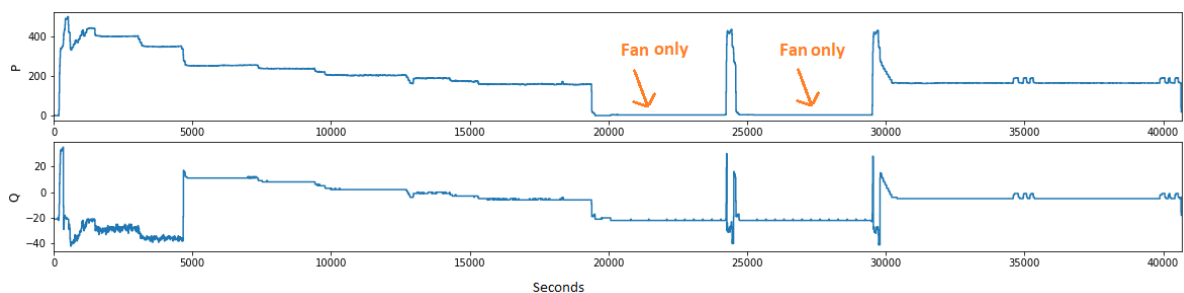


Figure 8-22: Heat pump power demand from measurements of 11 hours of operation.

## 8.5.4 Washing machine

### 8.5.4.1 Working principle and deployment

The deployment of washing machine in Norwegian and Western-European households is high, approximately 95% [43], [50]. The average number of washing cycles per week for European countries is between 3 and 5 per household according to [50]–[52].

There are many options to choose from when doing laundry with the washing machine to adjust the washing to the type of laundry subject to the washing. Options include water temperature, spin velocity and number of rinses performed in one washing program. There exist a variety of pre-programmed

washing programs suitable for different kinds of laundry. In addition, it is possible to do manual changes to the programs, by for instance increasing the number of rinses or changing the spin velocity.

In a report from the EIE project Smart-A [50], a technical description of typical European washing machine is provided. In references [1], [53] the different electrical characteristics of typical washing machine programs are broken down to load categories. The below table summarise the three basic stages of a washing cycle. The exact implementation of each stage may vary between washing machine models and washing programs.

Stage in washing cycle:	
<b>Cleaning/washing.</b>	This involves filling the machine with water, heating the water to the desired temperature and to rotate the drum to distribute water and washing detergent.
<b>Rinse</b>	In this stage, the detergent and dirty water should be removed from the clothes. This involves rotations of the drum, pumping out water and filling of new cold water.
<b>Spin</b>	As much water as possible should be removed from the clothes (according to the chosen washing program). This involves fast rotations of the drum.

Table 8-5: Washing machine cycle broken down to three stages: cleaning/washing, rinse and spin.

It is possible to sub-divide the washing cycle into more specific states, for instance the states identified in [51], namely: water filling, agitation, washing, draining, spinning and rinsing, of which some states may be repeated.

#### 8.5.4.2 Test details

To capture the varying nature of active and reactive power consumption throughout the washing cycle, two types of tests are performed in this thesis:

1. Tests of different washing programs. These are all performed with the same supplied voltage, namely 230V. The purpose of these tests is not to capture the voltage dependency of the load, but rather to investigate how different washing programs differ from each other.
2. Tests of the same washing program at different voltages. The same program is run at 210, 220, 225, 230, 235, 240 and 250V. The purpose of these tests is to investigate the voltage dependency of the active and reactive power consumption and how the voltage dependency changes throughout the washing cycle.

Details on the laundry load used for each test and the settings chosen for each tested washing cycle is provided in appendix C.3.

### 8.5.4.3 Results and observations

The below figure shows active power load curve for the different washing programs tested in this thesis.

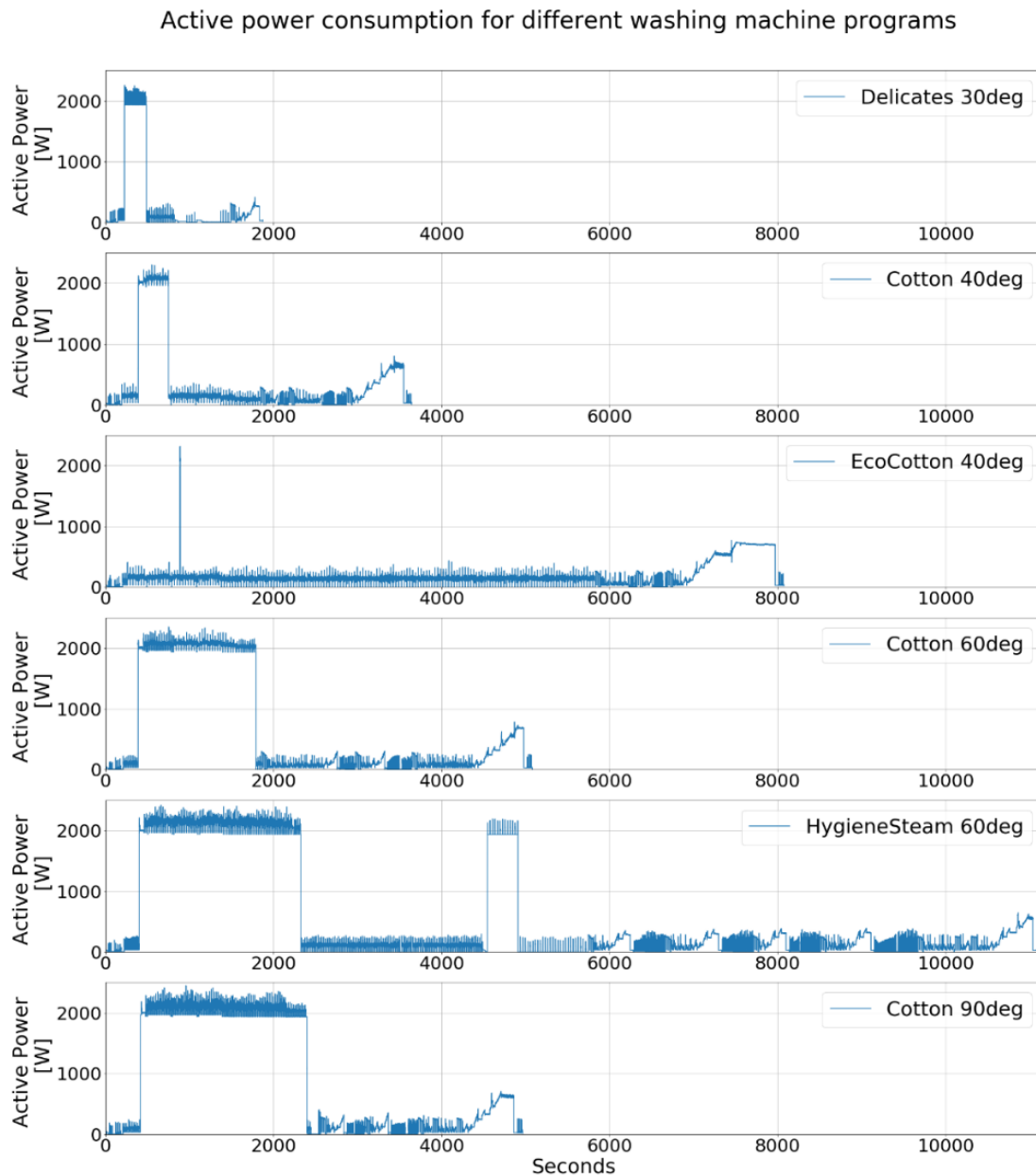


Figure 8-23: Washing machine load curves for different washing programs

The programs are different from each other in terms of total duration and the power drawn within the cycle. For all the programs, there are periods where the power demand is much higher than for the rest of the cycle. This occurs when the washing machine is heating water. For the 90- and 60-°C programs, the time used for heating water to the appropriate temperature is higher and thus the duration of the maximum power periods are longer than for the 30- and 40- degrees programs.

Reference [49] has performed measurement on two different washing machines for three different washing programs (in the U.S.). In [51], measurements on washing machines are done in 20 households, of which load curves for four washing machine cycles are presented in the paper. From the measurements performed in this thesis and in the mentioned references shown in the figures below, it is evident that the load curves may vary significantly between programs and washing machine models.

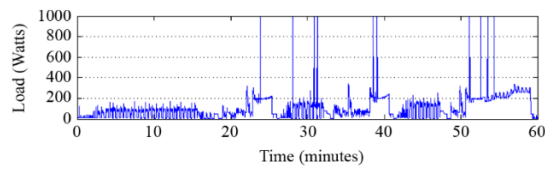


Figure 8-24: Washing machine load curve from measurements of a washing cycle from [49]

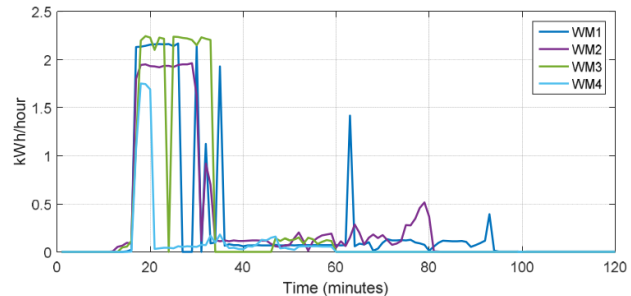


Figure 8-25: Washing machine load curves from measurements of four different washing cycles from [51]

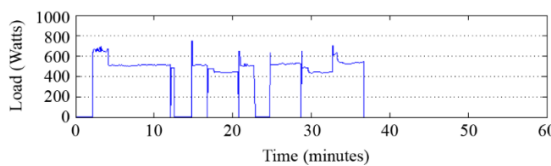


Figure 8-26: Washing machine load curve from measurements of a washing cycle from [49]

The below table presents the average values for some electrical parameters for the different washing programs tested in this thesis. The logged data from the tests is averaged over the entire washing cycle. In addition to average values, the table also contain the aggregated active energy demand for each washing program as well as the total duration of the cycle in minutes.

	<b>P [W]</b>	<b>Q [VAR]</b>	<b>Energy [Wh]</b>	<b>Duration [Min]</b>
<b>Delicates 30°C</b>	332	-8.1	173	31
<b>Cotton 40°C</b>	340	22	344	61
<b>EcoCotton 40°C</b>	179	26	402	135
<b>Cotton 60°C</b>	655	4.7	923	85
<b>HygieneSteam 60°C</b>	511	-1.2	1582	186
<b>Cotton 90°C</b>	903	-9.6	1245	83

Table 8-6: Average values of active and reactive power, true power factor and current and voltage THD for the tested washing machine programs. Tests are performed with 230V test voltage.

For investigating the voltage dependency of the washing machine, it is decided to look closer into the washing program “Cotton 40°C”. This program is run at voltages of 210, 220, 225 230,235, 240 and

250V. The below figure shows the power demand for the five of the voltage levels. The total duration of the washing program is almost the same for all the tested voltages. However, for the 210V test, the cycle lasted ca 10 minutes longer than the other tests. The stages of the washing cycle is marked in the figure.

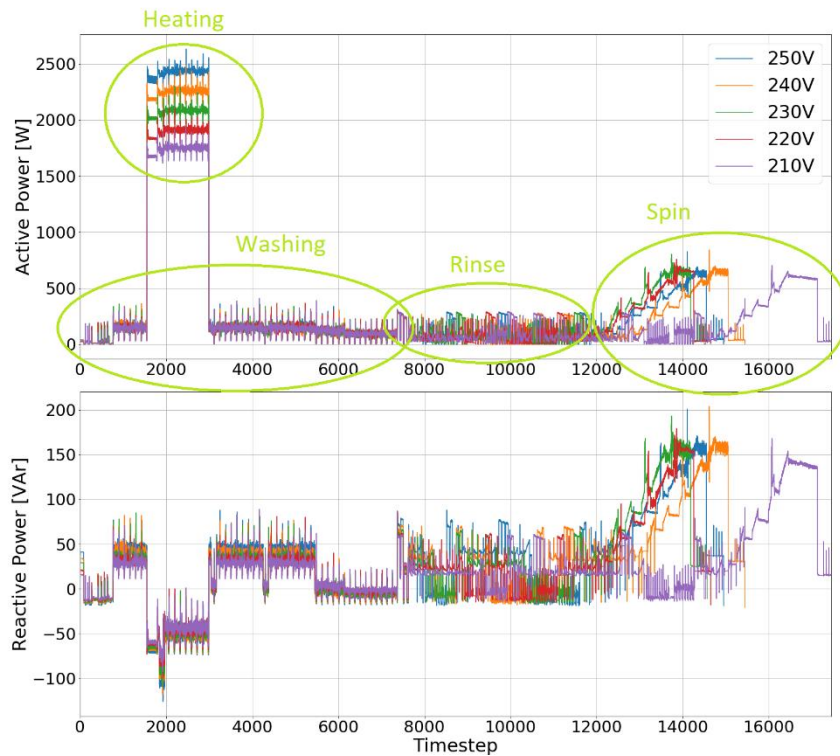


Figure 8-27: Active and reactive power demand for washing machine throughout washing cycle for different voltages. Each time step equals 0.25 seconds. The washing cycle stages washing, heating, rinse and spin are marked in the figure.

In the washing stage the drum is alternating between rotating clockwise and counterclockwise. Between the periods of rotation, the drum is standing still, which can be seen figure as small drops in the power demand (followed by peaks when the drum starts rotating again). The power demand increases significantly when the water is being heated. The rotations continue in the same pattern also in the heating-state.

For finding the load model parameters of the 40°C program, one option could be to find the load model parameters for the average behaviour of the whole washing cycle. Alternatively, the cycle can be split into parts with similar characteristics, for instance the washing stages heating, washing, rinse and spin, or the states identified in [51]. It could be possible to subdivide into subgroups of the washing stages by for instance distinguish between the parts of the cycle where the drum is rotating (i.e. the motor is running) and when it is not.

In this thesis, an attempt on finding the load model parameters of four different washing states have been made. Since the major power consumption takes place during the heating part of the washing

cycle, the heating state is the most important for the load modelling in this thesis by the fact that it contributes more to the peak power load in the network.

Load modelling results for the four stages are summarized in the table below. In Appendix D.4 some more details about the curve fitting procedures and results for each stage can be found.

	$P_n$ [W]	$Q_n$ [VAR]	$Z_P$	$I_P$	$P_P$	$Z_Q$	$I_Q$	$P_Q$	np	nq
<b>Washing</b>	121	16	0.77	-1.18	1.47	9.21	-16.2	7.99	0.35	2.27
<b>Heating</b>	2086	-57	0.77	0.37	-0.14	-3.23	7.57	-3.34	1.91	1.17
<b>Rinse</b>	84	18	- 0.23	1.40	-0.16	13.2	-23.4	11.2	0.93	3.12
<b>Spin</b>	381	92	0.63	-1.27	1.62	2.47	-4.14	2.68	0.01	0.78

*Table 8-7: Load model parameters for ZIP and exponential load models for the washing machine 40°C cotton program. Model parameters for each stage in the washing cycle are listed.*

It is worth noting that for the part of the cycle where the water is heating, there is a larger voltage dependency than in the other parts of the cycle. One could expect that the duration of the heating would depend on the voltage, since the energy needed to heat the water to the desired temperature is constant, and the duration therefor should increase if the power decrease. However, it seems like for this washing program, the heating is controlled by constant duration and not by thermostatic control.

### 8.5.5 Heat Pump Dryer

The penetration of tumble dryers in European households is in general considerably lower than washing machines, and also shows greater variations between countries. [50], [52]. The percentage of Norwegian households owning a clothes dryer (tumble dryer or drying cabinet) was 41% in 2001[55] and 47% according to a 2007 survey[43].

The basic principle of a tumble dryer is to blow warm air through/over the wet laundry to cause the water in the laundry to evaporate. Energy is needed to drive the drum rotation, heat the air to be blown over the laundry and drive fans to blow the warm air. The humid air can either be vented to the ambient or condensed by cooling it down in a heat exchanger via a second air stream. [50]

The most widely used technology in dryers used in European household is per 2008 to use resistive electrical heater to heat the air needed in the drying process[50]. An alternative to resistive heating is to use heat pump technology to heat the air. According to [50], many manufacturers have dryer models of this type, but this technology had (at least per 2008) much smaller penetration in the European market than its resistance-based countertype due to higher prices. The dryer tested in this thesis is of heat pump type.

The advantage of heat pump technology is that the energy contained in the humid air flow can be regained. The energy contained in the humid air going out of the drum can be used to heat the air going into the drum. According to [50] it is possible to save 40-50% of the total energy consumption by using this technology as oppose to the resistive heating technology.

### 8.5.5.1 Test details

Like the tested washing machine, the dryer offers many different programs for the user to choose from. Therefore, for the dryer the same two types of tests are conducted as for the washing machine, namely:

1. Tests of different drying programs with the same supplied voltage (230V)
2. Tests of the same drying program at different voltages. The same program is run at 210, 220, 225, 230, 235, 240 and 250V.

Details on the laundry load used for each test and the settings chosen for each tested drying cycle is provided in appendix C.4.

### 8.5.5.2 Results

There are various options for the user when drying clothes with this dryer. Several of them are categorized as “Optimal dry”-settings. In addition, there are some “Manual dry” settings.

The manual-dry programs have user defined duration, while the optimal-dry options adapt the duration to the laundry load. Some drying programs in both categories are tested.

The below figure shows the power demand of some different drying programs, all of them run at 230V.



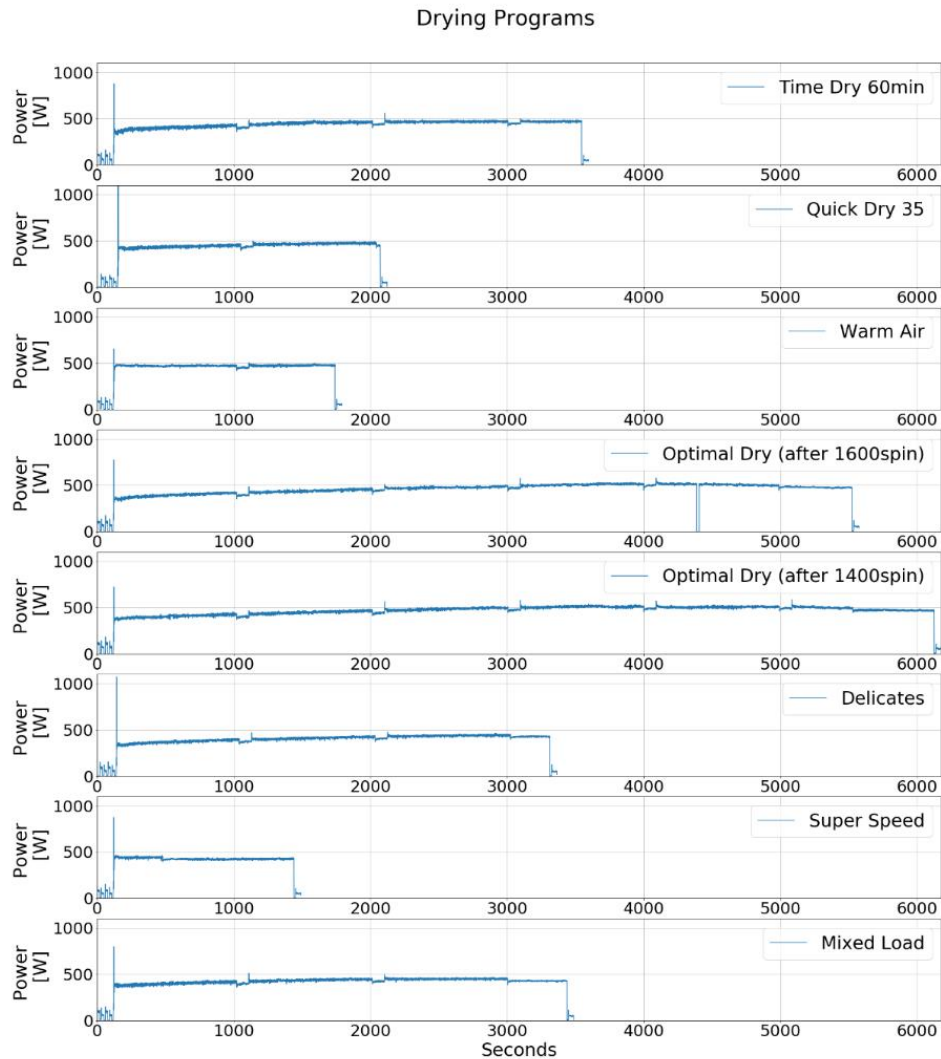


Figure 8-28: Drying programs active power demand

The load patterns of all the tested drying programs are very similar, with exception of the duration of the program. Some of the programs have slightly higher overall active power consumption than the others. The rated power from the user manual is 550-600W[56].

The table below presents some key parameters for the different drying cycles. The table shows the average values of some electrical parameters, averaged over drying cycle. It also shows the accumulated active energy and total duration of the cycles. The first two-three minutes (650 time steps) are excluded since the load behaviour is different in this period.

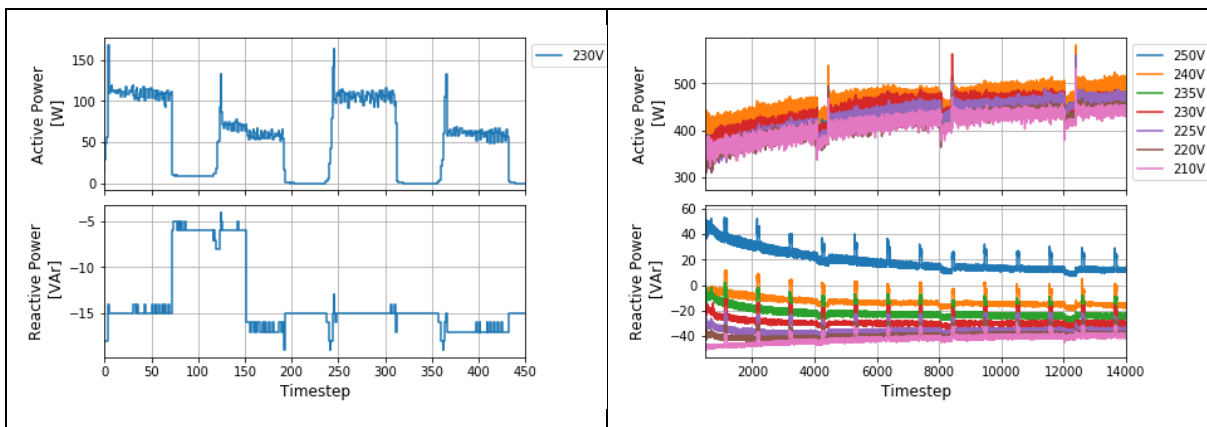
	P [W]	Q [VAR]	Energy [Wh]	Duration [Min]
<b>Time Dry 60min</b>	440	-28.3	419	57
<b>Quick Dry 35</b>	443	-28.5	241	33
<b>Warm Air</b>	458	-28.0	207	27
<b>Optimal Dry<sup>7</sup></b>	461	-28.6	694	90
<b>Optimal Dry<sup>8</sup></b>	470	-28.4	785	100
<b>Delicates</b>	402	-28.7	358	53
<b>Super Speed</b>	414	-29.9	153	22
<b>Mixed Load</b>	423	-29.4	391	55

Table 8-8: Average active and reactive power values for different drying programs

For testing the voltage dependency of the dryer, the same drying program is run at seven different voltages.

The drying program chosen in the test is “Time Dry”. This program allows the user to set the duration of the drying program. One can choose between 30, 60, 90, 120 or 150 minutes, of which 60 minutes are chosen in the tests.

The below figure shows the power consumption of the dryer throughout the 60 minutes drying cycle for applied voltage of 210, 220, 230, 240 and 250 Volts. In the load modelling, the first 500 time steps (ca 2 minutes) is excluded. The below figures show the load curve for the first ca 2 minutes of the drying cycle (left figure) and the load curves for the time window chosen for the load modelling (right figure). The curve fit result for the first 450 time steps is provided in appendix D.5.1.



<sup>7</sup> The clothes was washed with 1600 spin velocity before the drying.

<sup>8</sup> The clothes was washed with 1400 spin velocity before the drying

	$P_n$ [W]	$Q_n$ [VAR]	$Z_P$	$I_P$	$P_P$	$Z_Q$	$I_Q$	$P_Q$	np	nq
<b>Time-Dry 60min</b>	438	-27	-1.18	3.01	-0.83	-78.3	143	-64.1	0.66	-7.72

Table 8-9: Load model parameters for ZIP and exponential load models for the heat pump dryer for the Time Dry-setting

### 8.5.5.3 Observations

In references [49], [51] measurements on clothes dryers in the U.S and Norway are made. The measurements shown in ([51]) from dryers in Norwegian households have power consumption around 2 kW. The profiles measured in [49], have even higher peak demand and alternates between peak and a few hundred watts. The below figures show some load profiles of dryers found in the mentioned literature. The dryers from [49] are of resistive heating type. For the dryers measured in [51], the dryer models are not provided and therefore the technology is unknown to the author of this thesis.

Comparing the load curves measured in this thesis to the load curves from [49], [51] shown in Figure 8-29 and Figure 8-30, it can be seen that the power consumption of the tested heat pump dryer is significantly lower and less volatile throughout the drying cycles.

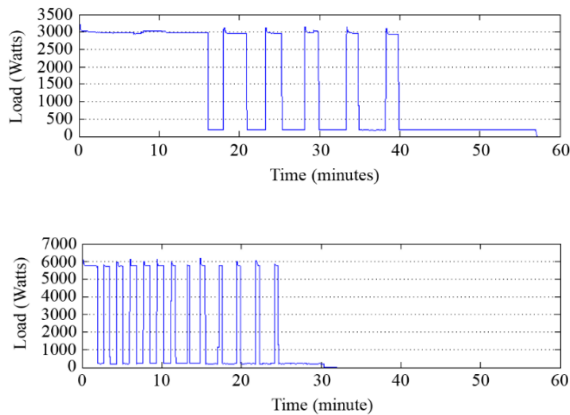


Figure 8-30: Load curves of drying programs for two different clothes dryer models measured in [49]

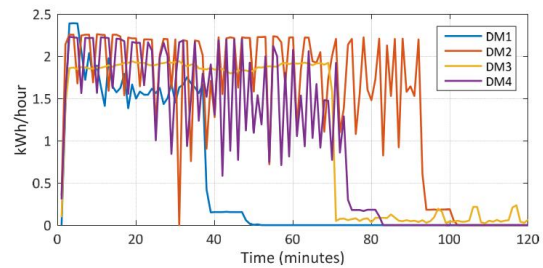


Figure 8-29: Load curves from four differed dryers measured in [51]

Another observation from the performed measurements is that the load behaviour is very similar for the different drying programs, except the duration of the program.

## 9 Discussion

In this part of the thesis, load modelling as well as voltage dependency of individual loads and network losses is addressed. Results from the lab work and associated curve fitting is presented for the tested loads: induction cooktop, resistance heater, heat pump, washing machine and heat pump dryer.

In literature it is a general agreement that load modelling not is a trivial task. In reference [4] it is pointed out that finding the *load composition* is the most challenging part in component-based load modelling. From the work with this thesis, it is clear that even finding the *load parameters of individual loads* poses some challenges. There are many causes of uncertainties in the modelling procedure. It is found that depending on how the measurement data is interpreted and analysed one can come to different modelling results.

Examples:

- Which part of the measurement time series that is used in the curve fitting can influence the model result. For instance, the induction cooktop running at max-power has an increasing active power consumption, especially for the first 1-2 minutes of operation. Including the first minutes gives other results than if they are not included.
- Each appliance has different available settings for the user to choose from. The choice of setting for the voltage dependency testing can thus impact the obtained load modelling results. From the devices tested in this thesis, the induction cooktop tests shows that the choice of setting can make a big difference. The cooktop namely exhibits a close-to constant impedance behaviour when the Max Power mode is chosen, and a constant power behaviour for the 1600W mode.
- For appliances with a load characteristic that changes throughout the cycle, there are several possibilities concerning the modelling. One can choose to find an average load model for the cycle or find several sets of load model parameters corresponding to different parts of the cycle which can be used to make a time dependent model for the appliance.
- For the induction cooktop test at Max Power mode, three tests are performed at the same voltage level (207V). These showed that the measured power is more different between the tests than what could be expected from normal measurement errors. This could indicate that there are some factors other than voltage level influencing the controllers in the cooktop, which has not been considered in the thesis.

When also taking into account all the different washing machine or cooktop models available on the market and penetrating households, it is obvious that there is a great diversity in load characteristics in even the same type of household equipment. As new models enter the market the “load stock” of the electricity consumers is gradually changing. The new appliance models may feature different kinds of components, different control loops and operation modes than the older models. Therefore, it is necessary to keep load models up to date with the changes by testing modern devices.

The tests performed in this thesis is a contribution to the work with keeping load models up to date. The heat pump and the heat pump dryer tested in the thesis are of relatively new technology which is not (at least as of yet) populating the households to as large extent as their conventional counterparts. The results from the measurements shows that their load behaviours differ from those found in literature for older technologies.

Concerning voltage control, different load types responds differently to voltage reduction or voltage increase.

- Constant impedance loads draw less current when lower voltage is applied, resulting in a reduced power demand proportional to the square of the voltage reduction.
- Constant current loads draw the same current independently of the voltage, and hence the power demand decrease linearly with reduced voltage.
- Constant power loads draw the same power independently of the voltage. Consequently, reduced voltage causes increased current draw.

When fitting the load behaviour of a device to the ZIP and exponential load models, many devices show a behaviour that is a combination of the three mentioned above. This is the case also for the devices tested in this thesis. However, it is possible to simplify the results obtained in the curve fits and categorize the devices as “close-to”-constant impedance, “close-to”-constant current and “close to”-constant power. The table below summarise the results from the tests in this thesis with emphasis on the voltage dependency of the active power demand.

	<b>Constant impedance</b> ZIP: $Z_p \approx 1, I_p \approx 0,$ $P_p \approx 0$ Exp: $np \approx 2$	<b>Constant current</b> ZIP: $Z_p \approx 0, I_p \approx 1,$ $P_p \approx 0$ Exp: $np \approx 1$	<b>Constant power</b> ZIP: $Z_p \approx 0, I_p \approx 0,$ $P_p \approx 1$ Exp: $np \approx 0$
<b>Induction cooktop</b>	Max Power-setting, 300W and 800W in “on-state”		1600W-setting
<b>Resistance heater</b>	Full-power and half- power settings		
<b>Heat pump</b>			All tested settings
<b>Washing machine</b>	Heating	Rinse	Washing and spin
<b>Tumble dryer</b>		Whole cycle of the tested program	

*Table 9-1: Summarising table for the curve fitting results. The results are simplified to categorise each tested appliance as either constant impedance, constant current or constant power. When relevant, individual settings or parts of operation cycle are categorised independently.*

It can be observed that the tested devices together represent all of the three characteristics. The washing machine exhibits all three characteristics in the different stages of the cycle. The induction cooktop shows different characteristics depending on the chosen setting.

The devices exhibiting a constant impedance and constant current characteristics will respond in the desired way if a CVR or Voltage-Led load management scheme were to be implemented, at least if only the initial response to the voltage change is considered. The initial response to a voltage reduction would for these devices be reduced active power demand. However, the resistance heater is equipped with a thermostatic control. Therefore, if the supplied voltage is reduced, the heater will be on for a longer

time period to achieve the same temperature increase in the room where it is located. Similarly, for the induction cooktop, the time it takes for the food to reach the desired temperature will be longer if the supplied voltage is lower. How the thermostatic control influences the effect of voltage control cannot be seen directly from the ZIP-parameters. This will be addressed more thoroughly in part III of the thesis.

## Part III - Aggregated loads and -load modelling

In part II of the thesis the emphasis is on load modelling of individual appliances as well as on the laboratory work performed in this thesis where load model parameters are estimated based on measurements and curve fitting techniques.

For voltage control and for assessing a network's response to a voltage control strategy, it is not the load characteristics of individual loads that are the main concern. The question is rather how the sum of all the loads connected to the network and used simultaneously responds to the voltage control strategy. Also in other power engineering applications, it is normally the total load or "the aggregate load" that is of interest.

Therefore, it is highly relevant to discuss how the knowledge of the individual load components obtained in Part II can be used in an aggregated load model. This is the scope of Part III of this thesis.

The outline of Part III is as follows:

Firstly, a brief presentation of the two main approaches to load model aggregation is given, namely the measurement- and the component-based approaches. This is followed by a more detailed introduction to the component-based approach.

Subsequently, modelling of closed-loop loads is discussed. Closed-loop loads are loads featuring control loops determining their duty-cycles, e.g. water- and space heaters. As these types of loads contribute to a large share of the Norwegian residential loads[43], their response to voltage is highly relevant when assessing VC strategies in Norwegian context. To illustrate how closed-loop loads can be modelled, the methodology and results from simulations of the voltage dependency of aggregation of water heaters is presented in chapter 11.1.

## 10 Measurement-based and component-based load modelling

There exist two main approaches to finding the load model parameters for aggregate loads: the measurement-based and component-based approaches. In this thesis the emphasis is on the component-based approach. This approach is a bottom-up approach for aggregating loads. The bottom layer is knowledge of individual load component's load characteristics. For instance how a washing machine's power consumption depends on the applied voltage. The next step for finding the aggregate load model, is knowledge about the composition of different load components, i.e. how large portion of the aggregate load that comes from the washing machine load.

The principle of the measurement-based approach on the other hand, is to perform measurements in the network itself to find the voltage dependency (and/or frequency-dependency) of the aggregated load directly. This approach can be classified as a top-down approach. Recommendations regarding the measurement procedures, data processing and parameter estimation for this approach is given in [4]. The idea is to measure voltage and other parameters at the busbar for which the load characteristics should be found or at other strategic locations in the grid. By analysing the measurement data for the network when it is subject to a deliberate or naturally occurring voltage change, the voltage dependency can be found (similar approach to find frequency dependency). Using this approach, no detailed knowledge about the individual load components and load classes connected to the network is necessary.

One advantage of the component-based approach over the measurement based, is that the models can be used for different operational conditions. A challenge in the measurement-based approach is to obtain measurements from different locations and for different load situations to obtain models that can be generalized to other locations and operational conditions. Simultaneously, the component-based approach requires extensive amounts of information about load composition which may be hard to obtain. [10]

In the following subchapter the component-based approach will be discussed in greater detail.

### 10.1 Component-based load modelling

Aggregation of loads by the component-based approach boils down to utilizing knowledge about individual loads and put together individual loads to form meaningful "groups of loads" with similar load characteristics (i.e. load classes, load components and load model categories). By also knowing how much each group contributes to the total load, one can find the load characteristics of the total load.

It is normal to distinguish between different *load classes*. Typically, the residential, commercial, industrial load classes are considered[4]. Other classes, like agricultural load class and general lightning can be added depending on the relevance for the considered area. Sub-classes of the main classes can be defined for instance by organizing the residential customers into one-dwelling or two-dwelling houses, apartments with electrical heating or apartments with central heating, etc. It can also be feasible to distinguish between rural and urban customers if that is assumed to impact the types of loads used by the customers or the utilization pattern for the use of the loads.

For commercial and industrial classes one can also organize into sub-classes based on the type of commercial/industrial activity and the expected types of electrical appliances and utilization pattern of the loads. The main goal of sub-dividing into sub-classes is to identify groups of customers that exhibit the same load behaviour. Typical load classes, sub-classes and load categories expected for the classes/sub-classes are described in [4].



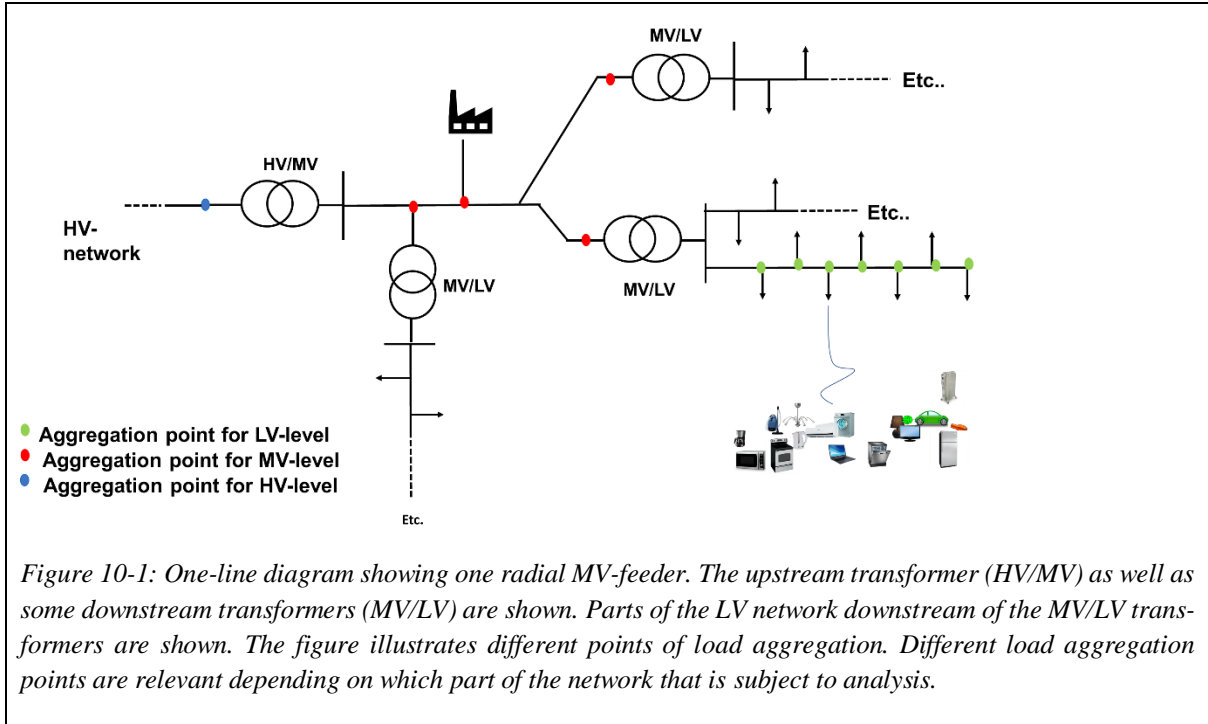
Within each load class or sub-class, the electricity demand is divided into several *load components* or *load model categories*. For instance, for the residential load sector, load categories may include resistive heating, lightning, power electronic devices, etc.

A major challenge for determining the aggregate load model parameters, is to find the *load composition* of different load categories within a load class as well as the load composition of the individual load classes with respect to the total load.

The load composition describes how sub-groups of loads contributes to the total load of the main group. Determining the load composition is not a trivial task, as it is not the same for all parts of the network and also varies with time. For example, the portion of the load coming from commercial versus residential load varies through the day and week with the opening hours of shops and workday in office buildings as well as occupancy of the residential buildings. Moreover, within the residential or other load sectors, the load composition of the different load components is determined by the user behaviour of the occupants of the building as well as the heat/cooling demand due to weather conditions and user-determined comfort levels.

To overcome this problem, load models are often found for “typical” load situations. For instance, one may find aggregate load model parameters for working days and holidays, seasons (summer, winter, spring, autumn) high-load and low-load, etc. To find the load composition for different situations, different sources of information are used, amongst others billing information, customer surveys covering ownership of different load components and time-of-use information, metering campaigns, smart meters, etc. Reference [8] describes how survey information, billing information and experimentally determined load model parameters of individual household appliances have been used to find load models for New York City for summer, winter and spring/autumn. By the Nordic TSOs, in the ZIP model parameters so far determined from the component-based approach, distinction is made between “high load” “low load” and “average load”. [32]

Depending on the level of aggregation to be performed, network components may also have to be included in the aggregated load. If the model should be used for load flow studies in LV-feeders with loads aggregated to customer level, the transformer and network is modelled as individual components (i.e. not included in the aggregate load). However, if it is desired to find an aggregated load model of the whole network downstream of a MV/LV-transformer or a HV/MV-transformer, not only the loads in terms of power consuming devices must be accounted for in the model, but also the network components like transformers, lines and cables. This is illustrated in the below figure, where “aggregation points” for different levels of aggregation is shown for a case where for instance load flow studies is to be performed in the HV, MV or LV-network.



When having estimated the ZIP model parameters for relevant load components and estimated the load composition, the aggregated load model parameters can be found by the below equation[57][7].

	$ZIP_{agg} = \sum_j^N \frac{S_{0,j}}{S_{agg}} ZIP_j$	N = number of load components/load classes to be aggregated
--	--	---

“ $ZIP_{agg}$ ” and “ $ZIP_j$ ” are substituted with the ZIP-coefficients  $Z_p, I_p, P_p, Z_q, I_q, P_q$  to find the respective aggregated coefficients. S can be substituted by P or Q for active and reactive components.

Below follows an example which shows how the ZIP-coefficient  $Z_{p,agg}$  for the aggregated load can be found when the coefficients for the residential, commercial and industrial load classes is known. The coefficients for the load classes are found using the similar approach, but then by finding the sum of the portions of all the load components/load categories that contributes to the total load class load.

	$Z_{p,agg} = \frac{P_{0,res}}{P_{agg}} Z_{p,res} + \frac{P_{0,com}}{P_{agg}} Z_{p,com} + \frac{P_{0,ind}}{P_{agg}} Z_{p,ind}$	Res= residential Com=commercial Ind=industrial
where	$P_{agg} = P_{0,res} + P_{0,com} + P_{0,ind}$	

The similar methodology can be used to find the other coefficients  $I_{p,agg}, P_{p,agg}, Z_{q,agg}, I_{q,agg}, P_{q,agg}$ .

The approach to load model aggregation may give sufficient accuracy for many applications. If model parameters are found for different load situations (different seasons, workday/holidays, peak-hours and off-peak hours, etc), they can provide valuable information and models to use in grid planning and operation. However, a drawback of the methodology is that the time-dependency is only captured to a

limited extent. Depending on the type of loads present in the network in question, this may or may not cause considerable weaknesses of the model.

## 11 Modelling and aggregation of thermal closed-loop loads

The methodology for aggregation of loads by the component-based approach described in the previous subchapter can be used to obtain load model parameters for different load situations in a selected part of the network. The model obtained by using this approach does not consider the effect of voltage on operation of *closed-loop loads*. Closed-loop loads, as oppose to open-loop loads, are loads containing one (or more) control loop(s). The most common closed-loop loads are different kinds of heating and cooling loads with thermostatic control. Closed-loop loads' operation can for instance also depend on humidity or other air quality parameters (e.g. for ventilation systems). In [26], motor drives and regulated constant power loads are also included under the closed-loop load type. However, in this subchapter the focus will be thermal closed-loop loads.

An aggregate ZIP model can be used for evaluating the effect of CVR or other VC strategies for open-loop loads. However, for closed-loop loads, a model considering the intertemporal effect of voltage on the load behaviour is required. For CVR assessment, this is addressed in [58] and [27], [59], where two different models are used to model thermal closed-loop loads.

Simulation-based assessment of VC strategies can be performed by doing power flow simulations for different load situations. To consider closed-loop loads in the simulation, one need to do time-series simulation for subsequent time steps where the load in timestep  $i$  is determined from the voltage-dependent load in timestep  $i-1$ . This is necessary since the voltage is decisive for how long time a closed-loop load will remain active.

A hypothetical example illustrating how the voltage dependency could influence the power demand of a water heater in a time step  $i$  could be:

- If the voltage applied to a water heater in time step  $i-1$  is 240V, the water temperature in the tank reaches the threshold temperature during that time step. Consequently, the thermostat deactivates the heating element so that in time step  $i$  the power drawn by the water heater is zero.
- If the voltage applied to the water heater is only 230V in time step  $i-1$ , the water temperature *do not* reach the threshold temperature. Thus, in time step  $i$  the heating element is still on and the power demand would be for instance 2kW.

To consider this in the simulation, different ways of modelling can be used, including:

1. Modelling thermostatically controlled loads as RC-circuits.[1], [58], [60]
  - Models the thermal characteristics of a load as a resistance and capacitor equivalent circuit. In reference [1], RC-parameters for house hold appliances are found using two different approaches: load monitoring and calculations based on information about materials' heat capacities, etc.
  - The voltage-dependency can be taken into account by using the exponential load model in combination with the RC-model, as implemented in [58].
2. Modelling thermostatically controlled loads with the Equivalent Thermal Parameter (ETP) model.
  - Models the thermal load with an ordinary differential equation.
  - Used in [27], [59] to model heating, ventilation and air conditioning systems (HVAC) with several input parameters: outdoor temperature, solar radiation, humidity, voltage and set-points of thermostatic controls.

- Voltage-dependency is considered by using the ZIP-models of the thermal loads in combination with the ETP models. [27], [59]
3. Incorporating the effect of voltage-dependency of thermostatically-control loads by changing coincident factors of the aggregate load.
- Coincidence factors are factors describing how much of the installed capacity that is being used simultaneously. For instance: in a household there may be electrical appliances capable of drawing 20kW if all appliances are used at the same time. Since this is normally not the case, the load at some time instance can be approximated by a coincidence factor. A factor of 0.5 would mean that the household with 20kW installed capacity, 10kW is estimated to run at the same time.
  - For a feeder coincidence factors can be used to estimate the peak load. If one assumes that the peak demand for all neighbours occurs at the same time, the coincidence factor for the peak demand of the neighbourhood is 1.
  - In [17] the aggregation of water and space heaters is simulated in different scenarios where different coincidence factors for the heaters are assumed. Monte Carlo simulations are used to incorporate the stochastic behaviour of activation and deactivation of the thermostatically controlled loads.
    - The study is scenario-based and do not incorporate how the coincidence factors are influenced by the voltage level. With deeper knowledge of the actual relationship between the voltage-dependency of loads and coincidence factors in the network of interest, this type of simulations could be enhanced to investigate VC strategies on real-world load compositions.

## 11.1 Example: simulation of aggregated effect of water heaters

This chapter will present an example of how aggregation of closed-loop loads can be simulated and how the thermal characteristics and voltage-dependency influence the aggregated load. The simulation is performed by researcher Nicolai Feilberg. The methodology and results are presented here with his permission. The purpose of including this in the thesis is:

- To give an example of how the stochasticity of power demand and aggregated effect of thermal closed-loop loads can be modelled.
- To present the results which can be interesting in the discussion regarding VC strategies in Norwegian distribution grids.

### 11.1.1 Method

The simulation is performed in Excel and uses Monte Carlo simulations to model the stochastic behaviour of hot water demand in 1000 households. Each household have one water heater and no other loads. There are no load flow calculations involved, and thus calculation of the network losses is not a part of the study. The objective of the simulation is to investigate how voltage impact the peak power demand for an aggregated load consisting of thermostatically controlled loads. Simulations are performed with a 1-minute resolution for a 24-hour period. 100 independent cases are modelled. Each “case” is a 24-hour period with a heat demand for each minute and each water heater simulated by Monte Carlo extraction.

1000 water heaters, each with a 2kW power rating and 200 litres of water are simulated. The total heat demand for a 24h period is assumed to be the same for all water heaters and is based on data from the REMODECE project<sup>9</sup>. How the energy demand is distributed during the 24 hours is modelled by Monte Carlo extraction to capture the stochastic behaviour of the load. Since the heat demand during the day is not totally random, each hour has an associated log-normal distribution with an expected value and standard deviation. This is to take into account that the heat demand to some extent follows typical user behaviour (the demand for hot water is larger at times a day when people typically shower, clean their dishes, etc.) In addition to user behaviour, the heat loss is taken account in the log-normal distributions. The normal distributions for each hour are based on data from measurement campaigns from the REMODECE project.

In the Monte Carlo extraction, the normal distributions of each hour are considered. Thus, for the hours during the day with higher expected values for heat demand, a larger number of the 1000 households will demand hot water during those hours. For which of the 60 minutes during the hour the hot-water demand is “triggered” is random since the same normal distribution is used for the whole hour.

Based on the modelled water demand for the 1440 timesteps (60min \* 24h= 1440), the electric power demand for the water heaters are determined based on:

- The temperature of the water in the previous time step
- The hot-water demand in the previous time step

If the water temperature in a given water tank is below the lower threshold value, the heating element in the water heater is “on” in the next timestep. The electric power demand when the heating element is “on” is determined by the voltage.

The heating element is modelled as a purely resistive constant-impedance load:

- $P_n = 2\text{kW}$ ,  $V_n = 230\text{V} = 1 \text{ pu}$
- $Z_P = 1$ ,  $I_P = 0$ ,  $P_P = 0$

The simulation is done at different voltage levels from 0.9 pu to 1.1 pu. The same Monte Carlo-simulated hot-water demand is used for all voltage levels.

## 11.1.2 Results

The figures below show the heat demand together with the electric power demand for one of the simulated 24h periods for voltage levels 1 pu and 0.9 pu. The heat demand is the same in both plots (i.e. comes from the same Monte Carlo simulation). The electric power demand follows the heat demand but has a more fluctuating behaviour due to the on- and- off switching of the thermostatically controlled heating elements.

The maximum power demand in this simulation is higher for the 0.9 pu case than the 1 pu case.

---

<sup>9</sup> <https://remodece.isr.uc.pt/>

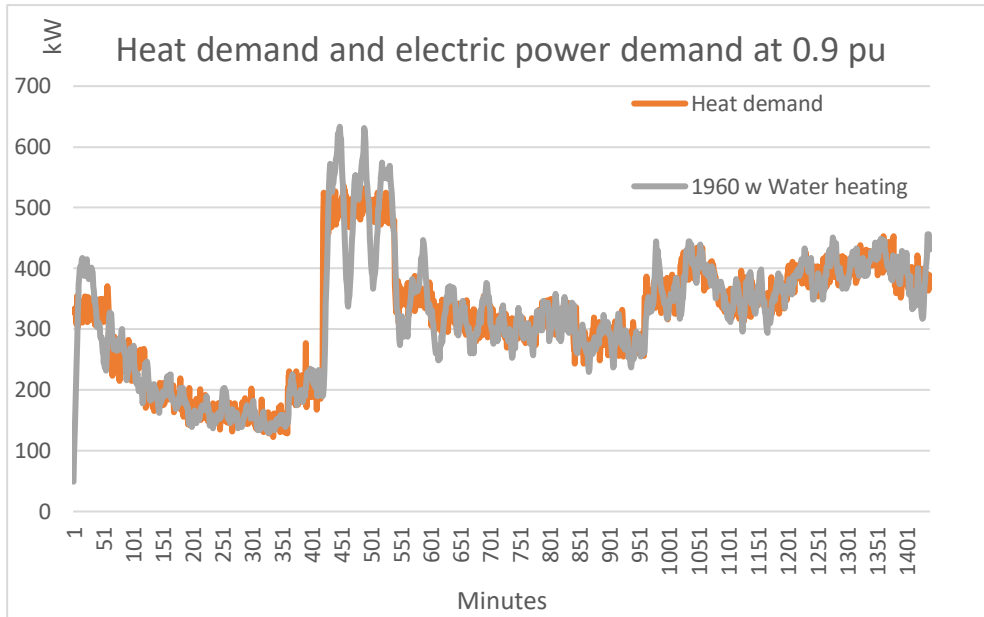


Figure 11-1: Heat demand and power demand from a 24-hour simulation of the aggregate effect of 1000 thermostatically controlled water heaters. The heat demand for each water heater comes from Monte Carlo simulation. The corresponding electric power demand for a water heater is a result of the heat demand and thermostat-controlled heating element's duty-cycle to keep the water in the water heater between threshold values. Each water heater has a nominal power of 2kW, but is here supplied with 0.9pu (207V) and therefore only supplying 1620Watts.

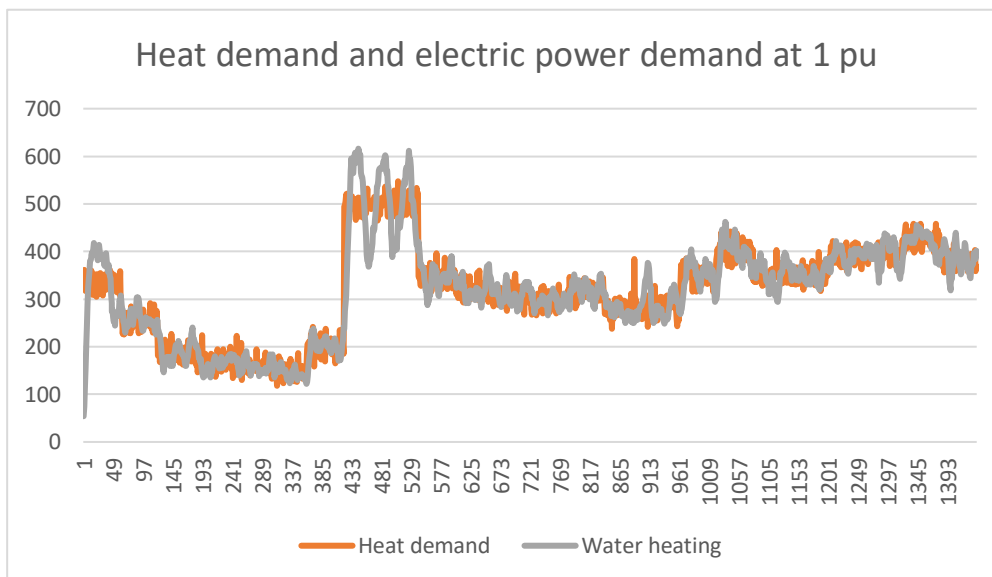


Figure 11-2: The heat demand is the same as for Figure 11-1 (refer to explanation above). Here however, the supply voltage for each water heater is 1 pu (230V) and thus each heating element delivers 2kW as long as they are active.

100 independent simulations of 24-hour periods have been performed. Due to the stochastic behaviour incorporated in the simulation by the Monte Carlo extraction, the 100 cases do not have the same heat demand curve. However, due to the probability distributions used in the Monte Carlo extraction, they

follow a similar load curve with higher demand in the morning hours and lower demand in the night and during the day when most people are at work/school etc.

From the 100 independent 24-hour periods, the peak power is found for each of the voltage levels simulated. The below figure shows the relationship between the voltage and the peak power demand from the simulations:

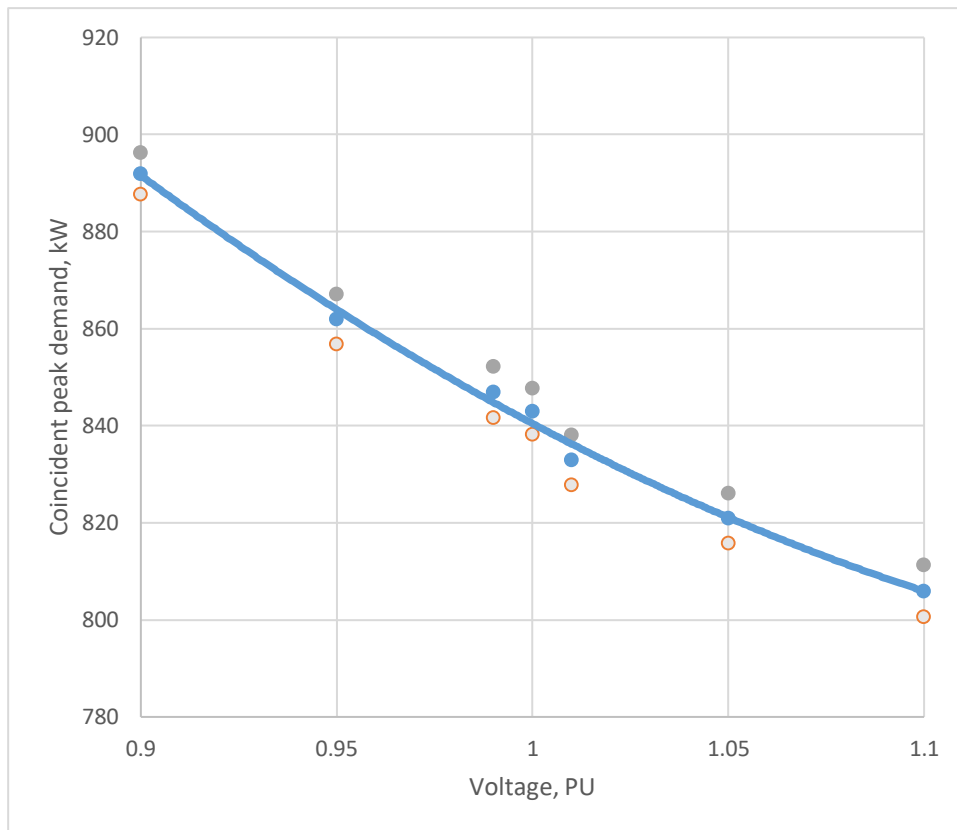


Figure 11-3: Expected values and 95% confidence interval resulting from 100 independent simulations of the aggregated effect of 1000 thermostatically controlled water heaters. Voltage of 1pu corresponds to 230V.

For each voltage level, three dots are plotted in the figure:

- the expected value (blue) based on the results from the 100 cases as well as
- a grey and orange dot showing the 95% confidence interval

According to the results from the simulations, the peak power demand of the aggregate load is expected to decrease with higher applied voltage. The energy demand of the water heaters on the other hand is independent of the voltage according to the simulation results.

### 11.1.3 Comments

Although the expected value of the peak power is higher for low voltages than for high voltages, it is important to notice that in practice, one may experience events where the case is the opposite. Due to the stochastic behaviour of the loads, in the worst case, all thermostatically controlled loads are on simultaneously. This is unlikely, but at least there may be instances in time where a large share of the appliances is on and thereby the power demand of the total load is high (i.e. high coincidence factor).



The probability of this to happen, seems to be higher when the voltage is lower, since lower voltage causes each appliance to be on for longer time intervals.

Comparable results from literature are found in [25]. In this reference, simulation results and field test from a load with large share of thermostatic controlled load in Montreal, Canada, is presented. It shows that following a voltage reduction, the power demand drops with the square of the voltage change (since the loads have a constant impedance characteristic). After about 15 minutes most of the load is restored to the level from before the voltage reduction. This is by the authors explained with the fact that the lower voltage causes the thermostatically controlled loads to remain on for longer time. In [58] where CVR is assessed by simulation including both open and closed loop loads. The simulation results show that the load-to-voltage relationship in one period of the simulated time series is negative, which can be due to the closed-loop load.

It should also be noted that the results from the simulation example would have been very different if a different thermostatically controlled appliance was used in the simulation. In the simulation, water heaters with an assumed constant-impedance characteristic is used (with power factor equal to unity). The rated power of each water heater at 1.0pu is 2kW, and hence at an applied voltage of 0.9pu the power demand is 1640 and at 1.1pu it is 2420W

Therefore, for higher voltages, shorter time is required to reach the upper temperature limit.

However, if the same simulation would be done for the heat pump tested in this thesis, the results would be different. The inverter-type heat pump has a constant-power characteristic. Hence, the power demand is determined only by the heat demand and the efficiency of the heat pump system and not by the voltage.

Thus, the energy demand as well as the expected value of the peak power for a collection of heat pumps would not be influenced by the voltage. Since the simulation is done without taking network losses into account, the voltage would not have any impact on the heat pump power and energy demand. However, if network losses are considered, lower voltage would cause higher current flows and higher losses.

In a real network there will be both water heaters, heat pumps, resistance heaters and other closed-loop loads. How the combination of all closed-loop and open-loop loads responds to a voltage strategy, will therefore be determined by the load composition. The impact of increase or reduction of losses in the total power and energy demand of the network depends on the type of lines, cables, transformers etc. in the area.

## 12 Discussion

Aggregation of loads is one of the major challenges for the component-based approach. For assessment of VC strategies in grids with considerable shares of closed-loop loads, the intertemporal effect of their voltage-dependency must be taken into account to obtain realistic results from simulations. Two approaches to doing so presented in literature is by representing loads as RC-circuits[58] or using the Equivalent Thermal Parameter model[27], [59]. In both cases, the voltage-dependency of the loads while turned “on” is taken into account, by using the exponential model or the ZIP model as done in [58] and [27], [59] respectively. Hence, the ZIP and exponential models obtained for the resistance heater, heat pump and induction cooktop in Part II of this thesis can be used in the modelling and simulation.

## Part IV - Conclusion and further work

### 13 Conclusion

This thesis addresses component-based load modelling and voltage control (VC) strategies. For determining the success of a given VC strategy, the voltage dependency of the loads connected to the network plays a vital role. Therefore, knowledge about the loads' voltage dependency and how this varies with time and load composition in the network is necessary if the effects of voltage control strategies are to be assessed before their implementation.

The thesis is divided into three parts, each addressing different aspects relevant for the scope of the thesis:

1. Voltage control and voltage control strategies
2. Voltage dependency of individual loads and network components
3. Load model aggregation

As part of the thesis, five electrical household appliances are tested in a laboratory and their voltage dependency is expressed in terms of two commonly used load models: the ZIP model and the exponential load model. The model coefficients of the load models for each tested device is estimated using curve fitting techniques. The tested devices are induction cooktop, resistance space heater, heat pump, washing machine and tumble dryer.

A general observation from the lab results is that the load characteristics of the individual devices vary according to the different user-defined settings applied. Both load curve, energy demand and voltage dependency characteristics vary between different user-defined settings for the same device. An example is the induction cooktop, which for some settings acts as a constant power load and for other settings exhibits a constant impedance characteristic. A different example is the washing machine, which throughout the different stages of the washing cycle incorporates constant impedance, constant current and constant power characteristics respectively.

For assessment of voltage control strategies and in many other power engineering applications, the behaviour of the aggregated load rather than the behaviour of individual appliances is the main concern. Load model aggregation is addressed in Part III of this thesis.

An important aspect of load model aggregation for VC strategy assessment is how closed-loop loads responds to voltage and how the aggregate effect of many individual closed-loop loads can be taken into consideration in load modelling and load flow simulations. Closed-loop loads that constitute a considerable share of the Norwegian residential load are thermostatically controlled space and water heating. These generally exhibit a constant impedance characteristic, and thus the short-term response to voltage reduction is reduced power demand. However, since the applied voltage influences the duty-cycle of the thermostatically controlled load, over time the aggregate power demand of the thermostatically controlled loads can be higher than the for the case with a higher voltage, since for low voltages the probability of more loads being active simultaneously is higher.

Some VC strategies implemented by DSOs in other countries are reviewed in the thesis, including Conservation Voltage Reduction (CVR). This strategy works on the assumption that the voltage dependency of the connected load is positive (i.e. reduction in voltage causes reduction in power and energy demand). Consequently, this strategy is only successful if large enough portions of the load demonstrate constant impedance or constant current characteristics. For closed-loop loads, the intertemporal effect

of the voltage strategy must also be taken into account. For such loads, voltage reduction does not lead to energy savings.

In a Norwegian context, VC strategies with the objective of reducing peak power may be more relevant than energy-conservation schemes. In the thesis, results from a simulation of the aggregate effect of voltage control on water heaters is presented. According to these results, the expected peak power of the aggregate load is reduced when voltage is increased. In further assessment of voltage control for peak power reduction, it is necessary to perform simulations that consider a wider collection of both closed-loop and open-loop loads as well as the network topology and associated losses.

As a conclusion it can be stated that since load characteristics are different in different networks and at different times a day/year, there is no one-size-fits-all for voltage control strategies. Additionally, since one may have different goals with implementation of a VC strategy, the desired strategy can vary between grid operators or even grid areas/feeders for the same grid operator. In all cases it is obvious that the behaviour of the loads connected to the network plays a significant role in determining the outcome of a strategy. Knowledge about the load composition in the network and the loads' dependency of voltage is therefore a crucial part of assessing different voltage control strategies. The results from the laboratory tests performed in this thesis contributes to enhanced knowledge about load behaviour and can be used in further work for VC strategy assessment as well as in other applications where load models and knowledge about load behaviour is needed.

## 14 Further work

The following points presents some aspects identified in the work with this thesis which can be relevant in future work:

- To obtain more robust results from the voltage-dependency tests and corresponding curve fitting, the devices can be tested at a larger number of different test voltages. Most of the tests in this thesis is performed with five to seven different voltages ranging from 210V to 250V. If more tests are performed, atypical results possibly resulting from errors introduced by mistakes in the test setup, environmental factors or other sources can easier be discovered and removed from the data set used in the analysis and curve fitting. Further, if more data points are used in the curve fitting procedure, the impact of extreme/atypical data points in the curve fit result is reduced.
- Obviously, there are many other appliances relevant in Norwegian households than the five devices tested in this thesis. The procedure followed in this thesis can be used to test other devices. It is especially interesting to test devices of newer date which may have other characteristics than older devices of similar types.
- Since closed-loop loads are highly relevant in Norway, it can be relevant to use the possibilities granted by the smart house and smart grid laboratory to do laboratory tests to find thermal characteristics for the loads widely used in Norway, for instance by using the RC-circuit model and the approach described in [1]
- In this thesis, the influence of voltage on the lifetime of loads is not considered. It is assumed that the devices are designed to operate at any voltage in the voltage range given by VQ limits. However, it should be noted that for some of the devices the operation voltage range specified in the user manuals is 220-240V. This can imply that voltages outside this range is not ideal for the optimal efficiency and/or lifetime of the appliance. Also, in the induction cooktop test at 253V, the device turned itself off due to internal overheating. In assessment of voltage control strategies this should be taken into account.

- All tested devices except the resistance heater feature power electronic controls. The current harmonics have been observed to be considerable for some of the appliances, especially in parts of the operation cycles. The harmonic contents have not been analysed as part of this thesis. However, the harmonic currents and voltages up to 40<sup>th</sup> order has been measured and logged and is available in the appendix for later research.
- In further work with assessing VC strategies for Norwegian DSOs, emphasis on modelling of closed-loop loads should be prioritized. In Norway, this type of load constitutes a large proportion of the total load and is therefore of special interest for Norwegian DSOs. Of the implemented VC strategies reviewed in this work, few are from grid areas with similar load behaviour. The majority of CVR implementations are from U.S. grids, and in many of these, air conditioning and cooling demand is a larger part of the load than what is the situation in the Norwegian residential load. Although the research on air conditioners can be useful for assessing the impact of increasing amounts of heat pumps amongst Norwegian households, the knowledge and experience from such research and real-world-implementation must be adapted to the load types, heating demand and load pattern reflecting the situation in Norway.
- This thesis focuses on residential loads. In assessing voltage strategies, it is also necessary to take into account commercial and industrial loads if the VC strategy is to be implemented in feeders where other loads than residential loads are connected.
- The number of electric vehicles is expected to increase rapidly in the years to come. If VC strategy is to be implemented it is important to investigate how charging of vehicles respond to the voltage level.
- The Norwegian energy regulatory authority, NVE, has presented plans to introduce price incentives in the grid tariffs in order to motivate consumers to reduce power peaks. When assessing voltage strategies, it should be taken into account that changes in tariff design may alter the future load mix in peak hours.

## References

- [1] K. McKenna and A. Keane, “Electrical and Thermal Characteristics of Household Appliances: Voltage Dependency, Harmonics and Thermal RC Parameters.” 2016.
- [2] IEC, “‘Electropedia: The World’s Online Electrotechnical Vocabulary’ by the International Electrotechnical Commission (IEC),” 2018. [Online]. Available: <http://www.electropedia.org>. [Accessed: 08-Dec-2018].
- [3] “Load representation for dynamic performance analysis (of power systems),” *IEEE Trans. Power Syst.*, vol. 8, no. 2, pp. 472–482, May 1993.
- [4] Cirgré Working Group C4.605, *Modelling and Aggregation of Loads in Flexible Power Networks*, no. February. 2014.
- [5] NVE, “Energi og effekt,” 2016. [Online]. Available: <https://www.nve.no/energibruk-og-effektivisering/energibruk-i-norge/energi-og-effekt/%0D>. [Accessed: 16-Jun-2019].
- [6] H. Kirkeby and M. Kolstad, “Nasjonalt potensiale for spenningsregulering,” SINTEF energi, 2016.
- [7] N. Lu, Y. Xie, Z. Huang, F. Puyleart, and S. Yang, “Load component database of household appliances and small office equipment,” 2008, pp. 1–5.
- [8] A. Bokhari *et al.*, “Experimental Determination of the ZIP Coefficients for Modern Residential, Commercial, and Industrial Loads,” *IEEE Trans. Power Deliv.*, vol. 29, no. 3, pp. 1372–1381, Jun. 2014.
- [9] P. Kundur, “Power system stability and control.” McGraw-Hill, New York, 1994.
- [10] A. Arif, Z. Wang, J. Wang, B. Mather, H. Bashualdo, and D. Zhao, “Load Modeling—A Review,” *IEEE Trans. Smart Grid*, vol. 9, no. 6, pp. 5986–5999, Nov. 2018.
- [11] “EN 50160, Voltage characteristics of electricity supplied by public electricity networks.” CENELEC, 2010.
- [12] “Forskrift om leveringskvalitet i kraftsystemet.” .
- [13] H. Kirkeby, “Virkningen av spenningsregulering på energibruk,” 2015.
- [14] “Conversation and e-mail correspondance with Rune Paulsen, NTE.” Trondheim, 2018.
- [15] “Conversation with Arnt-Magnar Forseth and Svein Skjevik , TrønderEnergi Nett.” Trondheim, 2018.
- [16] SINTEF Energi AS, “Kompensering i kraftnettet,” in *Planbok*, REN, 2016.
- [17] B. N. Torsæter, S. Garnås, and B. A. Høverstad, “Strategi for spenningsregulering i distribusjonsnettet,” Energi Norge, 2018.
- [18] J. Faiz and B. Siahkollah, “Past and Present,” in *Electronic Tap-changer for Distribution Transformers*, Berlin, Heidelberg: Springer Berlin Heidelberg, 2011, pp. 1–36.
- [19] C. R. Sarimuthu, V. K. Ramachandaramurthy, K. R. Agileswari, and H. Mokhlis, “A review on voltage control methods using on-load tap changer transformers for networks with renewable energy sources,” *Renew. Sustain. Energy Rev.*, vol. 62, pp. 1154–1161, Sep. 2016.
- [20] J. C. Das, *Power System Analysis - Short-Circuit Load Flow and Hamronics*. Marcel Dekker, Inc., 2002.

- [21] Magtech, “Magtech Voltage Booster, Technical data.” [Online]. Available: [http://www.magtech.no/userfiles/Model\\_overview\\_MVB\\_05.09.11\\_ENG.pdf](http://www.magtech.no/userfiles/Model_overview_MVB_05.09.11_ENG.pdf). [Accessed: 11-Dec-2018].
- [22] N. G. Hingorani, “Understanding FACTS : concepts and technology of flexible AC transmission systems.” IEEE Press, New York, 2000.
- [23] D. Pinney, “Costs and Benefits of Conservation Voltage Reduction,” 2013.
- [24] T. L. Wilson, “Measurement and verification of distribution voltage optimization results for the IEEE power & energy society,” *IEEE PES Gen. Meet. PES 2010*, pp. 1–9, 2010.
- [25] S. Lefebvre *et al.*, “Measuring the efficiency of voltage reduction at Hydro-Québec distribution,” in *2008 IEEE Power and Energy Society General Meeting - Conversion and Delivery of Electrical Energy in the 21st Century*, 2008, pp. 1–7.
- [26] Z. Wang and J. Wang, “Review on Implementation and Assessment of Conservation Voltage Reduction,” *IEEE Trans. Power Syst.*, vol. 29, no. 3, pp. 1306–1315, May 2014.
- [27] K. P. Schneider, J. C. Fuller, F. K. Tuffner, and R. Singh, “Evaluation of CVR on a National Level,” 2010.
- [28] A. Ballanti and L. F. Ochoa, “Voltage-Led Load Management in Whole Distribution Networks,” *IEEE Trans. Power Syst.*, vol. 33, no. 2, pp. 1544–1554, 2018.
- [29] A. Ballanti, L. N. Ochoa, K. Bailey, and S. Cox, “Unlocking New Sources of Flexibility: CLASS: the World’s Largest Voltage-Led Load-Management Project,” *IEEE Power Energy Mag.*, vol. 15, no. 3, pp. 52–63, 2017.
- [30] A. Kanicki, “Voltage Control in Distribution Systems,” in *Handbook of Power Quality*, A. Baghini, Ed. Chichester: Wiley, 2008, pp. 59–77.
- [31] J. V Milanovic, K. Yamashita, S. M. Villanueva, S. Ž. Djokic, and L. M. Korunović, “International Industry Practice on Power System Load Modeling,” *IEEE Trans. Power Syst.*, vol. 28, no. 3, pp. 3038–3046, Aug. 2013.
- [32] E. Hillberg *et al.*, “Development of improved aggregated load models for power system network planning in the Nordic power system Part 2 : Method verification,” *2018 Cigre Sess.*, 2018.
- [33] E. Hillberg *et al.*, “Development of improved aggregated load models for power system network planning in the Nordic power system Part 1 : Method development,” *c4 -104 cigre 2016*, no. C 4-104 CIGRE 2016, 2016.
- [34] Ecofys and Tractebel Engineering, “Identifying Energy Efficiency Improvements and Saving Potential in Energy Networks , Including Analysis of the value of Demand Response (Final report of the project ENER/C3/2013-423 Grid Energy Efficiency),” 2015.
- [35] “Western Power Distribution - Losses Strategy,” Western Power Distribution, 2018.
- [36] M. H. Heien, P. Melvær, R. Y. Sergieva, and T. H. Sliwinski, “Utvikling i nøkkeltal for nettselskap,” 2017.
- [37] P. S. Georgilakis, “Environmental cost of distribution transformer losses,” *Appl. Energy*, vol. 88, no. 9, pp. 3146–3155, Sep. 2011.
- [38] “National Smart Grid Laboratory, NTNU.” [Online]. Available: <https://www.ntnu.edu/smartgrid>. [Accessed: 27-Apr-2019].

- [39] “LMFIT documentation webpage.” [Online]. Available: <https://lmfit.github.io/lmfit-py/intro.html>. [Accessed: 21-May-2019].
- [40] J. Acero *et al.*, “The domestic induction heating appliance: An overview of recent research,” in *2008 Twenty-Third Annual IEEE Applied Power Electronics Conference and Exposition*, 2008, pp. 651–657.
- [41] M. Sweeney, J. Dols, B. Fortenbery, and F. Sharp, “Induction Cooking Technology Design and Assessment,” *2014 ACEEE Summer Study Energy Effic. Build.*, pp. 370–379, 2014.
- [42] “Online shop NetOnNet, product information about Wilfa Indux Induction Plate.” [Online]. Available: <https://www.netonnet.no/art/hjem-og-fritid/kjokkenapparater-kjokkenutstyr/kokeplaterogovner/wilfa-icp-2000/212367.11299/>. [Accessed: 12-May-2019].
- [43] B. Grinden and N. Feilberg, “Analysis of Monitoring Campaign in Norway (from REMODECE project),” 2008.
- [44] A. C. Bøeng, B. Halvorsen, and B. M. Larsen, “Kartlegging av oppvarmingsutstyr i husholdningene,” Statistisk sentralbyrå (SSB), 2014.
- [45] Energifakta Norge (Olje og Energidepartementet), “Energibruken i ulike sektorer.” [Online]. Available: <https://energifaktanorge.no/norsk-energibruk/energibruken-i-ulike-sektorer/>. [Accessed: 10-Jun-2019].
- [46] I. Staffell, D. Brett, N. Brandon, and A. Hawkes, “A review of domestic heat pumps,” *Energy Environ. Sci.*, vol. 5, no. 11, pp. 9291–9306, 2012.
- [47] N. Lu, Z. Huang, and Y. L. Xie, “Air Conditioner Compressor Performance Model,” no. August, 2008.
- [48] J. R. Turpin, “Inverters : Efficient , Comfortable , Quiet,” *Air Cond. Heat. Refrig. News*, vol. 255, no. 4, pp. 18–19, 2015.
- [49] M. Pipattanasomporn, M. Kuzlu, S. Rahman, and Y. Teklu, “Load Profiles of Selected Major Household Appliances and Their Demand Response Opportunities,” *IEEE Trans. Smart Grid*, vol. 5, no. 2, pp. 742–750, Mar. 2014.
- [50] R. Stamminger, “Synergy Potential of Smart Appliances - A report prepared as part of the EIE project „Smart Domestic Appliances in Sustainable Energy Systems (Smart-A)”,” Bonn, 2008.
- [51] M. Z. Degefa, H. Sæle, I. Petersen, and P. Ahcin, “Data-driven Household Load Flexibility Modelling: Shiftable Atomic Load,” in *2018 IEEE PES Innovative Smart Grid Technologies Conference Europe (ISGT-Europe)*, 2018, pp. 1–6.
- [52] A. Schmitz and R. Stamminger, “Usage behaviour and related energy consumption of European consumers for washing and drying,” *Energy Effic.*, vol. 7, no. 6, pp. 937–954, Dec. 2014.
- [53] G. Tsagarakis, A. Collin, and A. Kiprakis, “A statistical survey of the uk residential sector electrical loads,” *Int. J. Emerg. Electr. Power Syst.*, vol. 14, no. 5, pp. 509–523, 2013.
- [54] G. Tsagarakis, A. J. Collin, and A. Kiprakis, “Modelling the electrical loads of UK residential energy users,” 2012, pp. 1–6.
- [55] “Formålsfordeling av husholdningenes elektrisitetsforbruk i 2001. Sammenligning av

- formålsfordelingen i 1990 og 2001,” Statistisk sentralbyrå (SSB), 2005.
- [56] “User Manual, Heat Pump Dryer Samsung DV90N8289AW,” 2019. [Online]. Available: [http://downloadcenter.samsung.com/content/UM/201904/20190427123345970/DV8800N-DV6800N\\_DC68-03912J-03\\_EN.pdf](http://downloadcenter.samsung.com/content/UM/201904/20190427123345970/DV8800N-DV6800N_DC68-03912J-03_EN.pdf). [Accessed: 12-May-2019].
- [57] A. Perez Tellez, “Modelling aggregate loads in power systems.” 2017.
- [58] K. McKenna and A. Keane, “Open and Closed-Loop Residential Load Models for Assessment of Conservation Voltage Reduction,” *IEEE Trans. Power Syst.*, vol. 32, no. 4, 2017.
- [59] K. P. Schneider, J. C. Fuller, and D. Chassin, “Evaluating conservation voltage reduction: An application of GridLAB-D: An open source software package,” in *2011 IEEE Power and Energy Society General Meeting*, 2011, pp. 1–6.
- [60] S. Lefebvre and C. Desbiens, “Residential load modeling for predicting distribution transformer load behavior, feeder load and cold load pickup,” *Int. J. Electr. Power Energy Syst.*, vol. 24, no. 4, pp. 285–293, May 2002.
- [61] “Pandas webpage.” [Online]. Available: <https://pandas.pydata.org/>. [Accessed: 07-Apr-2019].
- [62] “Matplotlib webpage.” [Online]. Available: <https://matplotlib.org/>. [Accessed: 07-Apr-2019].
- [63] “NumPy webpage.” [Online]. Available: <http://www.numpy.org/>. [Accessed: 07-Apr-2019].
- [64] “Instrumentarkiv, Department of Electric Power Engineering, NTNU (Archive of lab instruments available in the Department’s laboratories).” [Online]. Available: <https://arkiv.elkraft.ntnu.no/instrumentarkiv/instsok.php>. [Accessed: 27-Apr-2019].
- [65] “Wilfa Indux ICP-2000 User Manual.” [Online]. Available: <https://www.manualsearcher.com/wilfa/icp-2000/manual?p=2>. [Accessed: 12-May-2019].
- [66] “Data Sheet ‘Siemens Unique varmeovn 2NC8,’” 2003. [Online]. Available: <http://efobasen.efo.no/ProductResources/933/ProductSheet/Unique.pdf>. [Accessed: 12-May-2019].
- [67] “User Manual, Washing machine Samsung WW10M86INOA,” 2018. [Online]. Available: [http://downloadcenter.samsung.com/content/UM/201802/20180220083317514/WW8800M\\_MANUAL\\_EN\\_DA\\_FI\\_NO\\_SV\\_DC68-03848J-00.pdf](http://downloadcenter.samsung.com/content/UM/201802/20180220083317514/WW8800M_MANUAL_EN_DA_FI_NO_SV_DC68-03848J-00.pdf). [Accessed: 12-May-2019].



## Appendices

### A Equipment

#### A.1 Test equipment

Device	Model, Serial number	Device number in NTNU instrument archive[64]	Specifications	Application in the test steup
<b>Programmable AC Power Supply</b>	ITECH 7626  Serial number 802325010737160006	B03-0614	Max output  300V  10 A when using the front panel  3 kVA	Used as the variable-voltage power supply in the tests.
<b>Power Quality and Motor Analyzer</b>	Fluke 438-II  Serial number 35603304  Firmware Revision V05.07	H02-0201		Used to measure current and voltage and log relevant electrical parameters during the tests.
<b>Current clamp</b>	Fluke i1000s AC Current Probe for Oscilloscope	I04-0480		Current measurement
<b>Current clamp</b>	Fluke i1000s AC Current Probe for Oscilloscope	I04-0481		Current measurement

<b>Extension cable with some of the outer insulation removed</b>	Clas Ohlson	N/A		To enable current measurement with current clamps, the individual phase conductors have to be accessible. The extension cable has one part where the outer insulation is removed. In that part, current clamps can be connected around the phase conductors.  The inner insulation is intact.
<b>PC with Fluke Power Log 5.6 software</b>	Power Log 430-II Software.  Version 5.6. 430-II-DLL: 1.2.0.14. Build: 5600. R: 2219		Data export can be done as tab-delimited .txt-files.	
<b>Temperature measurement device</b>		N02-0061		

#### A.1.1 Logged parameters and explanation regarding the data files

The measured parameters in the tests are current and voltage. Based on the measurements the Power Analyser calculates other power system parameters and logged those for each time step. The Power Analyser offer a wide range of optional parameters to be logged.

The time interval chosen for logging is 0.25 seconds, which is the most fine-grained time interval available for the Power Analyser. For each time step/time interval, both the minimum, maximum and average value for the time interval for each parameter is logged. In this thesis, the average values have been used in the data analysis and plotting.

Note that not all the logged parameters are meaningful. The real test configuration is a IT configuration, whereas the configuration setting chosen in the Power Analyser is TN. Therefore, the column names given for the logged parameters does not comply with the real setup.

For an IT configuration, one phase loads are connected line to line and there is no neutral wire. For TN, one-phase loads are connected between phase line and the neutral wire.

The following logged measurements and parameters are therefore not meaningful:

- Parameter marked with “NG”. NG should be the voltage between ground and neutral. However, the ITECH Power supply has a floating ground (is not grounded to the system ground), and the measurements ‘NG’ are therefore not meaningful.
- Current in line “N”.
- Power time series marked with “Total”

Parameter	Unit		Meaningful measurement
Voltage	V		L1N
Current	A		L1
Active power	W		L1N
Reactive power	VA <sub>r</sub>		L1N
Apparent Power	VA		L1N
Frequency	Hz		n/a
CosPhi	Unitless (0-1)		L1N
DPF	Unitless (0-1)		L1N
PF	Unitless (0-1)		L1N
THD voltage			L1N
THD current			L1
Voltage harmonics		1 <sup>st</sup> to 40 <sup>th</sup> harmonic	L1N
Current harmonics		1 <sup>st</sup> to 40 <sup>th</sup> harmonic	L1

The measurement files are added in a ZIP-file. For each measurement there are files with different formats:

- Fpqo -file. This is the type of file obtained from the Fluke software Power Log 5.6
- Txt-file with mixed encoding. The encoding in the header is different from the encoding in the rest of the file. This is the file exported from Power Log 5.6.
- Txt file with cp1252 encoding in both heading and body. This file can easily be read in Python using Pandas dataframes

- “Compact DF”-files. Since the original files are large and only some of the parameter time series were used in the thesis work, these files contain the relevant data used in the thesis. Rows in the start and end of the files witch were recorded before and after the test and therefor was not relevant is removed. Therefor these files are named “compact&clean”

The txt-files are tab-delimited.

## A.2 Tested devices

Table containing information about the household equipment that has been tested.

Type of device	Model	Serial number	Specifications and ratings	User manual or other product information
<b>Induction cook-top</b>	Wilfa Indux Induction plate ICP-2000	06/14  Device number in NTNU instrument archive [64]: P02-0306	220-240V 2000W	Information from vendor [42], user manual [65]
<b>Heat pump/ Air condition</b>	Samsung  Indoor: AC026KNADEH /EU  Outdoor: AC026JXSCEH/ EU	Indoor: 0FZHPAKK1000 04L  Outdoor: 0EE1PAFJ60002 0Z	220-240V Climate class T1  Refrigerant R410A  Rated power input: 26.5W Rated current: 0.3A  Capacity (cool/heat): 2.6/3.5 kW	<a href="https://manualzz.com/doc/49959296/samsung-cac--sieninis-laikiklis--šilumos-siurblys--lph-va...">https://manualzz.com/doc/49959296/samsung-cac--sieninis-laikiklis--šilumos-siurblys--lph-va...</a>
<b>Space heater</b>	Siemens Type: 2NC7 082 2LV	214/7801	230V 800W	Data Sheet for similar space heater (Type 2NC8) [66]

<b>Washing machine</b>	Samsung WW10M86INO A	0A3953AK20006 3N	220-240V 2000-2400 W	User manual[67]
<b>Heat Pump Dryer</b>	Samsung DV90N8289AW	0T5F5AEK3000 80P	Refrigerant R134a 220-240W 550-600W	User manual[56]

### A.3 Software

Two computers are used in the work with the thesis. PC 1 is used for downloading data from the Power Analyser and saving the data as txt-file in a format easily readable by the Python script.

PC 2 is used for writing the Python code and using the code to read the txt-files and analyse the data.

PC 1:

Intel(R) Core(TM) i3-2350M CPU @ 2.30GHz

4GB RAM

64-bit operating system, x64-based processor

PC 2:

Intel(R) Core(TM) i5-3210M CPU @ 2.50GHz

16GB RAM

64-bit operating system, x64-based processor

<b>Computer</b>	<b>Software used for the tests</b>	<b>Details</b>	<b>Use</b>
-----------------	------------------------------------	----------------	------------

<b>PC 1</b>	Windows 10 Enterprise	Version 1803 Installed on 14.03.2019 OS Build 17134.438  Control panel, location: format English (United States)	Operating system of the computer
	Power Log 5.6	Power Log 430-II Software. Version 5.6. 430-II-DLL: 1.2.0.14. Build: 5600. R: 2219	For downloading logged data from the Power Analyser and exporting the data as txt-file
	Microsoft Excel 2010	Date created 23.05.2012 Date Modified 23.05.2012	For importing the txt-file from the Power Log 5.6. and creating new txt-file with encoding windows-1252 (cp1252)
<b>PC 2</b>	Windows 10 Education	Version 1809 Installed on 23.03.2019 OS Build 17763.379	Operating system of the computer
	Anaconda, Spyder	Python 3.7.1	

## B Curve fitting

The nominal power in the load model expressions,  $P_n$  (or  $Q_n$ ), should be the active (or reactive) power drawn by the load when the nominal voltage ( $V_n$ ) is applied to it. However, as there are system losses and measurement errors in the test setup, none of the tests are done at exactly 230V. In general, the average measured voltages for the performed tests is 0.5-1V lower than the voltage referred to as the “test voltage” in this thesis. The test voltage is the voltage for a given test which the Power Supply is programmed to give as output voltage. The measured voltage on the other hand, is the voltage measured by the Power Analyser. Therefore, the nominal power values  $P_n$  and  $Q_n$  cannot be read directly from

the measured data. Instead, preliminary curve fits to find the nominal powers are performed before doing the curve fits to find the load model parameters.

Bokhari et al. [8] has conducted laboratory experiments to find ZIP model parameters for various loads. In this reference, the nominal power value is found by doing a preliminary least square fit in the voltage range  $V_{nom} \pm 3V$  with unconstrained coefficients (i.e. the sum  $Z+I+P$  are not bound to equal one). Afterwards a new, this time constrained, least square fit is performed to find the ZIP-coefficients.

A similar procedure is followed in this thesis. However, in cases where a device is only tested with five test voltages (210, 220, 230, 240, 250), all of these are used in the preliminary curve fit. In cases where more datasets are available, the datasets for the test-voltages closest to the nominal voltage (230V) are used in the preliminary curve fit.

The nominal voltage is fixed at 230V for all curve fits performed in the thesis since this is the nominal voltage for single-phase loads in the Norwegian power system

The following procedure is followed:

1. A “preliminary” least squares minimization is performed where the nominal power is included as a parameter to be found in the minimization (i.e. the nominal power is not fixed in the minimization). The result from this curve fit is used to calculate the nominal power.
2. The “final” least squares fit is performed. In this curve fit the nominal power found in step 1 is used and is fixed in the minimization.

The data points used in the curve fitting are from the measurements obtained from the lab tests. The below figure illustrates the procedure from the lab tests are performed until the load model coefficients are obtained.

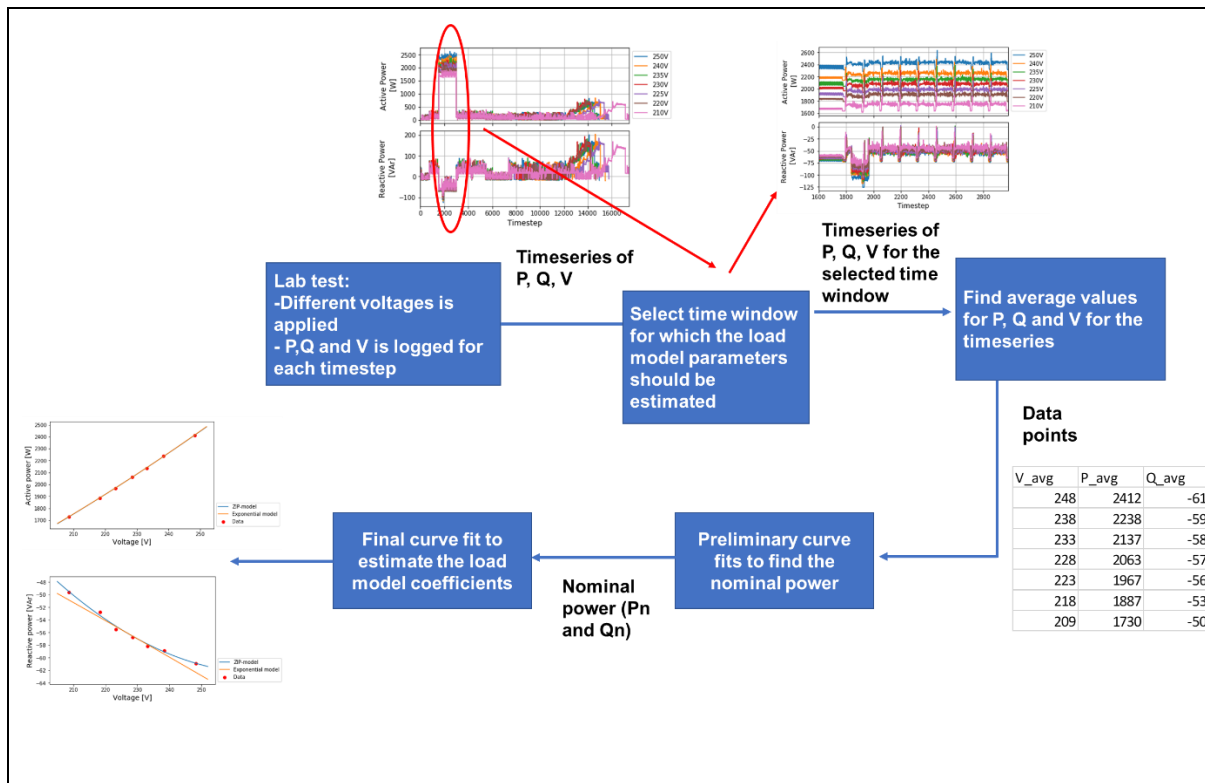


*Illustration of the procedure from lab tests is performed until the load model coefficients are estimated. The example used is for the washing machine test and estimation of the load model parameters for the time window where water is heated.*

The LMFIT package allows curve fitting with different fitting methods. The default method is Levenberg-Marquardt, for which much of the documentation and examples in [39] is based. Therefore, this method is mostly the method of choice in this thesis. Since the method has the disadvantage that it might only find the local minimum to an optimization problem where more than one minimum exists[39], the curve fitting has been tested with some other methods available in LMFIT as well (amongst others Truncated Newton). For the preliminary fitting Truncated Newton method is chosen, since for these curve fitting problems it is found that the results from the Levenberg-Marquardt method is more sensitive to the choice of initial guesses for the model parameters.

The tables with the curve fit results contains information about the size of the residuals obtained the curve fit. This information is listed using the names and definitions from LMFIT, namely:

Chi-square:	$X^2 = \sum_i^N [Residual_i]^2$	
Reduced chi-square:	$X = \frac{X^2}{N - N_{variables}}$	N = number of data points N <sub>variables</sub> = number of variables in the fit

I.e. the chi-square and reduced chi-square provided in the tables are from the “best fit” found in the curve fitting algorithm.

Details about the preliminary and final curve fits:

- A preliminary fit
  - o Objective: estimate the nominal power
  - o Method: Truncated Newton
    - (The default method is Levenberg-Marquardt, for which much of the documentation and examples in [39] is based. Therefore, this method is mostly the method of choice in this thesis. Since the method has the disadvantage that it might only find the local minimum to an optimization problem where more than one minimum exists[39], the curve fitting has been tested with some other methods available in LMFIT as well (amongst others Truncated Newton). For the preliminary fitting Truncated Newton method is chosen, since for these curve fitting problems it is found that the results from the Levenberg-Marquardt method is more sensitive to the choice of initial guesses for the model parameters.)
  - o The constraint Z+I+P = 1 is not applied
  - o The ZIP model is used. The result is later used for both the ZIP and exponential model.
  - o The data points for the tests closest to 230V are used. In some cases (where few datapoints are available), all datapoints is used in the fit.
- Final fit:



- Objective: estimate the model parameters (for ZIP and exponential model)
- Method: Levenberg-Marquardt
- The constraint  $Z+I+P = 1$  is applied
- Nominal voltage  $V_n = 230V$
- Nominal power: fixed to the value found from the preliminary fit.

## C Test details

A ZIP-file containing the fpqo- and txt-files with the measurement data from the tests is provided as appendix to the thesis. Each file name starts with “MEASxxx” where the xxx is a unique three-digit number identifying the respective tests. This number will hereafter be referred to as the MEAS-number (measurement number). In the following subchapters some information about the tests are provided together with the MEAS-number.

### C.1 Induction cooktop

All tests are performed with the same pan filled with 1 litre of water. Between each test the pan and cooktop are allowed to cool down to ensure similar starting conditions for all test. Each test is run with fresh water from the sink (the water is changed between the tests). The initial water temperature is around 19-24 degrees Celsius for the respective tests (see tables below). The cooktop is turned off when the measured water temperature reached approximately 100 degrees.

The test procedure is as follows:

1. Power supply is turned on
2. Measurement logging turned on
3. The cooktop is turned on and the desired setting is chosen
4. When measured water temperature reached 100 deg (50 deg in some tests), the cooktop is turned off.

The time from between step 2 and 3 may vary slightly between each test. Therefore, there is a varying amount of time steps in the test data which are measurements of the stand-by operation of the cooktop.

Test voltage	Cooktop setting	Initial water temperature (°C)	End water temperature (°C)	MEAS-number (saved as)
211.6	1600W	21.6	101.6	168
216.2	1600W	20.8	100.0	173
220.8	1600W	19.6	100.0	174
225.4	1600W	20.7	100.9	175
230	1600W	23.3	100.1	165
234.6	1600W	21.9	101.2	176

239.2	1600W	21.5	100.0	179
243.8	1600W	19.4	100.1	172
243.8	1600W	22.2	100.8	178
248.4	1600W	21.8	101.2	171
253	1600W	21.5	98.0*	166

\*Under this test, the cooktop went into error “E6 - internal overheating” and turned itself off. At the moment the error occurred, the water temperature is 98 °C.

Several attempts is made to do the test at 207V. Every time the cooktop seemed to go into “Max Power”-setting. Some of the time series obtained from these attempts are presented together with the other MaxPower-tests

Test voltage	Cooktop setting	Initial water temperature (°C)	End water temperature (°C)	MEAS-number (saved as)
207	Max Power	20.9	101.6	167
207	Max Power	24.8	100.1	198
207	Max Power	21.6	103.3	199
216.2	Max Power	20.2	100.8	169
230	Max Power	22.7	101.2	196
239.2	Max Power	22.2	100.9	177

Test voltage	Cooktop setting	Initial water temperature (°C)	End water temperature (°C)	MEAS-number (saved as)
210	300W	24.1	50.3	185
220	300W	25.1	52.0	184
230	300W	24.4	52.2	180
240	300W	24.5	51.2	181
250	300W	24.7	51.7	182

Test voltage	Cooktop setting	Initial water temperature (°C)	End water temperature (°C)	MEAS-number (saved as)
210	800W	22.8	101.5	193
220	800W	22.5	100.9	192
230	800W	24.8	100.5	187
240	800W	23.8	100.9	189
250	800W	21.3	100.5	191
260	800W	22.1	100.3	190

Test voltage	Cooktop setting	Initial water temperature (°C)	End water temperature (°C)	MEAS-number (saved as)
230	1100	25.1	100.7	186

## C.2 Space heater

Test voltage	Temperature setting	Power setting	MEAS-number (saved as)
210-250 (varied in steps)	Max	1	207
210-250 (varied in steps)	Max	2	206

## C.3 Washing machine

Laundry load	Weight
A	1.5 kg
B	4 kg
C	0.8 kg
D	0.5 kg

All tests are performed with the same clothes.

In all tests the “Auto Detergent” setting is used. This means that the washing machine regulates the amount of detergent. The amount of auto detergent is set to 2/3 lines, which is the default option for this washing machine.

Test voltage	Laundry load	Program	Washing time	Degrees [°C]	Rinse	Spin	MEAS-number (saved as)
230	A	Cotton	1h 6min	40	2	1600	209
240	A	Cotton	1h 6min	40	2	1600	212
220	A	Cotton	1h 6min	40	2	1600	233
210	A	Cotton	1h 6min	40	2	1600	226
250	A	Cotton	1h 6min	40	2	1600	228
225	A	Cotton	1h 6min	40	2	1600	239
235	A	Cotton	1h 6min	40	2	1600	241

Test voltage	Laundry load	Program	Degrees [°C]	Rinse	Spin	MEAS-number (saved as)
230	B	Cotton	90	2	1600	219
230	B	Hygiene Steam	60	4	1400	221
230	C	Delicates*	30	2	800	224

230	A	Cotton	60	2	1600	230
230	A	Eco Cotton	40	2	1600	217

\*Manual detergent is used instead of Auto detergent.

#### C.4 Heat Pump Dryer

Test voltage	Laundry load	Program	Dry time	Dry level		MEAS-number (saved as)
230	A	Time Dry	1 h	2		211
240	A	Time Dry	1 h	2		213
220	A	Time Dry	1 h	2		218
210	A	Time Dry	1 h	2		227
250	A	Time Dry	1 h	2		229
225	A	Time Dry	1 h	2		240
235	A	Time Dry	1 h	2		242

Test voltage	Laundry load	Program	Dry level		MEAS-number (saved as)
230	A	Quick Dry 35		Clothes did not dry. Quite moist	216
230	B	Optimal Dry: Cotton	2	Clothes are almost dry, but not 100%	220

230	B	Optimal Dry: Cotton	2	This is done after test 221 (spin 1400). Hence, the laundry might have been moister before drying than when using 1600 spin.	222
230	B	Manual Dry: Warm Air	N/A		223
230	D	Optimal dry: Delicates	2	Not entirely dry	225
230	A	Optimal Dry: Mixed Load		Dried	234
230	A	Optimal Dry: Super Speed	2	Did not dry properly	231
230	A	Optimal Dry: Super Speed	2	This is performed after MEAS231 since the clothes did not dry properly running the program only once.	232

\*Optimal Dry Cotton: The time showed when starting the drying program is 3h 8min. The program did not last that long.

## D Results

### D.1 Induction cooktop

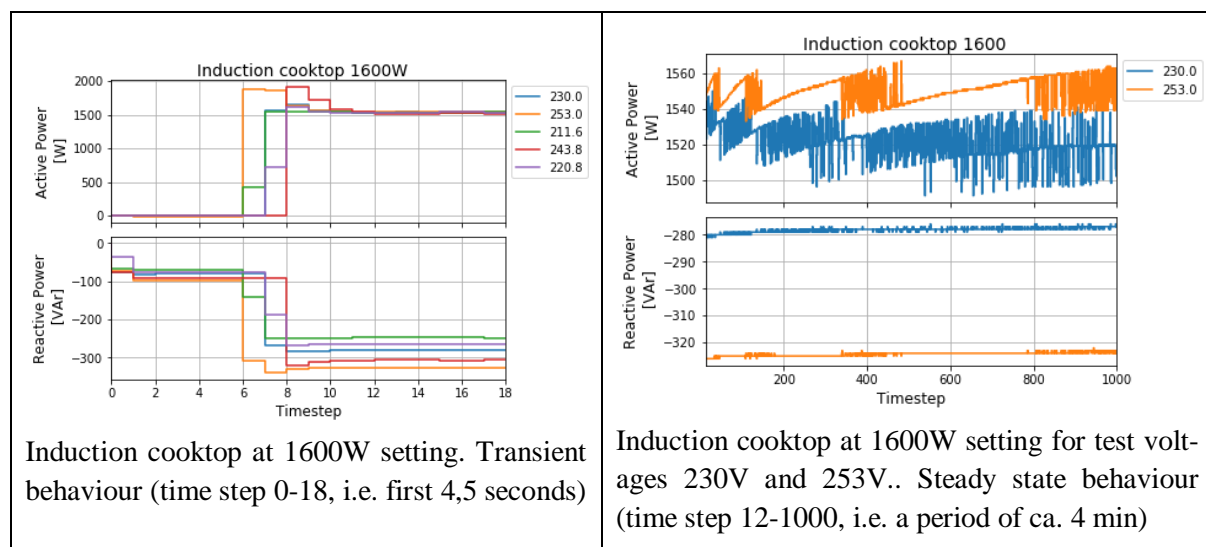
#### D.1.1 Test with 1600W setting

The option chosen at the cooktop is Power=1600W. No other parameters (time, temperature) are changed from the default options. The test is run at 10 different voltages from 211.6 to 253 V. Several attempts are done to perform a test at 207V. However, for all these tests the cooktop seemed to enter into “Max power”-mode, although the 1600W-setting is chosen.

All tests lasted for about four minutes. Throughout the whole cycle the cooktop draws approximately the same power. An exception is the first 0,5-1 seconds, where the power output is significantly higher than for the rest of the cycle. This start-up behaviour is shown for five of the ten tests in the below figure.

For the purpose of finding model parameters, the steady state behaviour is of interest. It has been chosen to use the time widow of time step 12-1000 in the analysis (which corresponds to a period of approximately 4 minutes).

By disregarding the first 11 time steps, the effects of the transient start-up behaviour is avoided. The figure to the right below shows the active and reactive load curve for the chosen time window (time step 12-1000). Only two of the ten voltage timeseries are plotted. The other eight show similar behaviours. However, the load pattern of each measured voltage level is not exactly equal and therefore no obvious “steady state” could be selected from the time series. Therefore, the whole 4-minute sequence is regarded as steady state. The average values for active and reactive power for the whole time window has been used to find the load model parameters.



The table below shows the average parameter values for the time window 12-1000. It also shows the variance for active and reactive power measurements within the time window. For finding the model parameters, the average values for power and voltage from the table is used in the curve fit. Due to losses in the system and measurement errors introduced by the Power Supply and the Power Analyser,

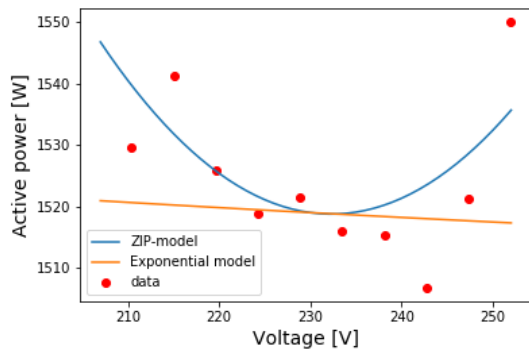
the measured voltages are not equal to the test-voltages applied from the Power supply but differ with ca 1V.

<b>Test voltage (supplied)</b>	<b>V_avg (measured voltage)</b>	<b>P_avg</b>	<b>P_var</b>	<b>Q_avg</b>	<b>Q_var</b>	<b>Energy [Wh]</b>	<b>Duration [Min]</b>
<b>253</b>	251.9	1550.1	44	-324.3	0.47	106	4
<b>248.4</b>	247.3	1521.3	32	-314.1	0.42	104	4
<b>243.8</b>	242.7	1506.8	107	-304.4	0.75	103	4
<b>239.2</b>	238.1	1515.4	102	-296.1	0.65	104	4
<b>234.6</b>	233.5	1516.0	87	-287.1	0.73	104	4
<b>230</b>	228.9	1521.5	110	-278.2	0.79	104	4
<b>225.4</b>	224.3	1518.8	78	-269.8	0.62	104	4
<b>220.8</b>	219.7	1525.8	74	-261.3	0.69	105	4
<b>216.2</b>	215.0	1541.3	63	-253.8	0.80	106	4
<b>211.6</b>	210.4	1529.7	84	-244.4	0.61	105	4

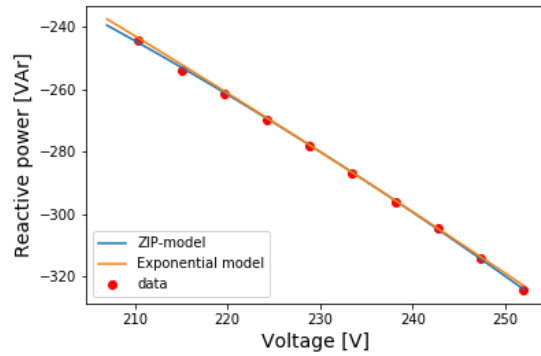
*Induction cooktop at 1600W setting. Average and variance values for power and voltage values for the steady state cycle (time step 12-1000)*

The preliminary least squares-fit for finding the nominal powers ( $P_n$  and  $Q_n$ ) is done using the five voltage tests from 220.8 to 239.2. In the least squares fit for finding the other load model parameters (ZIP-coefficients and exponents respectively), data from all the ten tests are used.





Induction cooktop at 1600W, active power. Data-points together with fitted curves for ZIP and exponential model.



Induction cooktop at 1600W, reactive power. Datapoints together with fitted curves for ZIP and exponential model.

Fit results for different time windows

Time window (time steps)	$P_{nom}$	$Z_p$	$I_p$	$P_p$	Power at 207 and 253 V
12-1000	1519	1.52	-3.07	2.55	1547 and 1537
500-1000	1519	1.36	-2.74	2.38	1542 and 1534
600-800	1519	1.43	-2.87	2.44	1544 and 1537
300-1000	1519	1.42	-2.87	2.44	1544 and 1537
400-700	1519	1.38	-2.79	2.41	1545 and 1535
12-400	1519	1.68	-3.40	2.72	1551 and 1538
<b>Variance:</b>	0	0.0117	0.0499	0.0133	8.25 and 1.556

*Induction cooktop at 1600W. ZIP-parameters for different time windows*

In reality, all the tests did not last equally long. However, since the starting and stopping conditions of the tests are not 100% comparable (water temperature and possibly other factors), the data is not of sufficient quality to compare the duration of heating the water at different voltages. Appendix C.1 presents some information about each test, including the starting and ending temperature of the water in each test.

### D.1.2 Test with 800W setting

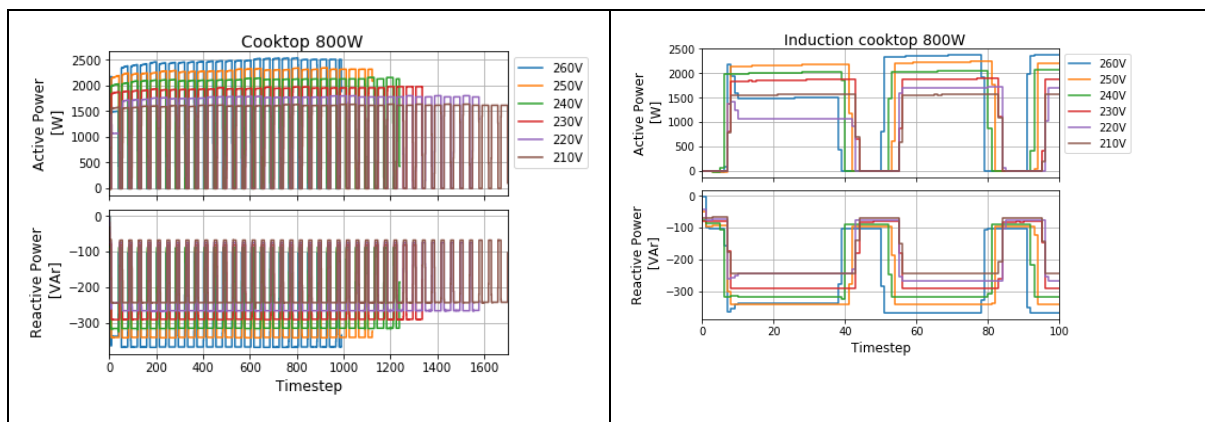
For this setting, the power is alternating between intervals of peak power and intervals with close-to-zero power. When in the peak-power period, or “on-state”, it shows a strong dependency on voltage.

For finding the voltage dependency, at least two alternative approaches are possible:

- Finding the model parameters for the on- and off-states independently, i.e. finding two independent sets of model parameters.
- Finding model parameters for the average behaviour of the cycle, i.e. taking into account both the on- and off-state in the same set of model parameters.

To disregard the transient behaviour in the load modelling, it is decided to exclude the first 50 time steps (12.5seconds). Since the duration of the measurements time series are not equally long, it is decided to choose a time window in the analysis for which all time series have values. Therefore the time window 50-900 is chosen. The reason for the varying durations of the time series is how the tests are conducted, namely by measuring the electrical parameters of the cooktop while the temperature of the water in the pan is measured. The tests are stopped when the water temperature reached approximately 100 °C (for details see appendix C.1). Since the power drawn by the cooktop differ between the tests, it is expected that also the time required for the water to boil, differ between the tests.

Three sets of model parameters will be found.

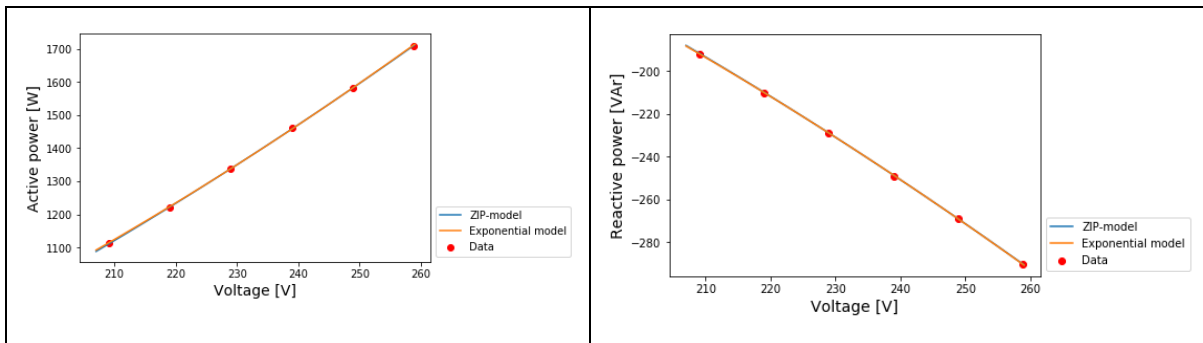


All of the datapoints (i.e. tests) are used in the preliminary fit to find the nominal powers,  $P_n$  and  $Q_n$ , since the total number of datapoints is quite small. With four unknown parameters in the model, at least four datapoints is required in the least squares fit. Time-window used is 50-900.

Firstly, the model parameters for the case where the average behaviour is considered will be presented.

	<b>Best fit</b>	<b>Chi-square (Reduced chi-square)</b>
<b>V<sub>nom</sub></b>	230 V	
<b>P<sub>nom</sub></b>	1350 W	

<b>Qnom</b>	-231 VAr	
<b>Zp</b>	0.826	7.996 (Reduced: 1.999)
<b>Ip</b>	0.369	
<b>Pp</b>	-0.195	
<b>Zq</b>	0.840	0.1600 (Reduced: 0.040)
<b>Iq</b>	0.262	
<b>Pq</b>	-0.102	
<b>Np</b>	2.010	9.963 (Reduced: 4.982)
<b>Nq</b>	1.938	0.230 (Reduced: 0.046)



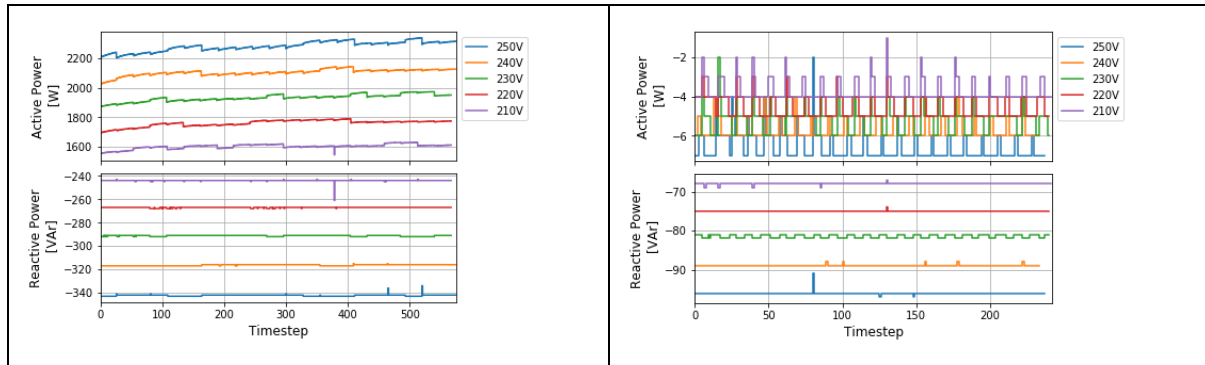
a) Finding the model parameters for the on- and off-states independently

For this case, the procedure of finding the parameters are as follows:

- For each test, the measured data time series for the electrical parameters (V, I, P, Q, THD, etc) are split into two datasets:
  - A dataset with all time steps where the active power (P) is above a threshold value. The threshold values are set for each test to a value which ensured that only the “steady-state on-state” measurements are included in the dataset. It is namely observed that between the on-state and off-state, the active power is measured at a value lying between the on- and offstate steady state values. For all the tests and for all changes from on to off state and from off to on-state, it is observed one time step measurement with a “transient” behaviour. Note that one time step represents the average of the measured values over 250ms. Hence, how the active power changes within this 250ms can not be

observed from the measurements with the resolution available from the Power Analyser used in this thesis. Since the goal of the tests and load modelling is to find the steady state behavior of the tested loads, the transients are excluded in the modelling.

- A dataset with all time step where the power is below 0 W, i.e. the “off-stat” of the cycle.

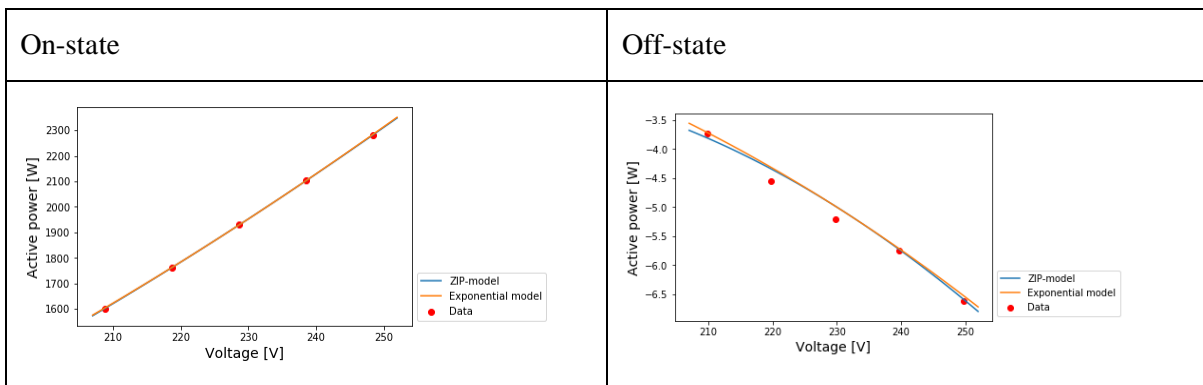


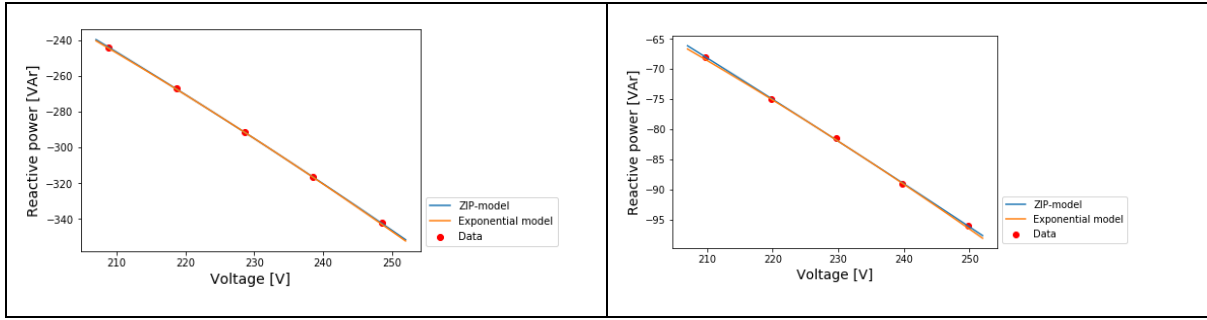
The above figures show the on- and offstates of the load cycle independently from each other. Hence the timesteps on the x-axis are not necessarily subsequent timesteps, but should only be used to get an idea of the duration of the variations in the load profiles.

	<b>Best fit, on-state</b>	<b>Chi-square (Reduced chi-square)</b>
<b>Vnom</b>	230 V	
<b>Pnom</b>	1952	
<b>Qnom</b>	-295	
<b>Zp</b>	0.91	21.48 (7.16)
<b>Ip</b>	0.21	
<b>Pp</b>	-0.12	
<b>Zq</b>	0.66	0.32 (0.11)
<b>Iq</b>	0.61	
<b>Pq</b>	-0.27	
<b>Np</b>	2.04	30.81 (7.70)

<b>Nq</b>	1.94	0.95 (0.24)
-----------	------	----------------

	<b>Best fit, off-state</b>	<b>Chi-square (Reduced chi-square)</b>
<b>Vnom</b>	230 V	
<b>Pnom</b>	-5	
<b>Qnom</b>	-82	
<b>Zp</b>	5.68	0.10 (0.03)
<b>Ip</b>	-8.15	
<b>Pp</b>	3.47	
<b>Zq</b>	0.32	0.13 (0.04)
<b>Iq</b>	1.33	
<b>Pq</b>	-0.65	
<b>Np</b>	3.23	0.11 (0.03)
<b>Nq</b>	1.96	0.13 (0.04)





By counting the instances of “on-state”-active power and “off-state”-active power in the measured time series of active power, it is found that the duration of the off-state is 11-12 time steps and the on-state is 27-28 time steps for each on/off -cycle. This corresponds to 3 seconds off and 7 seconds on. By using this information, one could make a time variant model of the cooktop load profile, utilizing the sets of model parameters found for the off- and on-states respectively.

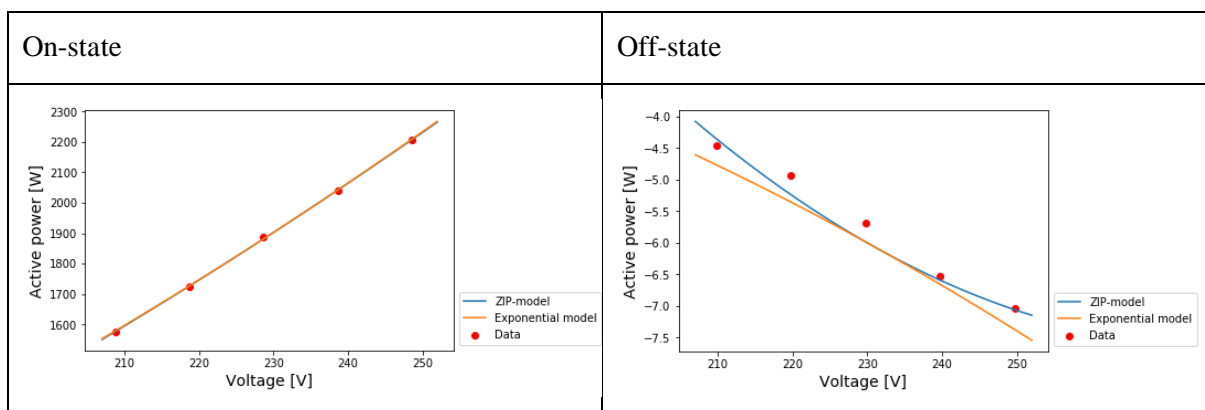
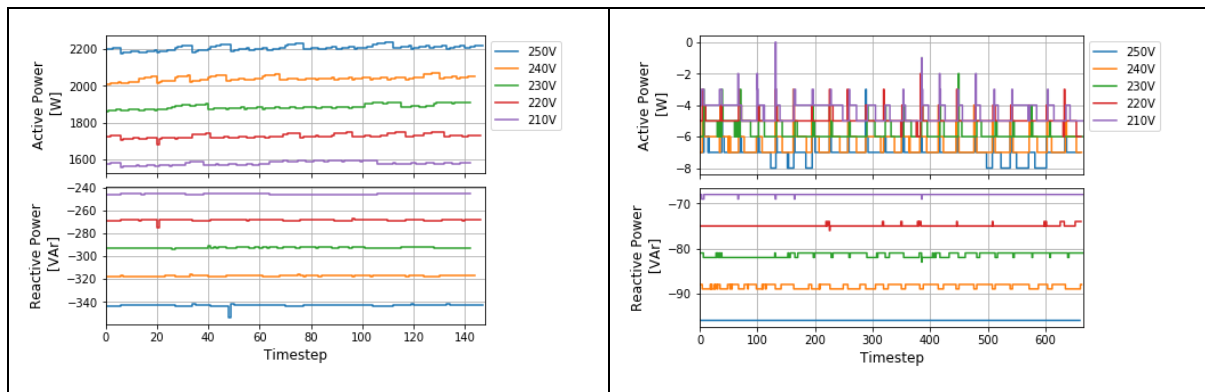
on-state	V	P	P_var	Q	Q_var	PF	THD_A	THD_V	Energy [Wh]	Duration [Min]
<b>250V</b>	248.5	2282	1047	-342	0.42	0.99	2.17	0.02	91.3	2.40
<b>240V</b>	238.6	2105	458	-316	0.24	0.99	2.20	0.02	84.0	2.40
<b>230V</b>	228.6	1932	536	-291	0.20	0.99	2.24	0.02	76.2	2.37
<b>220V</b>	218.7	1760	465	-267	0.08	0.99	2.23	0.02	69.4	2.37
<b>210V</b>	208.8	1602	250	-244	0.54	0.99	2.31	0.02	63.2	2.37

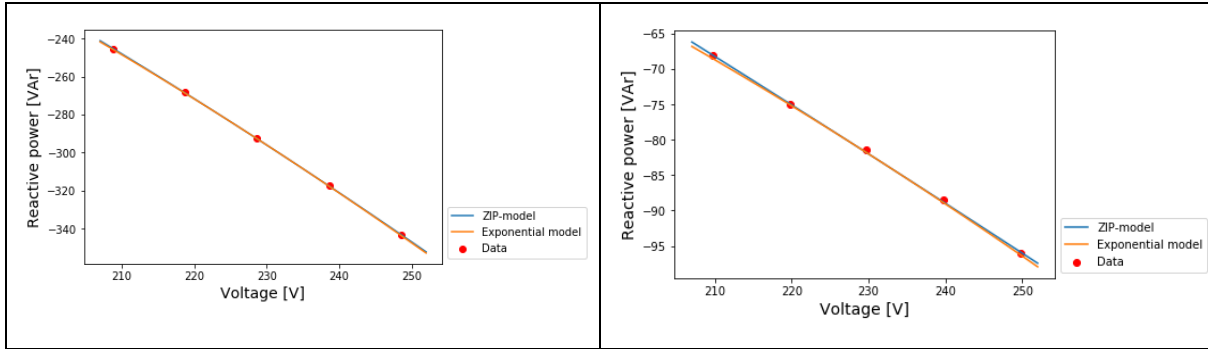
Off-state	V	P	P_var	Q	Q_var	PF	THD_A	THD_V	Energy [Wh]	Duration [Min]
<b>250V</b>	249.7	-6.6	0.43	-96.0	0.11	-0.07	10.4	0.01	-0.11	0.99
<b>240V</b>	239.7	-5.7	0.24	-89.0	0.02	-0.06	10.7	0.01	-0.09	0.98
<b>230V</b>	229.8	-5.2	0.38	-81.5	0.25	-0.06	11.3	0.01	-0.09	1.00
<b>220V</b>	219.8	-4.5	0.30	-75.0	0.00	-0.06	12.0	0.01	-0.08	1.00
<b>210V</b>	209.8	-3.7	0.28	-68.0	0.02	-0.05	12.8	0.01	-0.06	1.01

### D.1.3 Test with 300W setting

As for the 800W setting, the 300W setting shows a on-off-behaviour. Therefore load model parameters are found for the on and off states.

By counting the instances of “on-state”-active power and “off-state”-active power in the measured time series of active power, it is found that the duration of the off-state is ca 32 time steps and the on-state is 7 time steps for each on/off -cycle. This corresponds to 8 seconds off and 1.75 seconds on. By using this information, one could make a time variant model of the cooktop load profile, utilizing the sets of model parameters found for the off- and on-states respectively.





On-state	V	P_avg	P_var	Q_avg	Q_var	PF	THD_A	THD_V	Energy [Wh]	Duration [Min]
<b>250V</b>	248.6	2207	173	-343	1.01	0.99	2.15	0.02	22.7	0.6
<b>240V</b>	238.6	2040	164	-317	0.26	0.99	2.00	0.02	20.5	0.6
<b>230V</b>	228.7	1886	183	-293	0.27	0.99	1.90	0.02	18.7	0.6
<b>220V</b>	218.8	1726	127	-268	0.53	0.99	1.91	0.02	17.6	0.6
<b>210V</b>	208.8	1577	96	-245	0.24	0.99	1.89	0.02	15.7	0.6

Off-state	V	P	P_var	Q	Q_var	PF	THD_A	THD_V	Energy [Wh]	Duration [Min]
<b>250V</b>	249.7	-7.0	0.29	-96	0.00	-0.07	10.1	0.01	-0.32	2.75
<b>240V</b>	239.7	-6.5	0.36	-88	0.24	-0.07	10.6	0.01	-0.30	2.77
<b>230V</b>	229.8	-5.7	0.34	-81	0.25	-0.07	11.2	0.01	-0.26	2.78
<b>220V</b>	219.8	-4.9	0.15	-75	0.05	-0.07	11.9	0.01	-0.23	2.76
<b>210V</b>	209.8	-4.5	0.41	-68	0.01	-0.06	12.8	0.01	-0.21	2.78

The below table shows curve fit results when the average of the on- and off-states is considered.



	<b>Best fit, average of on- and off-states (time step 50-900)</b>	<b>Chi-square (Reduced chi-square)</b>
<b>Vnom</b>	230 V	
<b>Pnom</b>	363	
<b>Qnom</b>	-125	
<b>Zp</b>	0.91	14.98 (4.99)
<b>Ip</b>	0.10	
<b>Pp</b>	-0.01	
<b>Zq</b>	0.77	0.38 (0.13)
<b>Iq</b>	0.43	
<b>Pq</b>	-0.20	
<b>Np</b>	1.92	15.01 (3.75)
<b>Nq</b>	1.96	0.44 (0.11)

#### D.1.4 Test with MaxPower setting

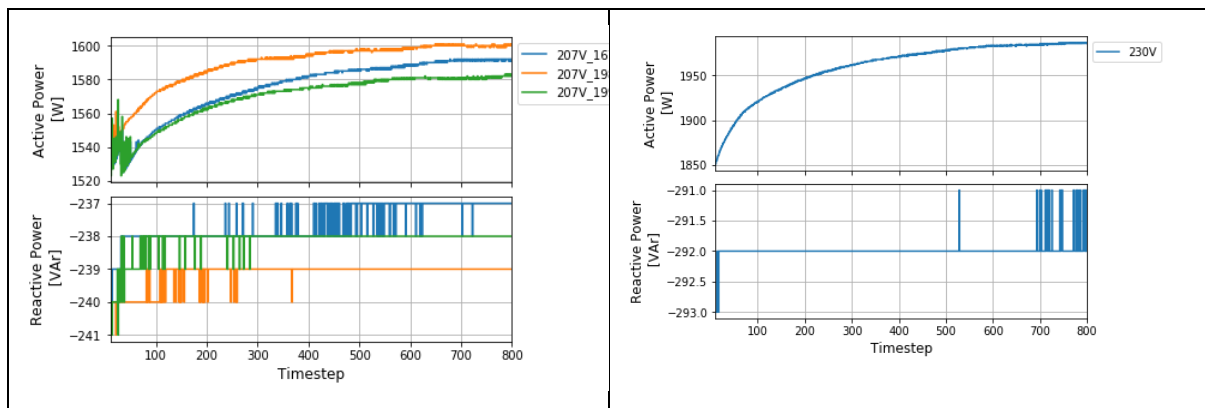
For this setting, tests at four different test voltages are conducted. In addition, tests for one of the voltages (207V), are executed in total three times. The selection of test voltages for this might seem a little bit random. The reason for this is that it is not found out during the tests, exactly why the cooktop entered the max power mode. The tests of the max power mode occurred unintentionally when trying to test other settings.

From the three tests performed at 207V, it is evident that the load curves are not exactly the same for the respective tests. The load curves are shown in the figure below for time step 10-800. The tests are labelled with the measurement number (See appendix C for more information on measurement number and the details for the respective tests with these numbers).

In the load modelling procedure, the average of the three 207V-tests is used. From the plots showing the load curves for the 207V and the 230V tests, it can be observed that the active power is increasing through the whole measurement window. The rate of change is higher in the beginning and slows down towards the end of the cycle. The observed pattern introduces several alternative approaches when it comes to choosing the steady state time window for the load modelling procedure. One possibility is to

include the whole time window (eg. Time step 10-800, corresponding to ca. 3 minutes) in the load modelling. A different approach would be to only include a time window where the active power curve has a more “flat” nature, e.g. from time step 500. Both approaches gives similar voltage dependency (similar load modelling result). Obviously, the nominal power  $P_n$ , in the load model results are different depending on the chosen approach. When considering only time step 10-300, the nominal power  $P_n$  from the preliminary curve fit is 1936W, whereas when considering the time window 500-800, the nominal active power result is 1995W.

It is interesting to notice that the loading is not equal given the same input voltage. Some of the differences may be due to measurement errors and the fact that the used measurement data is average values for 250ms time intervals. Other reasons may be the functionality of the power electronic controllers within the cooktop ...



	<b>Best fit, time step 500-800</b>	<b>Chi-square (Reduced chi-square)</b>
<b>Vnom</b>	230 V	
<b>Pnom</b>	1995 W	
<b>Qnom</b>	-295 VAR	
<b>Zp</b>	1.16	499.40 (249.70)
<b>Ip</b>	-0.23	
<b>Pp</b>	0.08	
<b>Zq</b>	0.78	0.93 (0.46)
<b>Iq</b>	0.37	
<b>Pq</b>	-0.15	

<b>Np</b>	2.08	499.98 (166.66)
<b>Nq</b>	1.93	0.96 (0.32)

	<b>Best fit, time step 10-300</b>	<b>Chi-square (Reduced chi-square)</b>
<b>Vnom</b>	230 V	
<b>Pnom</b>	1936 W	
<b>Qnom</b>	-295 VAr	
<b>Zp</b>	1.23	681.79 (340.90)
<b>Ip</b>	-0.46	
<b>Pp</b>	0.23	
<b>Zq</b>	0.92	1.50 (0.75)
<b>Iq</b>	0.09	
<b>Pq</b>	-0.01	
<b>Np</b>	1.98	687.55 (229.18)
<b>Nq</b>	1.92	1.50 (0.50)

	<b>Best fit, time step 10-800</b>	<b>Chi-square (Reduced chi-square)</b>
--	-----------------------------------	--

<b>Vnom</b>	230 V	
<b>Pnom</b>	1971 W	
<b>Qnom</b>	-295 VAr	
<b>Zp</b>	1.03	chi-square = 596.378985  reduced chi-square = 298.189492
<b>Ip</b>	-0.03	
<b>Pp</b>	0.00	
<b>Zq</b>	0.84	chi-square = 1.18347312  reduced chi-square = 0.59173656
<b>Iq</b>	0.25	
<b>Pq</b>	-0.08	
<b>Np</b>	2.04	chi-square = 596.656363  reduced chi-square = 198.885454
<b>Nq</b>	1.93	chi-square = 1.18747226  reduced chi-square = 0.39582409

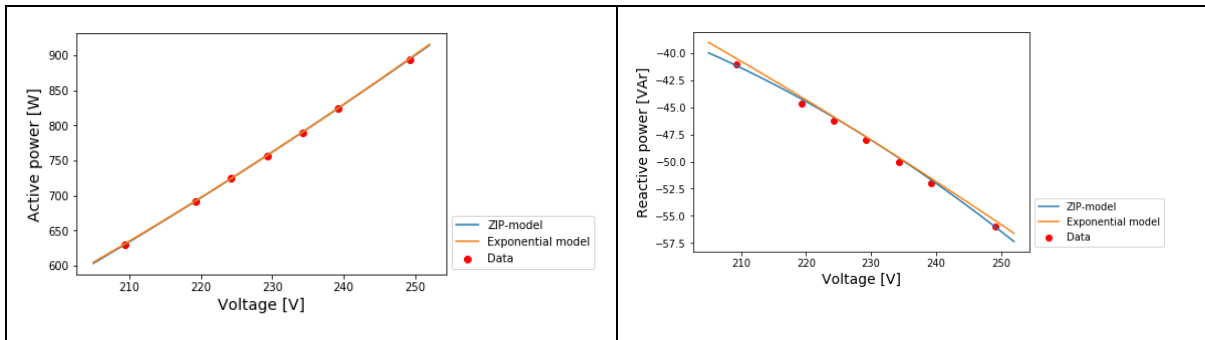
## D.2 Space heater

### D.2.1 Full power

The time interval from 750-1700 is used to find the model parameters.

	<b>Best fit</b>	<b>Chi-square (Reduced chi-square)</b>

<b>Vnom</b>	230 V	
<b>Pnom</b>	762 W	
<b>Qnom</b>	-48	
<b>Zp</b>	0.86	1.18 (0.24)
<b>Ip</b>	0.30	
<b>Pp</b>	-0.15	
<b>Zq</b>	2.45	0.61 (0.12)
<b>Iq</b>	-3.09	
<b>Pq</b>	1.64	
<b>Np</b>	2.01	2.91 (0.49)
<b>Nq</b>	1.81	1.44 (0.24)

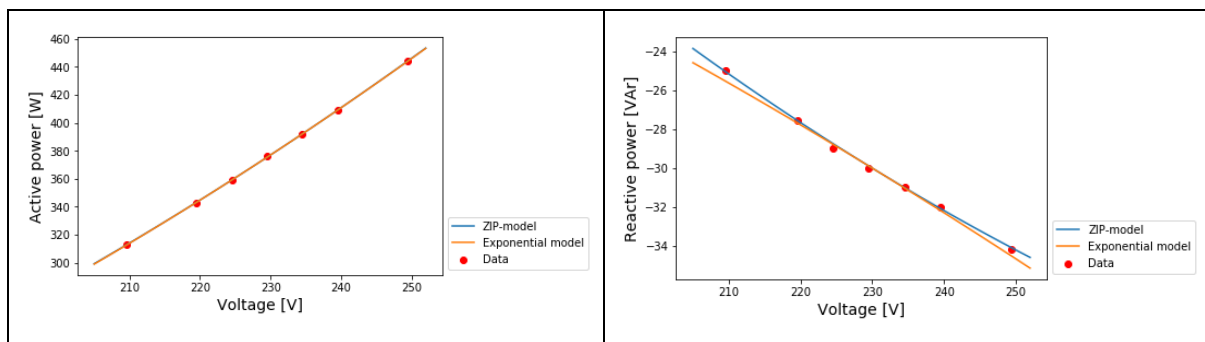


### D.2.2 Half power

The time interval 100-1100 is used in the modelling.

	<b>Best fit</b>	<b>Chi-square (Reduced chi-square)</b>
<b>Vnom</b>	230 V	

<b>P<sub>nom</sub></b>	377 W	
<b>Q<sub>nom</sub></b>	-30 VAr	
<b>Z<sub>p</sub></b>	1.08	0.53 (0.11)
<b>I<sub>p</sub></b>	-0.15	
<b>P<sub>p</sub></b>	0.07	
<b>Z<sub>q</sub></b>	-1.40	0.09 (0.02)
<b>I<sub>q</sub></b>	4.53	
<b>P<sub>q</sub></b>	-2.13	
<b>N<sub>p</sub></b>	2.01	0.60 (0.10)
<b>N<sub>q</sub></b>	1.73	0.54 (0.09)



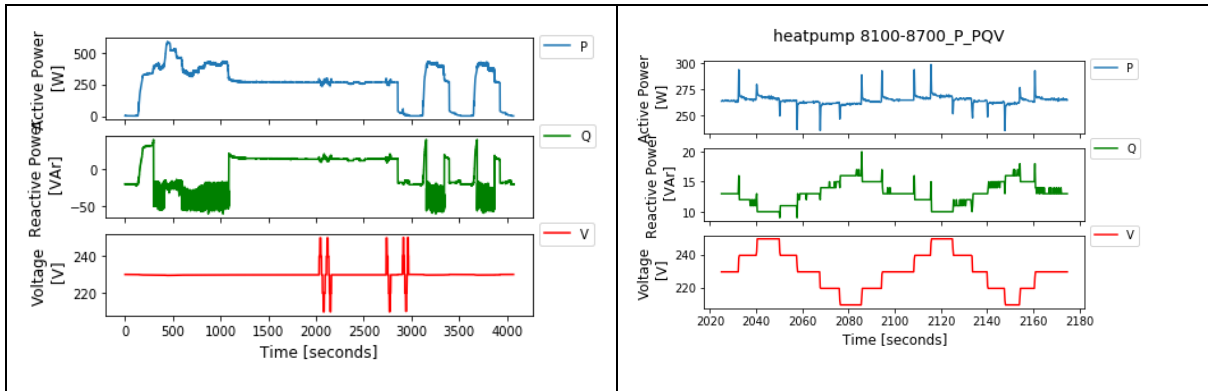
## D.3 Heat pump

### D.3.1 Test with 24deg setting

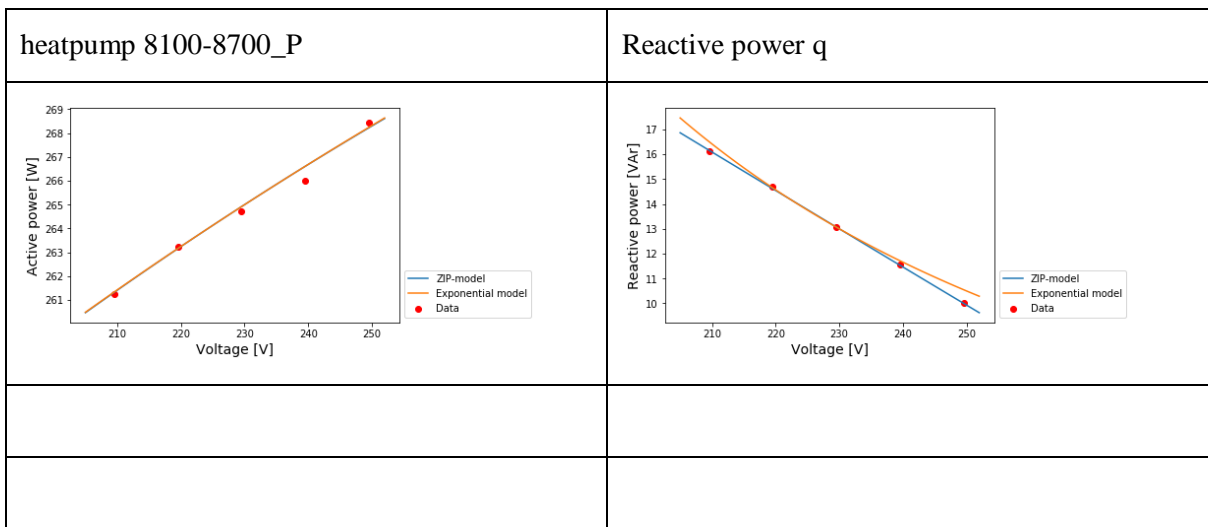
The below figures shows:

Left: The whole timeseries of MEAS243.

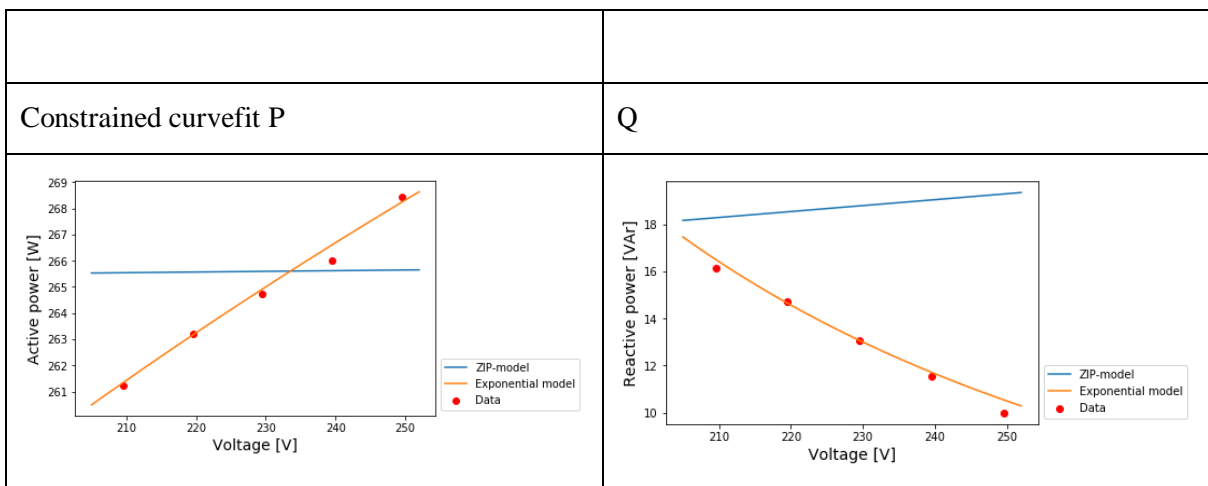
Right: Time window 8100-8700.



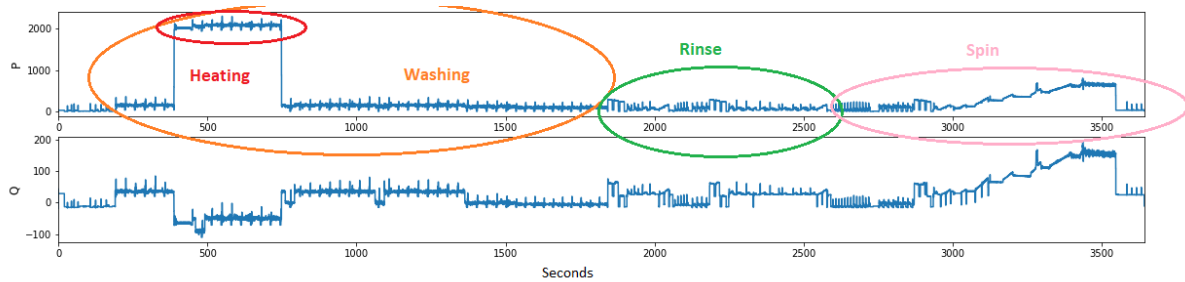
The below table contain the curve fit results from this time window. (accurate ZIP model is used)



Using the constrained ZIP model the fit result yields: (Note: the exponential model is unchanged from the one above)



## D.4 Washing machine



The table below shows the selected time intervals for the heating, washing, spin and rinse.

The rinse state did not last equally long for all tests. This may be caused by the voltage but can also be due to other factors. In the tests, the “auto detergent” option is chosen. This involves that some control in the washing machine adapts the amount of detergent to the laundry load. Although the same laundry load is used in all tests, the selected amount of detergent might have been different (the exact functioning of the auto detergent is not known by the author). Given that the amount of detergent is not the same in all tests, there might have been a need to continue the rinse state.

The state identified as “spin” in the load modelling is the very last part of the washing cycle where the active power increase and the spin velocity increase to dry the clothes. In this part of the cycle, the load pattern is very similar for all voltage levels. However, other definitions on when the “spin”-state started could have been chosen, as the limit between the rinse and spin states can be set differently depending on how one choose to define these states.

The “rinse” state is the state of the load modelling which contains most uncertainties in terms of defining comparable datasets for each state. By doing more detailed analysis in further work, it can be feasible to identify the different processes taking place in this state, for instance by distinguishing between what in [51] is identified as draining, rinsing and water filling. In the definition of rinse used in this thesis all these states are included. An alternative approach could be to divide the cycle into a number of equally long time-intervals and find model parameters for each interval. In [54] washing machine model parameters for eight subsequent periods of 10 minutes is used.

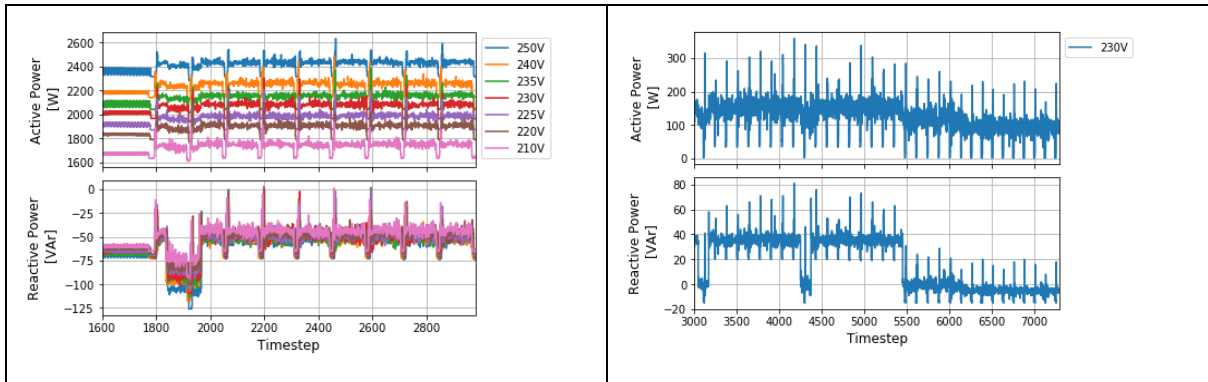
	Time step
Heating	1600-2980
Washing	3000-7300



Rinse	<pre>rinse_start= {'250V': 7375,               '240V': 7369,               '235V': 7377,               '230V': 7374,               '225V': 7373,               '220V':7374,               '210V':7368}  rinse_stop= {'250V':12250,              '240V': 12750,              '235V': 12100,              '230V': 11800,              '225V': 13000,              '220V': 11900,              '210V': 14800}</pre>
Spin	<pre>Spin_start           =rinse_stop spin_stop=None (to the end of the program. Var- ies between the tests since they are not equally long)</pre> <p>After the timeintercal had been chosen for each test, the indexing is started at 0 for each data-frame and the selected time window is 0-2300 to exclude the part of the cycle where the spin finishes and the drum stops (and makes some slow turns a few times, stopping in between each time).</p>

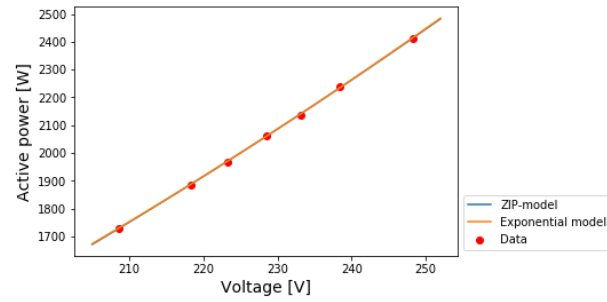
The preliminary curvefit is done with the five measurements closest to 230V.

#### D.4.1 Washing and heating

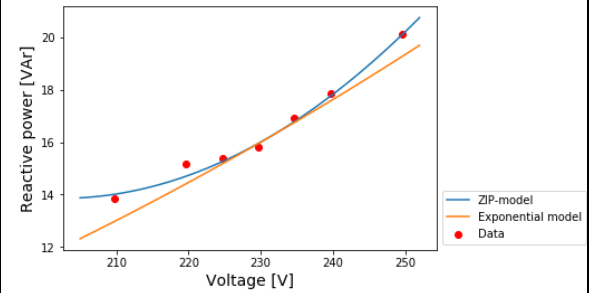
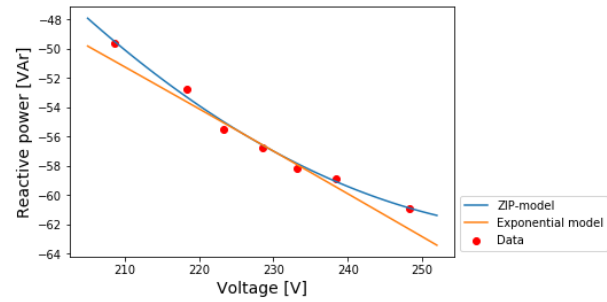
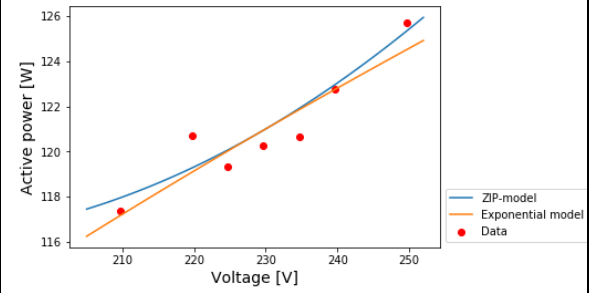


## Fit results

### Washing

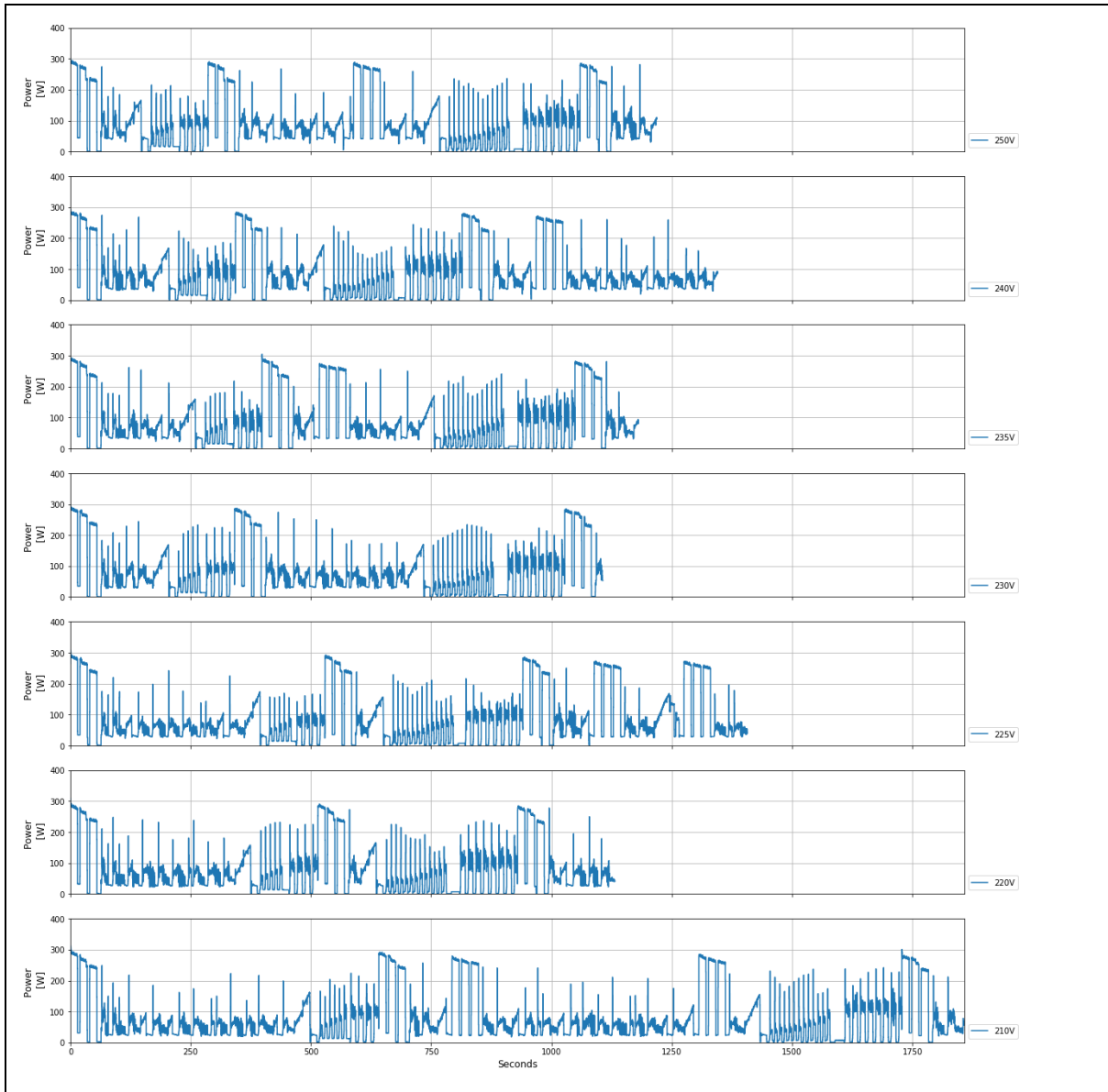


### Heating



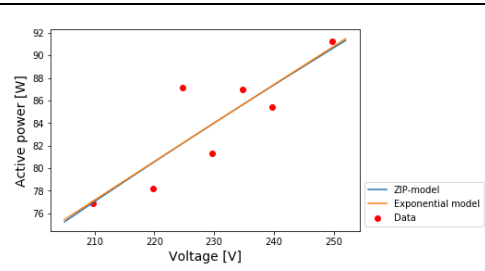
## D.4.2 Rinse

The plots shows the selected rinse states for the respective test voltages. They are not equally long.

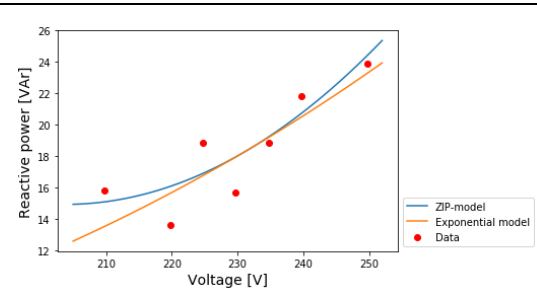


Curve fit results for the active and reactive power for RINSE state

P (active power)

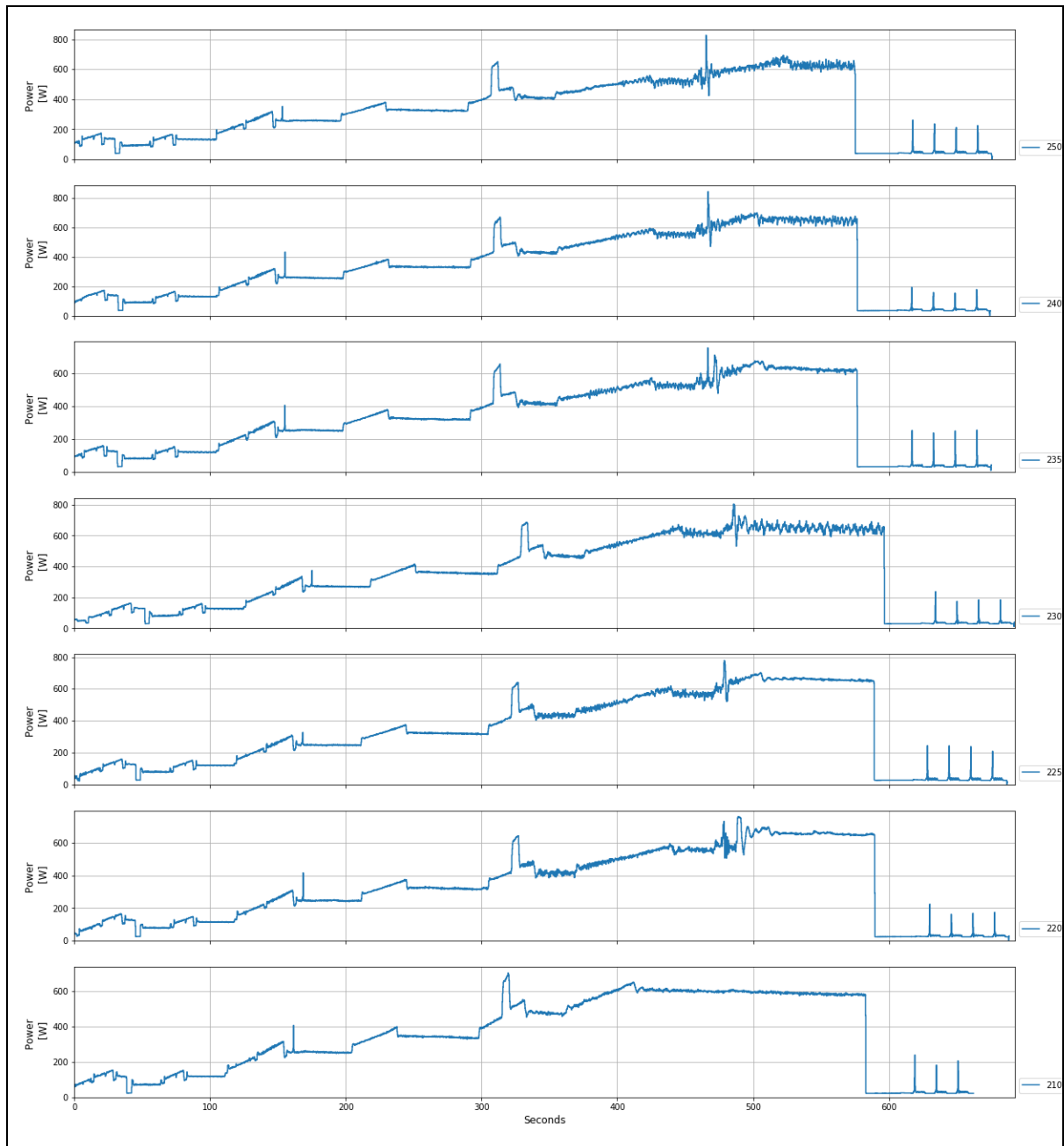


Q (reactive power)

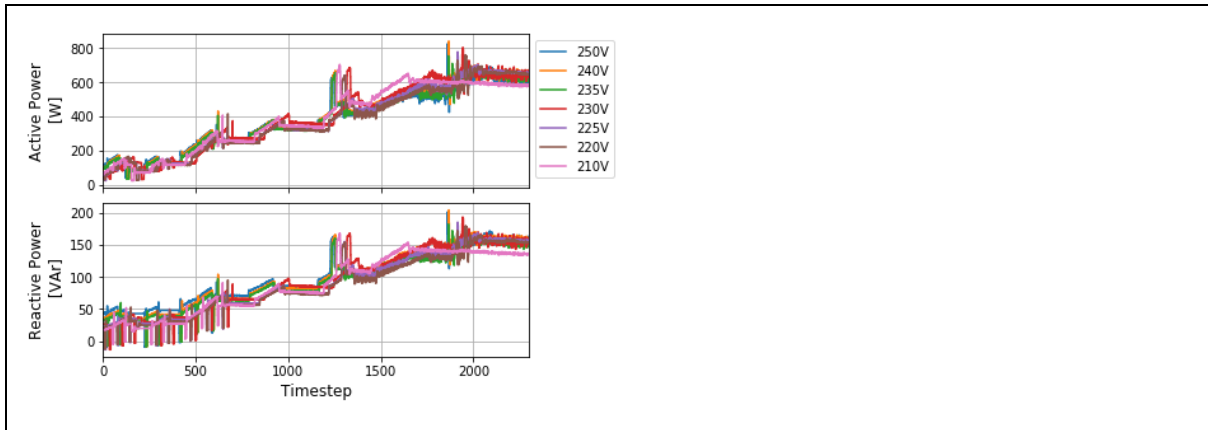


### D.4.3 Spin

The below figure shows the active power demand for the part of the washing cycle identified as “spin”. In the load modelling the last parts of the cycle are excluded (where the power demand drops when the high-velocity spinning of the drum is finished)

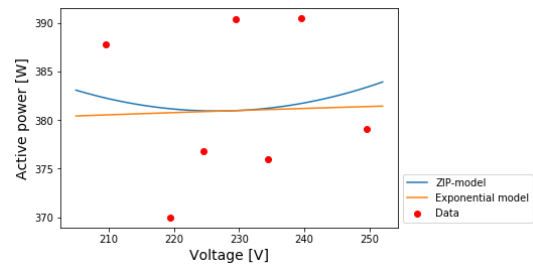


The part of the spin cycle used in load modelling is shown in the figure below.

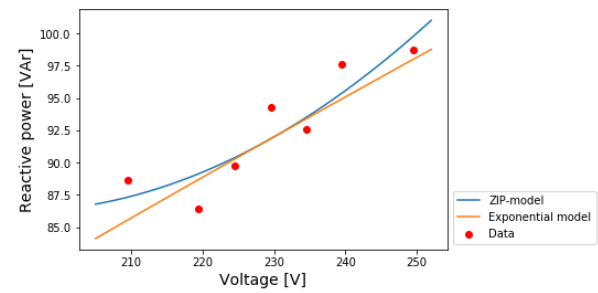


Spin P (0-2300 from spin-dataframes)

P – active power

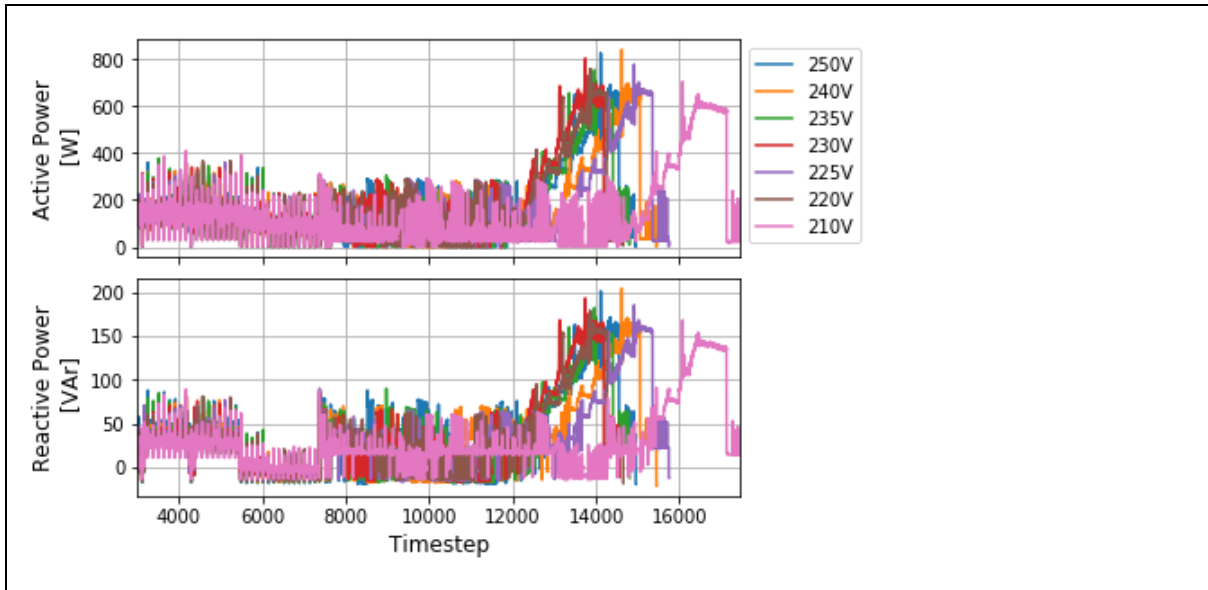


Q – reactive power



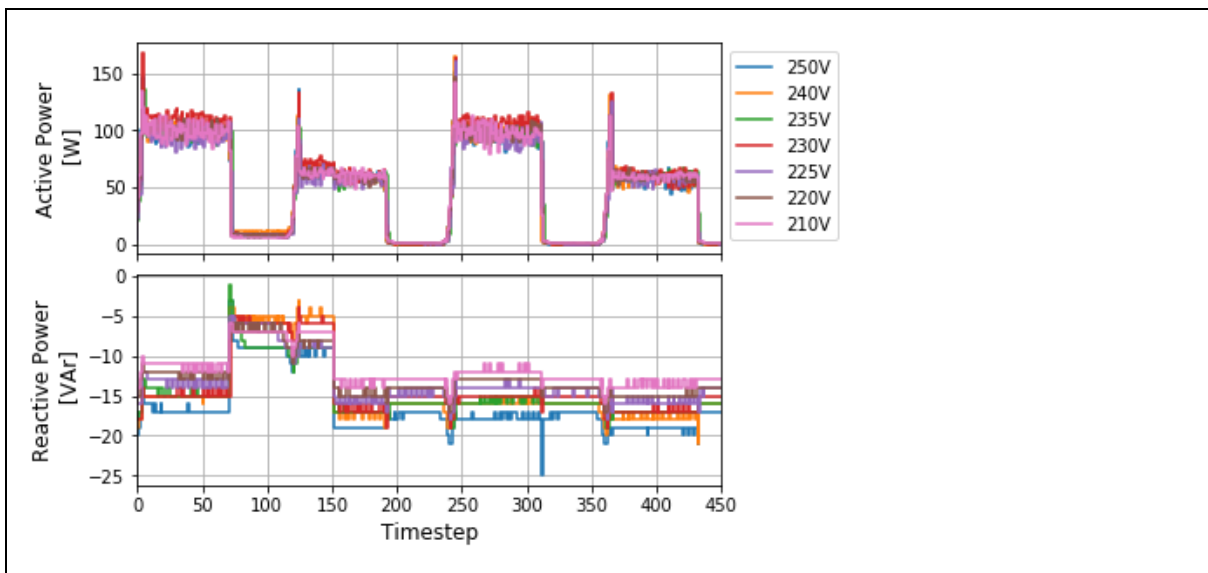
#### D.4.4 Cycle after water heating (time step 3000)

Load model parameters for the average behaviour after time step 3000.



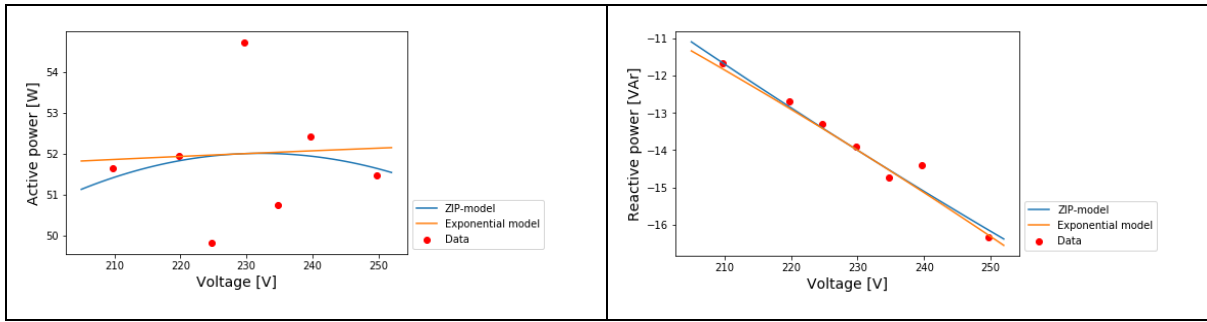
## D.5 Heat pump dryer

### D.5.1 Before time step 450



Active power

Reactive power



### D.5.2 Steady-state (time step 500-14000)

	<b>Best fit (time step 500-14000)</b>	<b>Chi-square (Reduced chi-square)</b>
<b>Vnom</b>	230 V	
<b>Pnom</b>	438	
<b>Qnom</b>	-27	
<b>Zp</b>	-1.18	756.6 (151.3)
<b>Ip</b>	3.01	
<b>Pp</b>	-0.83	
<b>Zq</b>	-78.3	16.86 (3.37)
<b>Iq</b>	143	
<b>Pq</b>	-64.1	
<b>Np</b>	0.66	783.1 (130.5)
<b>Nq</b>	-7.27	1397.63262 (232.9)

